Intravital visualization of hematopoietic stem cell and neutrophil behavior in long bones of mice

Dissertation

zur Erlangung des akademischen Grades

doctor rerum naturalium
(Dr. rer. nat.)

genehmigt durch die Fakultät für Naturwissenschaften
der Otto-von-Guericke-Universität Magdeburg

von Dipl. Biol. Anja Köhler

geb. am 05.07.1980 ***in*** Peine

Gutachter: Prof. Matthias Gunzer

Prof. Karl Welte

eingereicht am: 17.11.2010

verteidigt am: 21.02.2011

Declaration

I herewith confirm that I have written the present PhD thesis myself and independently, and that I have not submitted it at any other university worldwide.

Magdeburg, den

_____

Anja Köhler
Olvenstedter Str. 65
39108 Magdeburg

Publications during Thesis

Professional articles

Geiger H, **Köhler A**, Gunzer M

Stem cells, aging, niche, adhesion and Cdc42: a model for changes in cell-cell interactions and hematopoietic stem cell aging

Cell Cycle 2007; 6: 884-887

Köhler A, Smithorst V, Filippi M-D, Ryan MA, Daria D, Gunzer M and Geiger H

Altered cellular dynamics and endosteal location of aged early hematopoietic progenitor cells revealed by time-lapse intravital imaging in long bones

Blood 2009; 114:290-298

Ryan MA, Nattamai KJ, Xing E, Schleimer D, Daria D, Sengupta A, **Köhler A**, Liu W, Gunzer M, Jansen M, Ratner N, Le Cras TD, Waterstrat A, Van Zant G, Cancelas JA, Zheng Y, Geiger H.

Pharmacological inhibition of EGFR signaling enhances G-CSF-induced hematopoietic stem cell mobilization

Nat Med. 2010; 16(10):1141-6

Articles under revision

Köhler A, De Fillipo K, Hasenberg M, van den Brandt C, Nye E, Hosking MP, Lane TE, Männ L, Ransohoff RM, Hauser AE, Winter O, Schraven B, Geiger H, Hogg N and Gunzer M

G-CSF mediated Thrombopoietin release triggers neutrophil motility and mobilization from bone marrow via induction of CXCR2 ligands

Blood 2010

Gonzalez-Nieto D, Li L, **Köhler A**, Sengupta A, Madhu M, Arnett J, Santho R, Dunn SK, Fishman I, Gutstein D, Civitelli R, Barrio LC, Gunzer M, Cancelas JA

Osteolineage connexin-43 deficiency impairs trafficking of hematopoietic stem cells and progenitors and induces long-term hematopoietic stem cell failure

Cell stem cell 2010

Oral talks and poster presentations

Köhler A, Schmithorst V, Filippi M-D, Ryan MD, Daria D, Geiger H, Gunzer M.

Intravital 2-photon microscopy reveals the localization and motility of hematopoietic cells in long bones of mice

2nd Europoean Congress of Immunology, Berlin, September 13 – 16, 2009

Köhler A, De Filippo K, Hasenberg M, Männ L, Nitschke C, Nye E, Winter O, Hosking M, Lane TE, Hauser AE, Schraven B, Geiger H, Hogg N, Gunzer M

A novel intravital 2-photon microscopy approach to study neutrophil mobilization from the tibial bone marrow

14th International Congress of Immunology, Kobe, August 22 – 27, 2010

Mike

Abbreviations

°C	Grad Celsius
α	alpha
α	anti
µg	microgram
µl	microliter
µm	micrometer
µM	micromolar

A

aa	amino acid
7-AAD	7-aminoactinomycin
AB	antibody
ANG1	angiopoietin
APC	allophycocyanin
APCs	antigen presenting cells
avi	audio video interleave

B

B	bursa od fabricius
BD	Becton Dickinson
BFU	burst forming unit
BM	bone marrow
BMDC	bone marrow derived dendritic cell

C

C	carbon
CCD	charge-coupled device
CCHMC	Cincinnati Children's Hospital Medical Center
CD	cluster of differentiation
CFU	colony forming unit
Cl	chloride
CLP	common lymphoid progenitor
CMP	common myeloid progenitor
CNS	central nervous system
CFSE	carboxy fluorescein succinimidyl ester
c-Kit	stem cell factor receptor
col1a1	collagen type I alpha 1
CTO	Cell Tracker Orange
CTL	cytotoxic T-cell

D

3D	three dimensional
DC	dendritic cell
dist.	distilled

E

EAE	experimental allergic encephalitis
EDTA	ethylenediaminetetraacetic acid
e.g.	*Latin "exempli gratia"* = for example
EGFP	enhanced green fluorescent protein
eHPC	early hematopoietic progenitor cell
ELR	glutamic acid-leucine-arginine
ELISA	enzyme-linked immunosorbent assay
EPO	erythropoietin

F

FACS	fluorescence activated cell sorting
FC	fragment crystallizable region
FCS	fetal calf serum
FDA	Food and Drug Administration
FGF-4	fibroblast growth factor-4
FITC	fluorescein
FOXP-3	forkhead box protein 3
fps	frames per second
fs	femtosecond
FSC	forward scatter

G	
g	gram
g	earth's gravitational acceleration
G	gauge
G-CSF	granulocyte colony-stimulating factor
GEMM	granulocyte, erythrocyte, monocyte, megakaryocyte
GFP	green fluorescent protein
GM-CSF	granulocyte macrophage colony-stimulating factor
GMP	granulocyte-macrophage progenitor
GPI	glycosylphosphatidylinositol

H	
h	hour
H	hydrogen
HBSS	Hanks buffered salt solution
HPC	hematopoietic progenitor cells
HSC	hematopoietic stem cells

I	
ICAM1	inter-cellular-adhesion molecule
i.e.	*Latin: "id est"*
IFN	interferon
IgG	immunoglobulin G
IL	interleukin
IMDM	Iscove`s Modified Dulbecco`s Medium
i.p.	intraperitoneal
i.v.	intravenous

K	
K	potassium
K	c-kit
KC	keratinocyte chemoattractant
kD	kilodalton
kg	kilogram

L	
L	lineage
LFA1	lymphocyte function-associated antigen1
LIN	lineage
LPS	lipopolysaccharide
LSM	laser scanning microscope
LT	long term
Lys	lysozyme

M	
Mac-1	integrin alpha M
MC	macrophage
MEP	megakaryocyte-erythrocyte progenitor
mg	milligram
MHC	major histocompatibility complex
min	minute
MIP-2	macrophage inflammatory protein-2
ml	milliliter
mm	millimeter
mM	millimolar
Mpl	thrombopoietin receptor
MPP	multipotential progenitor
MSC	mesenchymal stem cell

N	
n	number
Na	sodium
NDD	non-descanned detector
NETs	neutrophil extracellular Traps
NK	natural killer
nm	nanometer
NRS	natural rabbit serum
n.s.	non significant

O	
O	oxygen
OvGU	Otto-von-Guericke University

P	
p	probability
PBS	phosphate buffered saline
PE	phycoerythrin
pH	the negative logarithm (base 10) of the molar concentration of dissolved hydrogen ions
PMN	polymorphonuclear leuco-cytes
PMT	photo-multiplier
PRR	pattern recognition receptor
PO	phosphate

R	
RT	room temperature

S	
S	Sca-1
Sca-1	stem cell antigen 1
SCF	stem cell factor
SDF-1	stromal cell-derived factor-1
SEM	structural equation modeling
SHG	second harmonic generation
SNO	spindle shaped N-cadherin osteoblast
SPF	specific pathogen free
SSC	side scatter
ST	short term
Strept.	streptavidin

T	
T	thymus
TGF-β	transforming growth factor beta
T_H-cell	T helper cell
TIE2	angiopoietin receptor
TNF	tumor necrosis factor
TPA	tetradecanoylphorbol 13-acetate
TPO	thrombopoietin
Treg	regulatory T cell

U	
U	unit
USA	United States of America

V	
V	volt
VLA	very-late antigen
v/v	volume per volume

W	
w/v	weight per volume

Y	
YFP	yellow fluorescent protein

Table of contents

Declaration 3

Publications during Thesis 3

Professional articles 3

Articles under revision 3

Oral talks and poster presentations 4

Abbreviations 6

Table of contents 9

1. Abstract 12

2. Introduction 14

2.1 Bone and bone marrow: structure and function 14

2.2 The hematopoietic system 17

2.2.1 Blood 17

2.2.2 Hematopoietic stem cells 18

2.2.3 Aging of hematopoietic stem cells 24

2.3 The mammalian immune system 25

2.4 Role of neutrophil granulocytes in the immune response 28

2.5 Chemokines 30

2.6 G-CSF 33

2.7 Megakaryocytes and Thrombopoietin 36

2.8 Neutrophil mobilization 37

2.9 Intravital 2-photon microscopy 40

2.10 Aim of the study 43

3. Materials and Methods 45

3.1 Materials 45

3.1.1 Mice 45

3.1.2 Buffers and additives 45

3.1.3 Antibodies and fluorescent markers 46

3.1.3.1 Antibodies for stem cell isolation (LIN-Cocktail) 46

3.1.3.2 Antibodies for stem cell isolation (FACS) 47

3.1.3.3 Antibodies for FACS analysis 47
3.1.3.4 Antibodies for mouse injections 48
3.1.3.5 Fluorescent dyes for *in vivo* imaging 48

3.2 Methods 49

3.2.1 General Methods 49
3.2.1.1 Mouse handling 49
3.2.1.1.1 Intraperitoneal injection 49
3.2.1.1.2 Retroorbital i.v. injection 49
3.2.1.1.3 Ketamin-Rompun narcosis 49
3.2.1.1.4 Bleeding 49
3.2.1.2 Isolation of bone marrow cells 49
3.2.1.3 Isolation of splenocytes 50
3.2.1.4 Estimation of cell numbers in a cell suspension 50
3.2.1.5 Fluorescence activated cell sorting (FACS) analysis 50
3.2.2 Stem cell specific methods 51
3.2.2.1 Preparation of hematopoietic progenitor cells (HPCs) and early hematopoietic progenitor cells (eHPCs) 51
3.2.3 Neutrophil specific methods 55
3.2.3.1 Neutrophil mobilization with G-CSF 55
3.2.3.2 Neutrophil mobilization with AMD3100 55
3.2.3.3 Neutrophil mobilization with thrombopoietin 55
3.2.3.4 Anti KC and anti MIP-2 treatment for inhibition of neutrophil mobilization 55
3.2.3.5 Inhibition of neutrophil mobilization by blocking CXCR2 55
3.2.3.6 Antibody mediated neutrophil depletion 56
3.2.3.7 Acute peritonitis model 56
3.2.4 Intravital 2-photon microscopy 56
3.2.4.1 Cell staining for 2-photon microscopy 56
3.2.4.2 Blood vessel staining for 2-photon microscopy 56
3.2.4.3 Mouse narcosis and bone preparation 57
3.2.4.4 Two-Photon microscopy 60
3.2.4.5 Data analysis 61
3.2.4.5.1 Processing of data with the rendering software “Volocity ®” 61
3.2.4.5.2 Cell tracking 61
3.2.4.5.3 Generation of “Kinetic overlays” 61
3.2.4.5.4 Calculation of cell distance to the endothelial layer 61
3.2.4.5.5 Statistical analysis 62

4. Results 63

4.1 Part I: Localization and dynamics of young and aged hematopoietic progenitor cells and early hematopoietic progenitor cells in the murine bone marrow revealed by intravital 2-photon microscopy 63

4.1.1 Visualization of hematopoietic progenitor cells and early hematopoietic progenitor cells in long bones of mice 63
4.1.2 Localization and dynamics of hematopoietic progenitor cells in long bones of mice 64
4.1.3 Dynamics of differentiated hematopoietic cells in the bone marrow 67
4.1.4 Altered localization and elevated dynamics of aged eHPCs 69
4.1.5 Summary - Part I 71

4.2 Part II: Analysis of G-CSF mediated neutrophil emergency release from the bone marrow of murine long bones 72
4.2.1 Visualization of the inner bone surface and blood staining for 2-photon microscopy 73
4.2.2 G-CSF treatment induces rapid neutrophil mobilization into the peripheral blood 75
4.2.3 Dramatic increase of neutrophil motility in the bone marrow after G-CSF injection 79
4.2.4 Long term behavior of neutrophils upon G-CSF stimulation 81
4.2.5 Monocyte mobilization with G-CSF in CX3CR-EGFP mice 84
4.2.6 Inhibition of G-CSF-induced neutrophil mobilization 85
4.2.7 Inhibition of neutrophil recruitment into the peripheral blood after CXCR2 antiserum treatment 88
4.2.8 Inhibition or depletion after CXCR2 treatment? 90
4.2.9 Influence of CXCR2 antiserum treatment on neutrophil behavior *in vivo* 93
4.2.10 Triggering of neutrophil motility with the CXCR4 antagonist AMD 3100 95
4.2.11 Thrombopoietin (TPO) as mediator of neutrophil mobilization 97
4.2.12 Summary - Part II 98

5. Discussion* *100

5.1 Localization and motility of HPCs und eHPCs from young and aged mice in murine long bones 100

5.2 Investigation of bone structure and blood flow in murine long bones 104

5.3 Important role for the chemokines KC and MIP-2 and their receptor CXCR2 in neutrophil mobilization from the bone marrow 105

5.4 Megakaryocytes produce and release KC and MIP-2 in response to thrombopoietin 106

5.5 Role of the CXCR4 antagonist AMD3100 in neutrophil mobilization 109

6. Outlook* *111

7. Reference list* *114

8. Appendix – DVD-Content* *132

9. Acknowledgement* *136

10. Curriculum vitae* *138

1. Abstract

Hematopoietic stem cells (HSC) are precursors of all blood cells and primarily located in the bone marrow (BM) of adults. They interact closely with a special BM microenvironment, referred to as stem cell niche, which regulates cell proliferation, self-renewal, differentiation and migration/mobilization. As a current hypothesis it is postulated that the impaired hematopoiesis of aged stem cells is a consequence of an altered interaction with their niche. With a newly developed experimental setup for intravital 2-photon microscopy the dynamics and spatial arrangement of young and aged primitive hematopoietic cells in the long bones of mice were investigated to reveal possible changes in cell-niche contact. Until now all microscopic observations of BM-resident hematopoietic cells were obtained from cells located in a small bone marrow patch of the calvarium, although this compartment has known limitations with regard to HSC-biology. Transplanted hematopoietic progenitor cells (HPCs) and early hematopoietic progenitor cells (eHPCs) were found to be completely immobile in murine long bones but displayed a permanent protrusion movement of the cell surface. Moreover, eHPCs of aged animals were located more distant from the inner bone surface and this correlated with an increase of the protrusion movement compared to eHPCs of young animals. This suggests a more quiescent microenvironment provided by the niche in areas close to the endosteum whereas cells that are located farther away from the inner bone surface are not longer in an extreme silent status.

In the second part of the thesis the new intravital 2-photon microscopy method was used to analyze cell behavior of neutrophils as an example for differentiated blood cells in the murine bone marrow. Neutrophils are the most abundant and, arguably, most important leukocyte type of the vertebrate immune system. Their lack or dysfunction is always associated with severe consequences to health. In “danger situations” such as peripheral infections, the release of neutrophils from bone marrow can be dramatically increased within hours, a process termed danger mobilization. The granulocyte colony-stimulating factor G-CSF is known to play an important role in this process and already a single injection of G-CSF leads to a massive neutrophil mobilization into the peripheral blood. However, although recombinant G-CSF has been used in clinical hematology for more than 20 years to overcome the severe problems of neutropenic patients the underlying molecular

mechanisms by which danger mobilization is mediated on single cell level in the BM still remains unknown. Neutrophils show a rapid and strong increase of motility in murine long bones after G-CSF treatment although it is known, that they can not respond directly to this trigger. The chemokines KC and MIP-2 were found to play a key role in recruiting neutrophils to the circulation by forming a gradient that neutrophils are able to follow after detection by their specific surface receptor CXCR2. Megakaryocytes were identified as a source of KC and MIP-2 production in the bone marrow. Moreover it could be demonstrated that both chemokines were released in response to thrombopoietin (TPO) stimulation, one major activation trigger for megakaryocytes. This factor might be released by a F4/80 positive subpopulation of macrophages that was identified to be positive for the G-CSF receptor and was also able to produce TPO.

2. Introduction

2.1 Bone and bone marrow: structure and function

The main functions of bones are to constitute the supporting apparatus of the body and the starting point of muscles to protect various organs of the body and to produce and store minerals. Moreover, they are responsible for the production of red and white blood cells [Junquiera *et al.* 2005].

Bones are composed of a highly specialized tissue which consists of living and dead cells embedded in a mineralized organic matrix. In addition they are covered by a connective tissue membrane called periosteum. Beneath the periosteum a dense zone, the compact bone or *Substantia compacta* is located which consists of the Haversian system, or osteon. Each osteon has concentric layers of mineralized matrix, which surround a central canal that contains blood vessels and nerves to support the bone with nutritive substances. The central part of the bone is filled with the bone marrow. Between the marrow cavity and the compact bone, the trabecular bone tissue, also called cancellous or spongy bone can be found as an open porous network. It consists of rod- and plate-like structures built up by bone trabeculae and the empty space is engaged by blood vessels and marrow. The function of this tissue is, to reduce the weight of

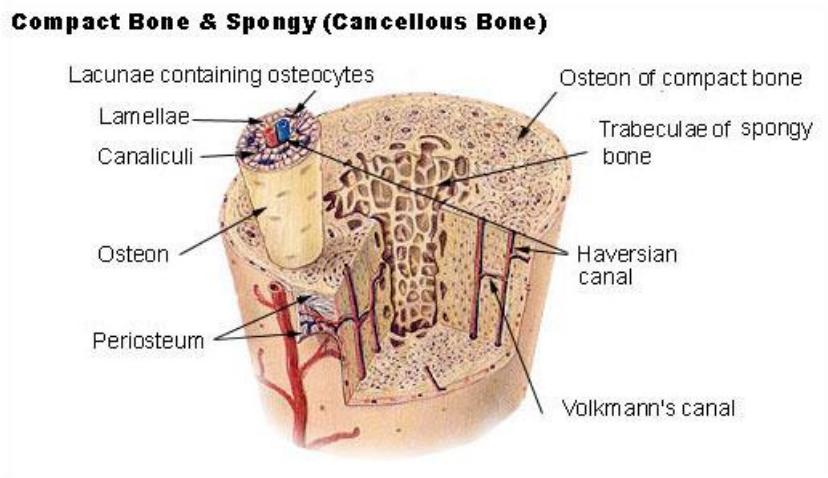

Figure 1 Bone constitution. Bone consists of a compact bone structure, which encloses the central bone marrow cavity. It is divided in many round units (osteon), long cylinders which run parallel to the diaphysis. Each osteon contains a Haversian canal in which blood vessels and nerves are located. Haversian canals can communicate with each other, with the periosteum or the bone marrow cavity by diagonal proceeding Volkmann canals. Spongy bone, a porous network of trabeculae is mostly located between the compact bone and the bone marrow cavity. The bone is covered by connective tissue which is referred to as periosteum at the outside of the bone and endosteum at the inner bone surface.

source: http://en.wikipedia.org/wiki/File:Illu_compact_spongy_bone.jpg

the bone [Schiebler 2005; Junquiera *et al.* 2005].

The bone substance is mainly built up by mononuclear bone-forming cells called osteoblasts. They form skin-like layers around bone structures and release collagen type-I, calcium phosphate and carbonate. Osteoblasts are not able to proliferate but they build up the bone matrix which gets mineralized and filled up with calcium over time. During this bone formation, also named ossification, a subset of osteoblasts undergoes a differentiation to osteocytes. These migrate into the bone as mature bone cells and, after reaching their final destination they become trapped and surrounded by bone matrix that they synthesize themselves. Osteocytes are characterized by their multiple nuclei and build up extensions towards osteoblasts and other osteocytes in order to influence bone formation, matrix maintenance and calcium homeostasis. In contrast to bone formation, osteoclasts are the cell type which is responsible for bone removal, namely bone resorption. They are located on the surfaces of bone trabeculae in indentations called howship-lacunae which they synthesize themselves by degradation of bone material. This degradation process is realized by a release of H^+-ions into the microenvironment between osteoclasts and the bone material resulting in a strong acidification of the small cavity. The organic constituents of the bone are drained by the acidic milieu and the resulting fragments are taken up by osteoclasts which degrade them subsequently [Schiebler 2005]. Because of their important role in regulating the amount of bone tissue and their ability to remodel the bone structure by phagocytic functions, osteoclasts are indispensable for the maintenance of bone integrity and always ensure a perfect functional status of bones [Junquiera *et al.* 2005; Schiebler 2005].

In almost any bone that holds cancellous tissue bone marrow can be found and according to unique characteristics it can be separated into two variants. The red bone marrow mainly consists of hematopoietic tissue which is responsible for the synthesis of all leukocytes, red blood cells and platelets. At birth almost the whole amount of BM consists of red BM but with age it gets more and more converted into the yellow type until only at specialized locations in the body functional hematopoiesis remains intact (e.g. the hip bone, breast bone, skull, ribs, vertebrae and shoulder blades and in the cancellous material of long bones). The main content of yellow BM are fat cells which serve as energy storage for the organism. This BM type is exclusively located in the center of long bones. Both BM variants are sup-

plied with a distinct network of blood vessels which enter the bone through many different pores which are spread all over the bone surface [Junquiera *et al.* 2005; Schiebler 2005].

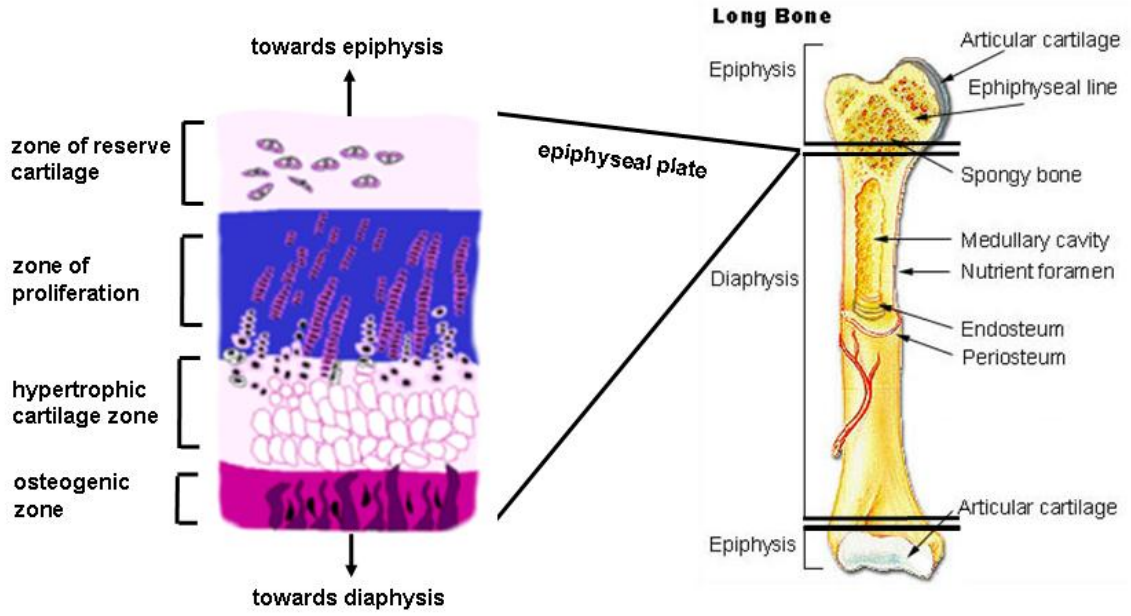

Figure 2 Scheme of long bone architecture and the epiphyseal plate. Long bones can be divided into a long diaphysis and two epiphyseal areas on each end. Over the period of time when the bone is growing an epiphyseal plate is located between both compartments, which is responsible for the linear growth of the bone. When the developmental bone growth is finalized the plate is replaced by the epiphyseal line. The epiphyseal plate can be divided into three major zones. The first one is a proliferation zone where chondrocytes divide heavily, leading to the bedding of new bone material. The hypertrophic cartilage zone consists of big apoptotic chondrocytes which are calcified step by step. The last zone is called osteogenic zone. This area is occupied by blood vessels and stem cells, which differentiate to osteoblasts that then build up new bone matrix. Between epiphysis and diaphysis a reserve zone of hyaline cartilage is located which is extremely elastic but not supplied by any nerves or blood vessels.

adapted from: http://en.wikipedia.org/wiki/File:Illu_long_bone.jpg and http://histology.leeds.ac.uk/bone/bone_ossify.php

Among all other types of bone that can be found in a mammalian organism, long bones are one special variant and they are characterized by unique features. They consist of compact bone with just a small amount of marrow in the center and, as their name indicates, their shaft is much longer than wide. Long bones display a characteristic assembly with a cylindrical diaphysis and two bone ends called epiphysis. In children, an epiphyseal plate is located between the diaphysis and epiphysis, which is responsible for the longitudinal growth of the bone. In adults

this plate is replaced by an epiphyseal line. Long bones arise from cartilage which is exclusively composed of chondrocytes. This special compartment is then coated by a bone collar. To support the bone with blood vessels, the bone collar is perforated by osteoclasts so that the vessels can grow through to reach the cartilage. By this route mesenchymal stem cells reach the inside of the bone. The diaphysis grows in the direction to the epiphysis, simultaneously osteoclasts remove material from the bone center to form the bone marrow cavity between both epiphyseal plates [Schiebler 2005]. During this development the ossification of the diaphysis goes on and in the end all cartilage is ossified, except that in the epiphyseal plate which is needed for the subsequent longitudinal growth of the bone. In this process the epiphyseal plate can be subdivided into three different zones. The first one is a proliferation zone in which the chondrocytes proliferate very fast. The hypertrophic cartilage zone is characterized by big chondrocytes which undergo apoptosis and are then ossified. After this process, blood vessels and stem cells migrate into the ossified region and differentiate to osteoblasts that build new bone matrix which is also ossified by and by. When the growth process is completed, the longitudinal growth is finalized by replacing the epiphyseal plate with new bone matrix, leading to a complete closing of the compartment [Junquiera *et al.* 2005]. Between the epiphyseal plate and the epiphysis a broad bar of hyaline cartilage is located which displays the last reservoir of cartilage in the full-grown bone [Schiebler 2005] (Figure 2).

2.2 The hematopoietic system

The blood building system of an organism is referred to as hematopoietic system. All cellular blood components which are important for a normal blood count, either the mature cells or their progenitors are mainly produced in the red bone marrow by a process that is called hematopoiesis [Murphy K *et al.* 2008]

2.2.1 Blood

Blood is responsible for the supply of organs and muscles with oxygen and other nutrients. Nevertheless, blood is not only indispensable for the transport of substances through the body moreover it is also responsible for the evacuation of waste products. An average healthy adult has a blood volume of about 5 liters and approximately $10^{11} – 10^{12}$ new blood cells are produced daily to maintain the num-

ber of all blood cells in the circulation. Blood cells can be divided into three major lineages: erythrocytes, lympho-cytes and myelocytes. The highest cell number in the vertebrate blood is provided by the oxygen carrying red blood cells or erythrocytes, which constitute about 43 % of the blood weight and 95 % weight of all blood cells. Lymphocytes are derived from common lymphoid progenitors and can be subdivided into two major groups, T-lymphocytes and B-lymphocytes. These cells are characterized by their ability to induce and modulate adaptive immune responses against foreign antigens (view 2.3) which makes them irreplaceable fighters against all kinds of infections. Granulocytes, megakaryocytes and macrophages are the cells belonging to the third group, termed myelocytes. All three sub-types have the same myeloid progenitor cell in common and they exhibit many important functions in adaptive, as well in innate immunity [Junquiera *et al.* 2005] [Murphy K *et al.* 2008].

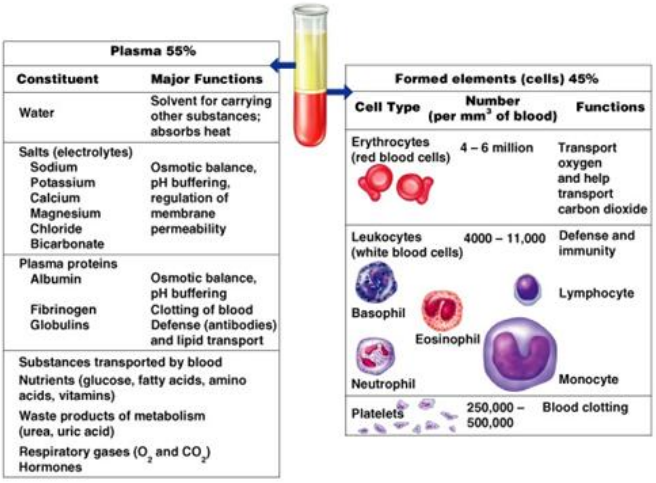

Figure 3 Blood composition and cell types of the blood. The main compounds of the blood plasma and their functions are displayed on the left side. On the right side the different types of blood cells are listed with a brief description of their major functions. Additionally their average numbers in a healthy adult are demonstrated.

adapted from: http://facweb.northseattle.edu/jlearn/ANP%20128/

Besides the blood cells, the blood plasma with a volume of around 55 % displays the second big blood component by weight. It contains many substances like proteins (antibodies, hormones) or lipids which are transported with the blood flow throughout the whole body to locations where they are needed. One very important protein that is part of the blood plasma is fibrinogen. During the process of blood clotting it polymerizes to fibrin thereby providing an indispensable substance for the closure of an open wound [Schiebler 2005; Junquiera *et al.* 2005].

2.2.2 Hematopoietic stem cells

All cellular blood components are derived from the same progenitor cells in the bone marrow which are called hematopoietic stem cells (HSCs). Because of their

special and unique ability to produce all types of blood cells they are designated as pluripotent [Abramson *et al.* 1977; Dick *et al.* 1985; Keller *et al.* 1985; Jordan *et al.* 1990; Szilvassy *et al.* 1994]. They reside only in the red blood marrow which in adults is mainly located in ribs, vertebrae, breastbone, hips and the end of the femurs. The population of pluripotent stem cells already develops in early embryos and renews itself mitotically while supporting the blood with all cellular compounds.

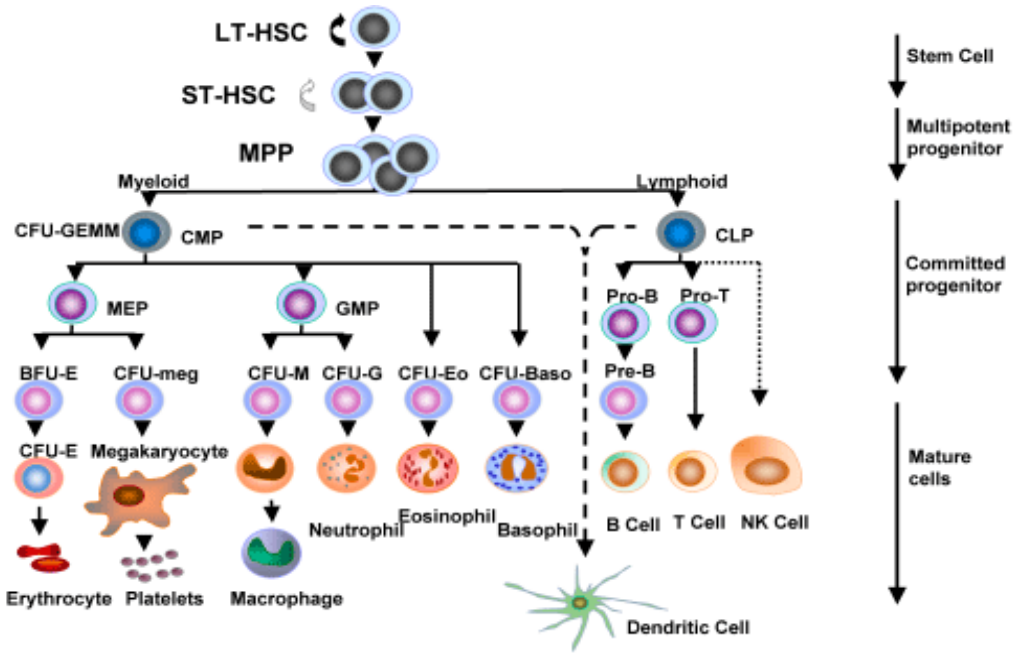

Figure 4 All blood cells and cells of the immune system are produced by multipotential hematopoietic stem cells. In the first step the stem cells differentiate into multipotent progenitor cells which then develop to progenitor cells either of the myeloid or lymphoid lineage in the bone marrow. In the end mature cells arise from a number of committed progenitors. The lymphoid lineage consists of natural killer cells and T- and B-lymphocytes. T-cell progenitors migrate to the thymus where they undergo further maturation. Afterwards T- cells as well as B-cells undergo further differentiation inside the lymph nodes like B-cells which develop into plasma cells after contact to an appropriate antigen. The myeloid progenitor cells differentiate to erythrocytes, megakaryocytes, mast cells and myeloblasts. Megakaryocytes are responsible for the production of thrombocytes (platelets) whereas the myeloblasts further develop to basophils, neutrophils, eosinophils and monocytes. Monocytes leave the bone marrow and enter body tissues to differentiate to macrophages. Mast cells also invade other tissues for further maturation. LT-HSC: long-term hematopoietic stem cell; ST-HSC: short-term hematopoietic stem cell; MPP: multipotential progenitor; CFU: colony forming unit; GEMM: granulocyte, erythrocyte, monocyte, megakaryocyte; CMP: common myeloid progenitor; CLP: common lymphoid progenitor; MEP: megakaryocyte-erythrocyte progenitor; GMP: granulocyte-macrophage progenitor; BFU: burst forming unit;

source: http://contanatura.weblog.com.pt/arquivo/stem-cell.jpg

The hematopoietic stem cell which can be isolated from adult bone marrow or peripheral blood belongs to the group of adult stem cells and it is the best characterized somatic stem cell [Weissman 2000; Kondo *et al.* 2003]. Adult stem cells are present in most self-renewing tissues like skin, intestinal epithelium and the hematopoietic system. In contrast to embryonic stem cells which can, independent of their location, develop to all kinds of tissue, adult stem cells can only form cells of the tissue which they are derived from. They have the capacity to produce further stem cells of their own type, which indicates the ability of self-renewal. This gives rise to a distinct, mature and differentiated offspring which efficiently maintains or repairs host tissue [Osawa *et al.* 1996]. In addition to the ability of self-renewal and the fact that they are pluripotent it is generally expected that a hematopoietic stem cell fulfills a third criterion to be considered as stem cell and this is an extremely high potential of proliferation. An average adult has approximately 50 million HSC in his body, some of which can generate up to 10^{13} mature blood cells over a normal lifespan. In contrast mice possess just 10.000-15.000 HSCs but remarkably it has been shown that a single stem cell can reconstitute the entire lympho-hematopoietic system of a mouse, following transplantation into an irradiated recipient [Osawa *et al.* 1996; Morrison *et al.* 1995; Krause *et al.* 2001]. In cases of injury, this enormous proliferation potential is needed to rapidly compensate the blood loss. Under normal conditions up to 75 % of HSC reside quiescently in the bone marrow [Cheshier *et al.* 1999]. Just very few cells are constantly dividing to ensure the maintenance of the hematopoietic system. The exact process of this division remains unclear at present but it is commonly accepted that HSC divide asymmetrically in order to obtain a cell that is able to conserve a constant population of quiescent long-term (LT) stem cells [Wilson *et al.* 2006a]. The second cell is believed to differentiate into a cell of the hematopoietic system. From all cells in the bone marrow just about 0.1 % are pluripotent stem cells. HSCs are characterized by a variety of surface markers. A lot of them have been identified during the last 20 years [Visser *et al.* 1990; Civin *et al.* 1993; Uchida *et al.* 1993], but just a few of them are routinely used for the characterization and isolation of HCS. The most important markers are c-kit, a receptor tyrosine-kinase recognizing the cytokine SCF (stem cell factor) and Sca-1 which is a glycosylphosphatidylinositol(GPI)-linked cell surface protein [Hanson *et al.* 2003] whose function is still unclear. It seems to have different roles in the normal HSC function like homing or lineage

development [Bradfute *et al.* 2005]. Studies on Sca-1 knock-out mice have identified an influence of the factor in HSC self-renewal [Ito *et al.* 2003] but there have also conflicting data been published [Bradfute *et al.* 2005]. Another important criterion to identify a HCS is the absence of lineage markers. Every cell that orientates to a distinct cell lineage during maturation is provided with a unique set of surface markers. Based on this fact a common protocol for the isolation of HSCs is to remove all cell types that have underwent differentiation from a cell suspension by positive selection with an antibody cocktail consisting of all typical markers for their lineages. In mice a suitable AB cocktail contains the following antibodies: B220 directed against B-cells, Gr-1 directed against neutrophils, Mac-1 directed against macrophages, CD5 directed against B- and T-cells, CD8a directed against cytotoxic T-cells and TER-119 directed against erythrocytes. The HSCs are designated to be completely unspecialized, so none of these markers should be detectable on them. It is now widely appreciated that the only valid test that defines a HSC is to demonstrate its capacity to completely and lastingly regenerate the lymphohematopoietic system following transplantation into lethally irradiated hosts [Szilvassy 2003]. As a critical test for HSC self-renewal serial transplantations are performed to finally identify a real stem cell which can reconstitute recipients 4–6 times [SIMINOVITCH *et al.* 1964; CUDKOWICZ *et al.* 1964].

A possibility to mobilize the usually quiescent HSC out of the bone marrow into the blood stream is the treatment of an organism with the granulocyte colony stimulating factor G-CSF, a glycoprotein that is involved in many processes of HSC homeostasis (view 2.6). G-CSF probably induces the release of proteases leading to a degradation of chemokines like SDF-1 (CXCL12) which acts as the main anchorage for HSC in the bone marrow through the binding to its receptor CXCR4 [Lapidot *et al.* 2002]. Treatment with G-CSF over several days leads to a strong increase of HSC in the peripheral blood which allows the isolation of HSC directly from this source. After transplantation HSC have the ability to return to the bone marrow of the recipient by specific migration, a behavior called “homing” [Nilsson *et al.* 2004]. Several cell surface adhesion molecules, including selectins and integrins are crucial for this HSC homing process (e.g. β_1- integrins, the very late antigen 4 (VLA4) and VLA5 or the β_2-Integrin “lymphocyte function-associated antigen 1 (LFA-1)) [Papayannopoulou 2003; Lapidot *et al.* 2005]. The lack of one or more of these molecules leads to a strongly diminished or complete loss of the

HSCs' possibility to home into bone marrow after transplantation. In principle, homing to the bone marrow is an unselective process which can be performed by all hematopoietic cells with almost the same frequency. The specialty of HSCs in contrast to other cell types is their ability to migrate through endothelial barriers into extra-vascular compartments of the bone marrow and in addition into distinct endothelial domains of the bone, which are designated as stem cell niche [Nilsson *et al.* 2004; Nilsson *et al.* 2005; Nilsson *et al.* 2003]. The concept of a distinct cell niche for the hematopoietic system was first established in 1978 [Schofield 1978]. The special three-dimensional microenvironment of this compartment is expected to regulate self-renewal, differentiation and proliferation of HSCs *in vivo* [Curry *et al.* 1967]. Mediators which are secreted by cells of the endosteum, displaying the inner bone surface, recruit the cells to the niche. One crucial factor involved in migration, mobilization and retention of HSCs is CXCL12 which is expressed by several types of bone marrow stromal cells, including osteoblasts and vascular endothelial cells [Ara *et al.* 2003; Ponomaryov *et al.* 2000]. CXCL12 binds to the CXC-chemokine receptor 4 (CXCR4) which is expressed on the surface of HSCs and by this action it is believed that HSCs migrate directed and specifically to their niche [Wright *et al.* 2002].

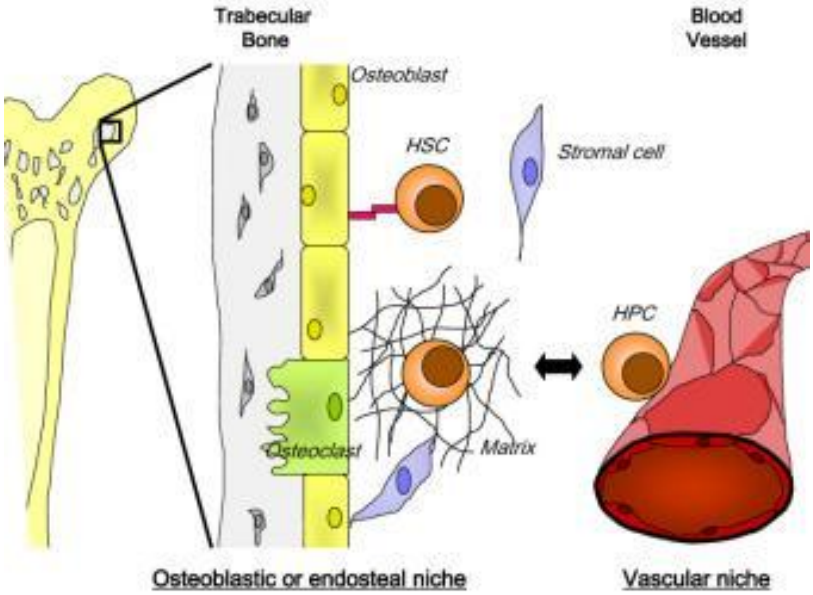

Figure 5 Endosteal and vascular hematopoietic stem cell niche in the bone marrow. Stem cells seem to reside at distinct places in the bone marrow that provide a special microenvironment to support stem cell quiescence and self-renewal. At these specific places called niche stem cells are in close contact, mainly to osteoblasts. If stem cells become more active it is believed that they enter a second niche in the bone marrow close to a blood vessel which is therefore termed vascular niche. This niche supports stem cell differentiation, proliferation and migration.

source: http://www.regmed.uni-tuebingen.de/files/3the_stem_cell_niche_338x252.jpg

Until now, two types of niches have been characterized in the bone marrow. A few stem cells can be found close to blood vessels. This microenvironment seems to support stem cell proliferation, differentiation and migration and is designated as vascular niche [Kiel *et al.* 2005; Kiel *et al.* 2006; Sugiyama *et al.* 2006]. In contrast, most of the stem cells reside in the endosteal niche. The main difference to the vascular niche is that this distinct area is located close to the endosteum where the cells reside in close vicinity to the bone what promotes stem cell quiescence and self-renewal [Wilson *et al.* 2006a]. In this compartment stem cells are attached to special stroma cells [Nilsson *et al.* 2001] or osteoblasts which mainly build up the endosteal stroma. These special osteoblasts are called “spindle-shaped osteoblasts” or SNO-cells and the strong adhesion and the resulting communication is known to play a crucial role in regulating stem cell fate [Zhang *et al.* 2003; Yin *et al.* 2006; Jung *et al.* 2005; Neiva *et al.* 2005]. Only the SNO-cells express the adhesion molecule N-cadherin which is also expressed on hematopoietic stem cells and which seems to be a central molecule mediating the strong adhesion between both cell types [Zhang *et al.* 2003; Wilson *et al.* 2004]. Moreover, it was shown that SNO-cells also produce other adhesion molecules and cytokines which have a strong influence on stem cell behavior. In example angiopoietin 1 (ANG1) activates the tyrosine kinase receptor (TIE2) that is expressed on stem cells. TIE2 increases the N-cadherin expression on stem cells resulting in a better adhesion to osteoblasts. Additionally the ANG1-TIE2 bond and the activated downstream pathway inhibits stem cell proliferation and keeps the cells in a resting status *in vitro* and *in vivo* [Fleming *et al.* 1993; Spangrude *et al.* 1990; Arai *et al.* 2004; Cheng *et al.* 2000]. Many other significant interactions between both cell types have been described in the last years. For example one important observation was that a depletion of osteoblasts leads to a reduction of the HSC number and interestingly, this effect has been shown to be reversible [Visnjic *et al.* 2001; Visnjic *et al.* 2004]. This finding underlines the crucial influence of osteoblasts on hematopoietic stem cell regulation and the importance of their close interactions. Very recently it has been demonstrated that mesenchymal stem cells (MSCs) expressing high levels of nestin are an indispensable part of the stem cell niche. This study demonstrated that hematopoietic stem cells, after transplantation into lethally irradiated recipients, migrate into distinct areas close to MSCs whereas the depletion of nestin positive MSCs clearly diminishes the number of homing HSCs.

Moreover, MSCs express high levels of SDF-1 which is supposed to be the main anchor that attach HSCs to the bone marrow by binding to CXCR4. These data imply a new kind of stem cell niche in which two different stem cell types interact very closely [Mendez-Ferrer *et al.* 2010].

2.2.3 Aging of hematopoietic stem cells

By comparing stem cells from young and old organisms a big difference in cell activity can be observed. These differences are not induced by the microenvironment in the niche but they are stem cell specific [Geiger *et al.* 2002; Geiger *et al.* 2005; Rossi *et al.* 2005]. As stem cells are responsible for the maintenance and renewal of all tissues it is assumed that the development of the individual's aging process is related to an impaired activity of old stem cells. During their own aging they seem to loose their regenerative tissue repair activity and in addition their ability to react to replicative and oxidative stress. These facts limit the normal life-span of every organism [Geiger *et al.* 2002; van Zant *et al.* 2003; Sharpless *et al.* 2004; Torella *et al.* 2004].

By FACS analysis [Morrison *et al.* 1996; Sudo *et al.* 2000] and *in vitro* experiments [de Haan *et al.* 1999] it has been clearly shown, that the number of stem cells in old mice is several-fold increased compared to young animals. This finding suggests that not the number of cells is critical for aging but the quality of their action. A proof for this hypothesis are experiments which have shown that hematopoietic stem cells from old animals contributed just half as good to hematopoiesis in irradiated hosts than stem cells from young mice did [Morrison *et al.* 1996; Chen *et al.* 2000]. Moreover, also their homing ability is impaired after transplantation [Liang *et al.* 2005] and they show a reduced capacity of self-renewal as well as an increased apoptosis rate [Janzen *et al.* 2006]. Another difference between young and aged stem cells seems to be their adhesion to stromal cells within their niche which in turn could also influence their homing capacity. At least it was shown that an impaired adhesion can lead to elevated cell mobilization [Papayannopoulou 2004; Semerad *et al.* 2005b; Thomas *et al.* 2002]. As Xing *et al.* found that old mice release more stem cells into the peripheral blood after G-CSF treatment than young mice [Xing *et al.* 2006] one could speculate that their interaction with stroma cells is somehow modified, leading to a facilitated detachment from stromal cells. In this context it is also not a big surprise that the aging of stem cells is accompa-

nied by dramatic changes in the expression of different adhesion molecules like VLA4 or VCAM1 which are expressed much less in old cells whereas the expression of the adhesion molecule P-selectin and the α6 integrin is elevated in them [Xing *et al.* 2006; Rossi *et al.* 2005].

2.3 The mammalian immune system

Every second living creatures are in danger of infections for example through bacteria or a viral disease and for that reason all organisms need to protect themselves against external, harmful influences to ensure their survival in the natural environment. During the last millions of years a complex system with distinct mechanisms has developed that is able to protect the organism from diseases very efficiently.

The first line of defense against pathogens that induce disease to the host organism is displayed by physical barriers like skin or mucosa. If pathogens get over the physical barriers and start to proliferate within the body, other cellular mechanisms are needed to recognize and clear the infection. Therefore the immune system has evolved in a way that two major arms of immunity were established: the innate and the adaptive immune system [Murphy K *et al.* 2008]. The cells of innate immunity provide the first defense against microorganisms or toxins that successfully enter an organism and the following cell types are involved in these immunological responses: Phagocytes, including macrophages, neutrophils, dendritic cells as well as mast cells, eosinophils, basophils and natural killer cells which have different other opportunities to kill pathogens. Their responses are usually triggered when the microbes are identified by pattern recognition receptors (PRR) which detect components that are conserved on a broad spectrum of microorganisms. Alternatively also injured or stressed cells are able to send out alert signals when they are damaged and many of these are recognized by the same receptors as those that recognize pathogens [McDonald *et al.* 2010]. In most cases macrophages are the first cells which get in contact with invading pathogens. They continuously mature from circulating monocytes and leave the blood vessels to invade all body tissues. The recognition of pathogens by the macrophage's surface receptors leads to a fast phagocytosis of the invaders. Moreover, this process leads to a secretion of biologically active proteins like cytokines or chemokines (view 2.5). These proteins recruit another very important cell type of the innate immune system to the site of

inflammation, the neutrophil granulocyte, which can then unfold its full antimicrobial repertoire (view 2.4). Innate immune defenses are non-specific, meaning these systems respond to pathogens in a vey general way and they are also not able to build up a distinct protective mechanism against any re-infection. However, the innate immune system removes the majority of invading microorganisms fast and effectively through mechanisms like phagocytosis. This way of action prevents the establishment of more severe infections [Murphy K *et al.* 2008].

While innate immunity fights to remove an infection the adaptive immunity displays the next line of immune responses. The unique ability of the adaptive immunity is to recognize pathogens specifically and build up an immunological memory that provides a stronger protection against a re-infection. It is induced, when an immature dendritic cell (DC) recognizes and phagocytoses a pathogen. Thereby, the DC gets activated and migrates to the closest draining lymph node, where it presents specific antigens of the pathogen to naive lymphocytes, mainly T cells. As a result these cells differentiate into effector cells and react with strong proliferation to produce a high number of them [Murphy K *et al.* 2008].

Different types of T effector cells are known so far. On the one hand cytotoxic T cells (CTLs) are characterized by expression of the cell surface marker CD8. The immunological role of CTLs is to eliminate infected or abnormal somatic cells directly. The recognition of these cells is mediated by presentation of pathogenic or tumor protein residues (peptides) in specific membrane bound glycoproteins, the major histocompatibility complex (MHC) class 1. Upon recognition of the somatic target cells by CTLs the effectors release the cytotoxins perforin, granzymes and granulysin thereby inducing the cell death cascade apoptosis of the pathogen [Russell *et al.* 2002]. They can also induce apoptosis in the target cell by triggering the apoptosis receptor FAS via the FAS-ligand (CD95 ligand) [Ju *et al.* 1995; Kagi *et al.* 1994]. The second type of T cells expresses the co-receptor CD4 on its surface and it is known as T helper cell (T_H-cell). Their main role is to mediate the activity of other cell types, during an ongoing innate or adaptive immune response. In contrast to cytotoxic T cells, they are activated by recognition of a foreign peptide which is presented by a MHC molecule of class 2. T_H-cells can be divided into different functional different sub-types. T_H1-cells play an important role in the abatement of intracellular bacterial infections which mainly reside in vesicles of macrophages, like the *Mycobacterium tubercolosis* causing tuberculosis infections. In

this setting T_H1-cells induce the fusion of vesicles with the lysosomes of macrophages, which contain antimicrobial enzymes and substances that kill the bacteria. Moreover, they release cytokines which recruit cells of the innate arm of immunity to the site of infection. For the fight against extracellular pathogens T_H2-cells are indispensable. After specific contact to an external antigen and activation by a T_H2-cell, B cells differentiate into an effector-cell type called plasma cell. Their main function is to release specific antibodies which recognize foreign pathogenic antigens. One function of these agents is to bind and neutralize epitopes on the particular target which are crucial for their harmful activity. Moreover, pathogens are marked by antibodies to facilitate their recognition by phagocytes (opsonization) [Murphy K *et al.* 2008].

Recently, an additional subset of T helper cells was identified and named as T_H17-cell because of their IL-17 production [Harrington *et al.* 2005; Park *et al.* 2005]. They are a subset of CD4-positive T cells and are involved in many T cell mediated autoimmune diseases like experimental autoimmune encephalomyelitis (EAE) demonstrated in IL-17 deficient animals which develop a milder form of EAE [Nakae *et al.* 2003].

Besides that, another special group of T cells is known which can be characterized by the production of the transcription factor forkhead box protein 3 (FOXP3). The function of these T regulatory cells (Tregs) is to arrange for the tolerance of self-antigens by suppressing overreactions of the adaptive immune system to prevent the establishment of autoimmune diseases. For that they can e.g. release the immunosuppressive cytokines IL-10 and the transforming growth factor TGF-β. The deletion of Tregs leads to increased immune reactions against the own organism or for example against transplanted tissue [Murphy K *et al.* 2008].

After clearance of an infection most T effector cells undergo apoptosis except for a small population that subsequently forms memory cells. In case of a re-infection they can induce a much stronger and faster immune response against the specific antigen. This behavior builds the basis for all vaccinations [Murphy K *et al.* 2008].

2.4 Role of neutrophil granulocytes in the immune response

In addition to macrophages, neutrophils display the second major group of phagocytes in mammalians. Typical und unique for neutrophils is their characteristically formed nucleus which is, depending on the cell maturation status, divided into 2-5 lobes. This feature is responsible for the name of the cell family neutrophils belong to together with basophils and eosinophils: the polymorphonuclear cells or PMNs. In human beings, neutrophils are the most abundant white blood cells. They constitute around 70 % of all leukocytes [Murphy K *et al.* 2008] and have a very short life period, meaning that they undergo apoptosis after only 6 h in circulation independent of whether they have encountered a pathogen or not [Hoebe *et al.* 2004].

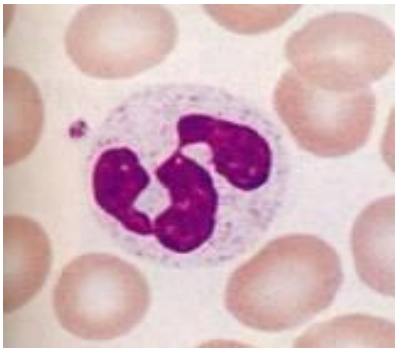

Figure 6 Neutrophil granulocyte. Wright Giemsa staining of blood smear. Neutrophils can be easily identified by their characteristic segmented nucleus.

source: http://www.oncolink.org/coping/images/neutrophil.jpg

Neutrophils have three different strategies to directly attack microorganisms. The first is phagocytosis,which involves the engulfment and elimination of pathogens in specialized phagolysosomal compartments. Secondly, neutrophils can release soluble antimicrobial molecules from their granules in close vicinity to the infection in a process called degranulation. The generation of neutrophil extracellular traps (NETs) is the third defense mechanism. In a just recently discovered cell death mechanism they release nuclear contents, composed of decondensed chromatin decorated with granula as well as with cytoplasmic proteins into the extracellular space. These structures trap various microbes and can kill them by high local concentrations of antimicrobial components [Bruns *et al.* 2010; Brinkmann *et al.* 2004; Brinkmann *et al.* 2007].

The major neutrophil population resides in the bone marrow of long bones but a small percentage always circulates with the blood flow to reach infected tissue very quickly. In cases of an infection the circulating PMNs are attracted inside the blood vessels to the emergency area and migrate from the blood flow into the inflamed tissue. This step is called extravasation.

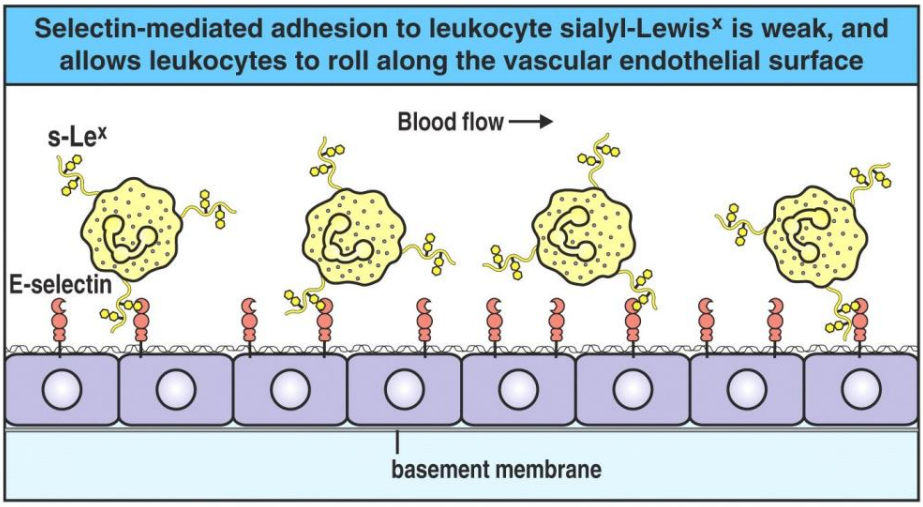

Figure 7 Neutrophil adhesion and rolling on the vascular endothelium. Reversible binding of neutrophils through selectins on the endothelium and its receptor sialyl-Lewis^x moiety (s-Le^x) located on the neutrophil surface induce a slowdown of neutrophils in the circulation. This results in a rolling of the cells on the endosteal surface and allows the forming of stronger bindings.

source: http://0-www.ncbi.nlm.nih.gov.www.elgar.govt.nz/bookshelf/br.fcgi?book=imm&part=A203

In the first step of this process TNFα stimulates the endothelial cells lining blood vessels to express the surface adhesion molecule P-selectin. Within a couple of hours a second surface adhesion molecule E-selectin is produced. Together, E- and P-selectin slow down the speed of leukocytes through the bloodstream by inducing their rolling along the endothelium via s-Le^x structures on the surface of the granulocyte [Murphy K *et al.* 2008].

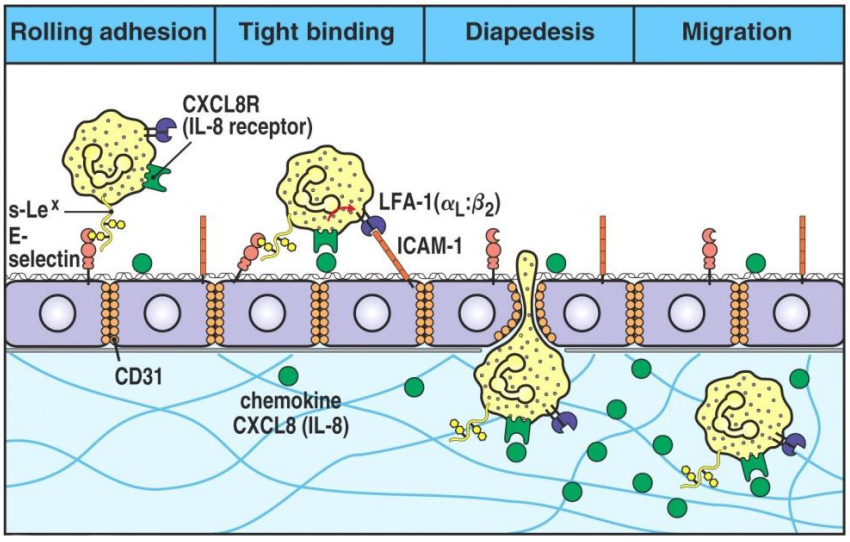

Figure 8 Neutrophil migration through the vascular endothelium into infected tissue. After rolling adhesion neutrophils form stronger bindings to ICAM-1 on the vascular endothelium through

their receptor LFA-1 that gets activated by contact with the chemokine IL-8. This adhesion completely stops the neutrophils and allows the migration through the vascular endothelium (extravasation) towards chemoattractants.

source: http://0-www.ncbi.nlm.nih.gov.www.elgar.govt.nz/bookshelf/br.fcgi?book=imm&part=A203

That allows other molecules to interact with the slowed leukocytes to stop them and promote their movement into the tissues. E- and P-selectin expression can also be stimulated by interleukin-1 (IL-1) and lipopolysaccharide (LPS) [Leeuwenberg *et al.* 1992]. Leukocyte rolling occurs due to the brief, reversible binding of E- and P-selectin with their complementary molecules, which are expressed on the surface of passing neutrophils. Tight adhesion to the rolling leukocyte is mediated by another molecule, the intercellular adhesion molecule 1 (ICAM- 1) whose expression is also induced by TNFα. ICAM-1 binds to both integrins LFA-1 and Mac-1 on the surface of neutrophils and arrests the motion of the rolling leukocytes by strong adhesion to the endothelium. After stopping, the leukocyte is able to enter the tissues by secreting proteases to breach the endothelial basement membrane, a process known as diapedesis. Again, the integrins LFA-1 and Mac-1 play a major role in this process, as well as adhesive interactions with the molecule PECAM (CD31). This protein is expressed on neutrophils and epithelial cells and the interaction allows the invasion of leukocytes through the endothelial cell layer [Murphy K *et al.* 2008]. The driving signal for the influx of PMNs comes from a pro-inflammatory chemokine gradient, which is for example built up by Il-8, which in turn is released by macrophages after contact to a pathogen [Baggiolini *et al.* 1994; Holmes *et al.* 1991; Strieter *et al.* 1992; Terashima *et al.* 1998].

2.5 Chemokines

Chemokines are a subclass of cytokines which mainly act as chemoattractants for leukocytes. They activate different phagocytic leukocytes upon binding to G protein-coupled seven-transmembrane receptors [Murphy 1994] thereby guiding immune cells straight and fast to the site of infection in order to ensure an efficient host defense against invading pathogens. All chemokines are relatively small molecules with a molecular mass between 6 and 14 kD and a homology of 20-50 % to each other [Le *et al.* 2004].

A great variety of cell types can produce chemokines. Some are permanently re-

leased under homeostatic conditions, for example to regulate the constant migration of leukocytes or dendritic cells. Others are released in response to an inflammatory stimulus [Murphy K *et al.* 2008].

Until now over 50 mammalian chemokines and 19 different corresponding chemokine receptors have been cloned and molecularly characterized [Murphy *et al.* 2000; Horuk 2001]. Based on their structural characteristics chemokines can be classified in four different groups [Murdoch *et al.* 2000] representing similar spatial arrangements of the first two, closely paired cysteine residues of the particular chemokine ("C chemokines", "CC chemokines", "CXC chemokines" and "CX3C chemokine"). The chemokine receptor families are equally termed according to the group of chemokines they bind. Among these reside six "CXC receptors" (CXCR1-6), eleven "CC receptors" (CCR1-11), one "CX3C" (CX3CR1) and one "C receptor" (XCR1) [Le *et al.* 2004].

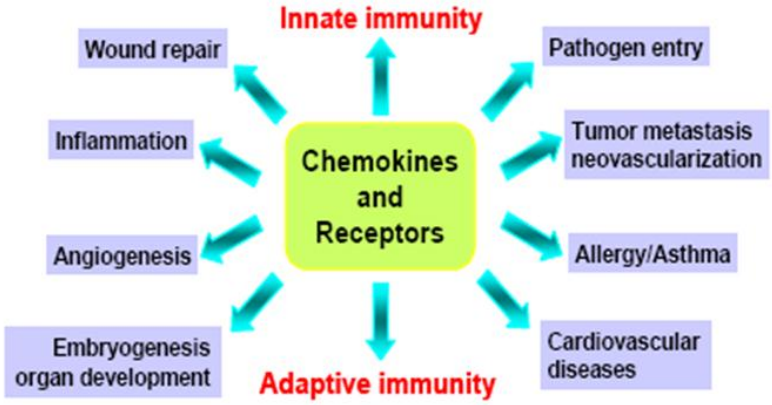

Figure 9 Overview over the multiple roles of chemokines. Chemokines and their receptors play an important role in many different situations, under homeostatic as well as inflammation conditions [Le *et al.* 2004].

The subgroup of "CC chemokines" is characterized by two adjacent cysteines close to their amino terminus. They are also called "CC chemokine ligands" (CCL) and bind to CC chemokine receptors. This group mainly induces the migration of monocytes and other cell types such as NK cells or dendritic cells [Murphy K *et al.* 2008]. The two N-terminal cysteines of "CXC chemokines" are separated by one additional amino acid. They can be divided into two different sub-groups: Those with a specific tripeptide structure motif of glutamic acid-leucine-arginine (ELR) located in front of the first cysteine of the CXC motif (designated as ELR-positive) and those without an ELR motif (ELR-negative) [Murphy *et al.* 2000]. ELR-positive "CXC chemokines" like interleukin-8 (IL-8), specifically mediate the migration of neutrophils and interact with the chemokine receptors CXCR1 and CXCR2. IL-8 is the human analogue for the murine chemokines keratinocyte chemoattractant (KC) and macrophage inflammatory protein-2 (MIP-2), which are all stimulators of

neutrophils to leave the bloodstream and enter the surrounding tissue [Murphy K *et al.* 2008]. In contrast, ELR-negative chemokines tend to be chemo attractive for lymphocytes.

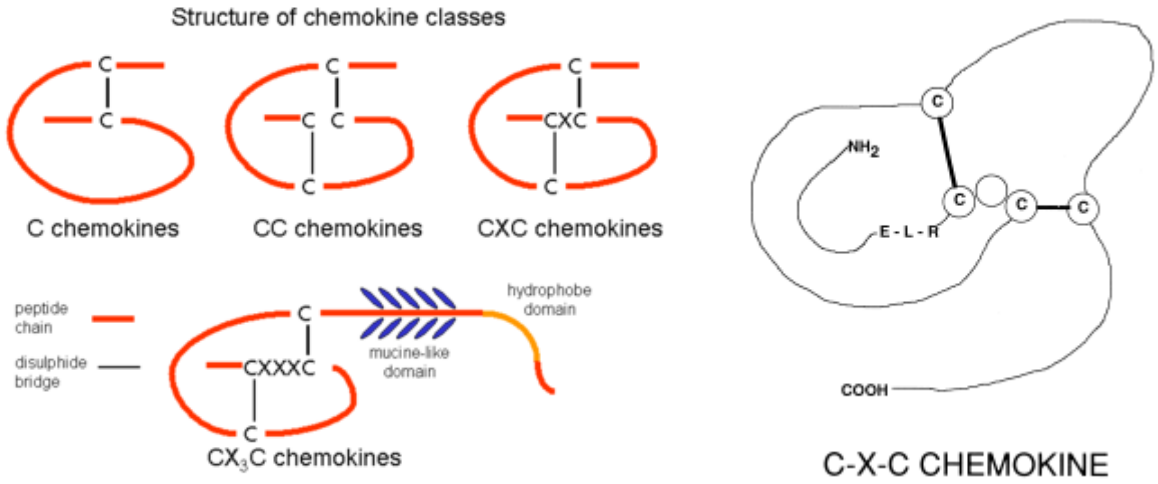

Figure 10 Structure of chemokine classes. Chemokines are distributed into four sub-groups, characterized by the first two cysteine residues. CXC chemokines can be divided in two subgroups, those with a specific tripeptide structure motif of glutamic acid-leucine-arginine (ELR) in front of the first cysteine and those without such a motif.

source left: http://www.absoluteastronomy.com/topics/Chemotaxis
source right: http://journals.prous.com/journals/dnp/19991201/html/dn120005/images/Coll1.gif

Additionally, two more small groups of chemokines have been described so far. One is the termed “C chemokines” family which is characterized by one N-terminal cysteine and another almost C-terminally located one. Just two chemokines have been described in this sub-group, XCL1 (lymphotactin-α) and XCL2 (lymphotactin-ß) which both attract T-cell precursors to the thymus. The only “CX3C chemokine” discovered until now, the fractalkine, displays the fourth group of chemokines. According to the other groups, three amino acids are located between both cysteines (CX3CL1). This chemokine has an interesting property as it is membrane bound and acts both as a chemoattractant as well as an adhesion molecule [Murphy K *et al.* 2008].

By examining the interaction of chemokines to their receptors, big differences can be observed. In some cases, chemokines can bind to only one specific receptor and vice versa it is also very common, that one certain receptor is just able to bind one specific, single chemokine, like the interaction of CXCR4 with CXCL12 (SDF-

1) by which resting neutrophils are kept inside the BM cavities. However, there are also many other examples, where chemokines interact with more than one single receptor or receptors, that can bind different chemokines. For instance the chemokine CCL7 that can bind to CCR1, 2 and 3 or the receptor CXCR1 which is able to bind the chemokines CXCL 2, 3, 5, 6, 7 and 8 [Le *et al.* 2004].

As mentioned earlier inflammatory chemokines are indispensable for guiding immune cells as response to microbial infections and agents that cause physical tissue damage. As pioneer cells different leukocytes build up a chemokine gradient along the tissues and blood stream, so that immunocytes can orientate themselves at the increasing concentration of chemokines that guide them directly to the invading pathogens. Their release is often stimulated by pro-inflammatory cytokines such as IL-1 [Le *et al.* 2004].

Besides that, chemokines are involved in various other incidents. Notably, some chemokines are also known for their roles in cell and tissue development, for example in vascularization or cerebellar development [Tachibana *et al.* 1998; Zou *et al.* 1998]. Moreover, they are able to promote angiogenesis [Strieter *et al.* 1992; Koch *et al.* 1992], play multiple roles in tumor growth [Wang *et al.* 1998; Murphy 2001] and are also involved in different autoimmune diseases like asthma or multiple sclerosis [Murdoch *et al.* 2000]. However, each single chemokine and receptor has a special position in the complex network of immune response and homeostasis to recruit almost every different cell type to the place, where it is needed.

2.6 G-CSF

The glycoprotein granulocyte colony-stimulating factor (G-CSF) is essential for many processes that are involved in neutrophil or stem cell homeostasis.

An adult of average size produces approximately 120 million granulocytes per day, simply to replace the loss of short living neutrophils. This enormous production can be increased at least 10-fold under stress conditions and G-CSF is likely to play an important role in the basal regulation of neutrophil production as well as a primary regulatory factor controlling the neutrophil response to inflammatory stimuli. After its discovery (murine: 1980 [Burgess *et al.* 1980]; human: 1986 [Souza *et al.* 1986; Nagata *et al.* 1986c]) and further characterization, the enormous potential of G-CSF for clinical applications was assessed very fast. In phase 1 clinical trials with cancer patients G-CSF was shown to be a potent well tolerated agent that could

increase the number of circulating neutrophils in a dose dependent manner [Morstyn *et al.* 1988; Gabrilove *et al.* 1988a; Gabrilove *et al.* 1988b]. For that reason, G-CSF was recommended for approval in December 1990 by an advisory panel of the United States Food and Drug Administration (FDA) for commercial use in cancer chemotherapy. This has led to the final approval of this molecule in February 1991 [Demetri *et al.* 1991]. Since this time G-CSF is heavily used in cancer patients to refill the neutrophil population very fast after chemotherapy. Administration of G-CSF after cytotoxic chemotherapy was associated with significant reductions in the duration of severe neutropenia and correspondently the incidence of fever and hospitalizations with neutropenia and moreover the requirement for antibiotics strongly declined [Crawford *et al.* 1991]. Besides the mobilization of neutrophils from the BM into the blood G-CSF has been shown to activate the production of neutrophil granulocytes and it also stimulates their survival, proliferation, differentiation, and function [von Vietinghoff *et al.* 2008; Metcalf 2008].

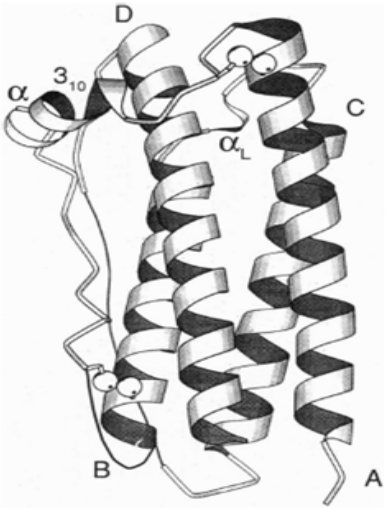

Figure 11 Chrystal structure of recombinant human G-CSF. It consists of four main bundle helices termed A, B, C and D. [Hill *et al.* 1993b]

Interestingly this soluble mediator has not only effects on neutrophils but also on HPCs. It directly influences the production of the progenitors and moreover it appears to modulate the distribution of neutrophil and progenitor cells within the organism [Demetri *et al.* 1991]. With such a potential G-CSF is also intensively used in the clinics for the mobilization of hematopoietic stem cells into peripheral blood. In the past it was common for bone marrow transplantations that HSC were isolated from a big bone of the donor, typically the pelvis, through a needle that reaches the centre of the bone. This technique is referred to as bone marrow harvest and is performed under general anesthesia. With the availability of the stem cell growth factor G-CSF, most hematopoietic stem cell transplantation procedures are now performed using stem cells collected from the peripheral blood, rather than directly from the bone marrow. Collecting peripheral blood stem cells provides a bigger graft, does not require a general anesthesia to collect the graft and results in a shorter time to engraftment [Cutler *et al.* 2001].

The mobilization of HPCs from their reservoir in the bone marrow into the circulation is mediated by G-CSF but interestingly it could be shown, that G-CSF cannot act directly on the hematopoietic progenitor cells, because they do not express the G-CSF receptor [Thomas *et al.* 2002]. Moreover, although mature neutrophils do express the receptor for G-CSF [Avalos 1996], conflicting data are reported regarding to the direct role of G-CSF in recruiting neutrophils [Knapp *et al.* 2004] [Witowski *et al.* 2007]. How G-CSF acts on single cells *in vivo* in their natural environment of long bones marrow, as well as the underlying mechanism of cell mobilization are completely unknown.

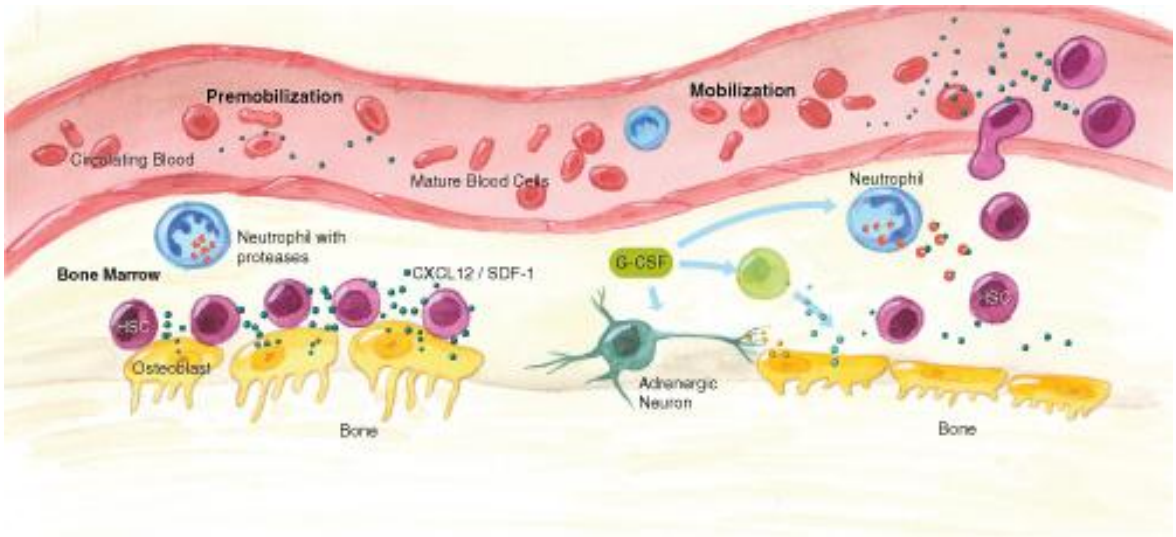

Figure 12 Neutrophil mobilization from bone marrow by G-CSF. Neutrophils are attached in the bone marrow by expression of CXCR4 that binds to SDF-1. SDF-1 is strongly expressed by endosteal cells, mainly osteoblasts, in the bone marrow. G-CSF release induces neutrophil proteases that cleave the SDF-1 CXCR4 binding and neutrophils are mobilized into the peripheral blood flow.

source: http://www.rndsystems.com/dam_public/5827.jpg

As G-CSF is so indispensable for the functionality of neutrophils and therefore for a crucial part of the innate immunity, it is produced by a variety of different cells, e.g. vascular endothelial cells [Zsebo *et al.* 1988], fibroblasts [Koeffler *et al.* 1987] and mesothelial cells [Demetri *et al.* 1989]. Also T_H17-cells are able to produce G-CSF. In response to an infection they leave the lymph node and migrate to the inflamed tissue, where they recruit neutrophils to the distinct place by releasing G-CSF [Murphy K *et al.* 2008]. Nevertheless, the most important source of G-CSF is provided by cells of the monocyte/macrophage lineage [Demetri *et al.* 1991]. The

natural occurring human G-CSF exists in two forms, as 174 aa- and as 180 aa-long protein [Hill *et al.* 1993a], whereas the more abundant and more active 174 aa form has been used for the development of pharmaceutical products by recombinant DNA technology. Human G-CSF is encoded by a single gene [Nagata *et al.* 1986a; Nagata *et al.* 1986c] that is located on chromosome 17 [Le Beau *et al.* 1987; Simmers *et al.* 1987]. Two different polypeptides are synthesized from the same gene by differential splicing of mRNA, in one form is shortened by three amino acids but both display the same G-CSF activity [Nagata *et al.* 1986b]. The murine G-CSF is located on chromosome 11 in a region that is homologous to the human chromosome 17 [Demetri *et al.* 1991]. Compared to the human G-CSF, the murine form is very similar [Tsuchiya *et al.* 1986]. The production of G-CSF can be induced *in vitro* by a variety of stimulatory agents, including LPS [Ernst *et al.* 1989; Vellenga *et al.* 1988], TNF-α [Koeffler *et al.* 1987], IL-1 [Zsebo *et al.* 1988; Fibbe *et al.* 1988], TPA [Koeffler *et al.* 1988; Demetri *et al.* 1989], GM-CSF [Vellenga *et al.* 1988; Oster *et al.* 1989], IL-3 [Oster *et al.* 1989], IL-4 [Wieser *et al.* 1989] and IFN-γ [Herrmann *et al.* 1986].

2.7 Megakaryocytes and Thrombopoietin

Megakaryocytes are produced by megakaryoblasts and they are mainly located in the bone marrow. With a diameter of 35-150 µm they are the biggest cell type in this compartment. Normally, just a relatively small number resides in the bone marrow, but in cases of an infection the number can rapidly increase more than 10-fold [Branehog *et al.* 1975]. These cells are characterized by many cell nuclei which posses a 16-fold set of chromosomes and their main function is to produce platelets. This is a thrombopoietin (TPO; see below) regulated process, triggered by the fusion of intracellular membranes leads to a constriction of single platelets and takes place in the Golgi-apparatus. Megakaryocytes can release between 500-5000 platelets and after this cell disrupting event the remaining nucleus is removed by macrophages [Junquiera *et al.* 2005]. Recently it was demonstrated that megakaryocytes release pro-platelets by extending cell elongations into micro vessels in the bone marrow. In these intravascular compartments pro-platelets are abrupted by shearing forces of the blood flow [Junt *et al.* 2007].

TPO, the main trigger for megakaryocyte synthesis is produced in several organs, like the liver or the kidney induced by interleukin 6 (IL-6), but also from stromal cells in the bone marrow [Kaushansky 2006]. Although TPO is very important for megakaryocyte production it was shown, that TPO is not the only stimulus for the so called megakaryocytopoiesis [Bunting *et al.* 1997]. Other molecules that are involved in this activity are GM-CSF, IL-3, IL-6, IL-11, the chemokines SDF-1 and FGF-4 [Avecilla *et al.* 2004] and erythropoietin (EPO) [Deutsch *et al.* 2006]. Nevertheless, TPO is also absolutely essential for the formation of platelets which was clearly demonstrated in transgenic mice lacking TPO or the TPO receptor (Mpl). Although in these animals the platelets look normal in morphology and are able to function properly, the number of circulating platelets in the animals is remarkably reduced by about 90 % [Murone *et al.* 1998].

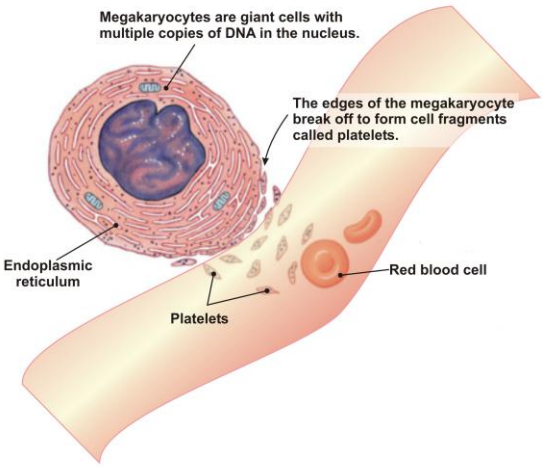

Figure 13 Platelet production by megakaryocytes. Megakaryocytes release platelets directly into the blood flow. Single platelets are constricted through the formation of new membranes by a process that is triggered by thrombopoietin.

adapted from http://www.rndsystems.com/cb_detail_objectname_sp06_hspc.aspx

2.8 Neutrophil mobilization

The regulation of circulating neutrophil numbers and their localization inside the body are extremely critical parameters for efficient innate immune responses. It is absolutely essential, that neutrophils are able to reach all tissues of an organism very fast to immediately display their antimicrobial actions thereby preventing the local settlement and, furthermore the systemic dissemination of pathogens. Besides constituting a huge storage for resting neutrophils, bone marrow plays a central role in the regulation of their release into the blood stream under at least two different circumstances: on the one hand the homeostatic release of mature neutrophils that patrol through the blood in search of potential pathogens and on the other hand the emergency release of neutrophils in response to an acute inflammatory signal. The complex mechanisms of neutrophil release remain very unclear

at present. A variety of chemotactic factors, like the leukotriene B4, C5a and the chemokine interleukin (IL)-8, have been shown to induce a rapid blood neutrophilia after i.v. injection into rabbits or mice. It is possible that such factors are able to build up a chemotactic gradient across the sinusoidal endothelium which guides neutrophils from the bone marrow into the blood stream and further directly to the infected tissue [Jagels *et al.* 1992; Jagels *et al.* 1995; Terashima *et al.* 1998].

As noted earlier, peripheral blood neutrophil counts can increase rapidly in response to an infection or other stress triggers. Although, the downstream signals that regulate this response are mainly undefined, recent reports suggest that CXCR4 may play an important role in this context. CXCR4 is expressed by neutrophils as well as by many other hematopoietic cells and its ligand, SDF-1 (CXCL12), is constitutively expressed at high levels in the bone marrow stroma [Suratt *et al.* 2004] or in nestin positive MSCs [Mendez-Ferrer *et al.* 2010]. If individuals are treated with G-CSF this results in a decrease of SDF-1 expression in the bone marrow and in the down-regulation of CXCR4 expression on neutrophils [Kim *et al.* 2006; Semerad *et al.* 2002; Semerad *et al.* 2005a; Levesque *et al.* 2003a]. This observation suggests the hypothesis that disruption of the CXCR4-SDF-1 bond might play a key step in mediating neutrophil release by G-CSF. Furthermore, animals in which either SDF-1 or CXCR4 has been knocked out show a massive spreading of immature myeloid progenitor cells into the blood circulation [Ma *et al.* 1998] and additionally, a treatment of individuals with AMD3100, a selective antagonist for CXCR4 leads to the development of peripheral neutrophilia in both mice and men [Hendrix *et al.* 2000], further supporting that CXCR4 is a crucial mediator of neutrophil mobilization. The same effect was observed by administration of CXCR4-blocking antibodies [Liles *et al.* 2003; Broxmeyer *et al.* 2005; Suratt *et al.* 2004]. A recent work has demonstrated that SDF-1 and CXCR4 also play a key role in controlling neutrophil homeostasis [Link 2005].

Yet, the mechanisms by which CXCR4 signaling leads to migration of neutrophils towards the bone marrow venous sinuses and into the circulation in response to treatment with G-CSF are not well defined. Based on their well-characterized role in other aspects of neutrophil biology, like in various infection models [Murphy 1997], it was recently hypothesized that G-CSF may trigger ELR+ CXC chemokines to induce neutrophil migration into the bone marrow vascular space, by acting contrary to the CXCR4/CXCL12 axis [Eash *et al.* 2010]. Thereby, the ELR+

CXC chemokines KC and MIP-2 seemed to be the major inducer of neutrophil migration and both are strongly expressed in infected tissues [Safirstein *et al.* 1991; Huang *et al.* 1992; Bozic *et al.* 1995; Rovai *et al.* 1998; Fahey, III *et al.* 1990]. They can be characterized by their specific influence on neutrophils and they are able to signal through CXCR1 and CXCR2 [Eash *et al.* 2010]. Furthermore, ELR+ chemokines are known to be potent neutrophil chemoattractants and activators in cases of exogenous administration [Burdon *et al.* 2005; Laterveer *et al.* 1995; Opdenakker *et al.* 1998; King *et al.* 2001; Burdon *et al.* 2008]. Like many genes of chemokines, the gene expression of KC and MIP-2 is inducible in multiple different cell types and in response to a variety of proinflammatory stimuli [Rovai *et al.* 1998; Sherry *et al.* 1992; Ohmori *et al.* 1994b; Ohmori *et al.* 1994a]. Moreover, both chemokines are known to be expressed in a great variety of acute and chronic inflammatory situations. They seem to be the essential activators of the occurring immune response, which controls the kind and also the extent of the resulting inflammation [Safirstein *et al.* 1991; Huang *et al.* 1992; Rovai *et al.* 1998; Fahey, III *et al.* 1990; Dilulio *et al.* 1999; Kielian *et al.* 2001; Miura *et al.* 2001].

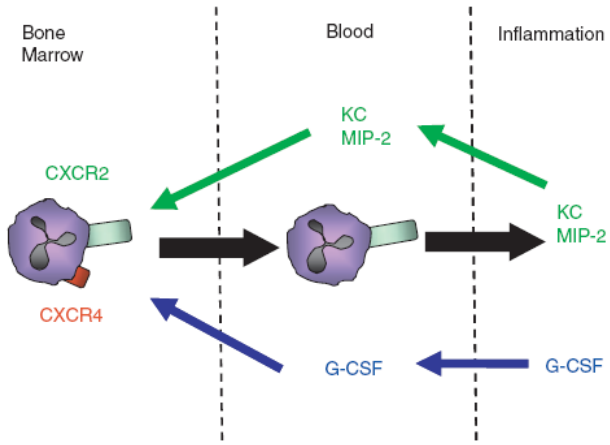

Figure 14 G-CSF and the both chemokines KC and MIP-2 act together to mobilize neutrophils from the bone marrow into the circulation. G-CSF reduces the expression of CXCR4 on neutrophils which results in a diminished adhesion of neutrophils to the bone marrow via SDF-1. The chemokines KC and MIP-2 act on the CXCR2 receptor on neutrophils and guide the cells out of the bone marrow to the side of infection by building up a chemokine gradient [Furze *et al.* 2008].

KC (CXCL1) and MIP-2 (CXCL2) are both ligands of the receptor CXCR2 and are constitutively expressed in bone marrow endothelium. Interestingly also MIP-2 expression in endothelial cells is increased during G-CSF–induced neutrophil mobilization [Eash *et al.* 2010].

It was shown that G-CSF and the chemokines KC and MIP-2 act together to mobilize and recruit neutrophils to infected tissue. In this concept, G-CSF down-

regulates the expression of CXCR4 on neutrophils, which leads to a reduced retention of the cells via the CXCR4/SDF-1 axis [Wengner *et al.* 2008]. In a very recent study a important role of CXCR2 was spotlighted besides the known significance of CXCR4 during G-CSF mobilization [Eash *et al.* 2010]. By the using CXCR2-/- mixed bone marrow chimeras an extended model to explain neutrophil mobilization from the bone marrow was established. Interestingly it could be shown that CXCR2 and CXCR4 act antagonistically to regulate neutrophil release. Moreover it was demonstrated that under basal conditions more chemokines are produced which are responsible for neutrophil adhesion, preferentially CXCL12, whereas under stress conditions KC and MIP-2 are heavily produced to exceed the level of retention signals and to direct a high number of neutrophils into the circulation. But this was only shown during long term experiments, where mice were treated with G-CSF repetitively over seven days [Eash *et al.* 2010].

2.9 Intravital 2-photon microscopy

In the last years 2-photon microscopy became a heavily used technique to clarify open questions in the field of immunology. Despite multiple possibilities to analyze immune cell motility and interactions *in vitro* the most relevant method to analyze this behavior is to directly observe cells in their natural environment in different organs and tissue. The idea of intravital microscopy came up in the nineteen's century, but multi-photon microscopy is a relatively recent approach [Williams B.Swaim 2010]. It is based on a concept of Maria Göppert-Mayer [Göppert-Mayer M. 1931] and was finally developed from Winfried Denk in 1990 [Denk *et al.* 1990]. The concept of this special microscopy technique is based on a long wavelength excitation that allows a deep tissue penetration. For that, a phenomenon is used which is called optical window. It describes the wavelengths between 800 – 1200 nm where light have the ability to penetrate tissues with the maximum depth [Tromberg *et al.* 2000].

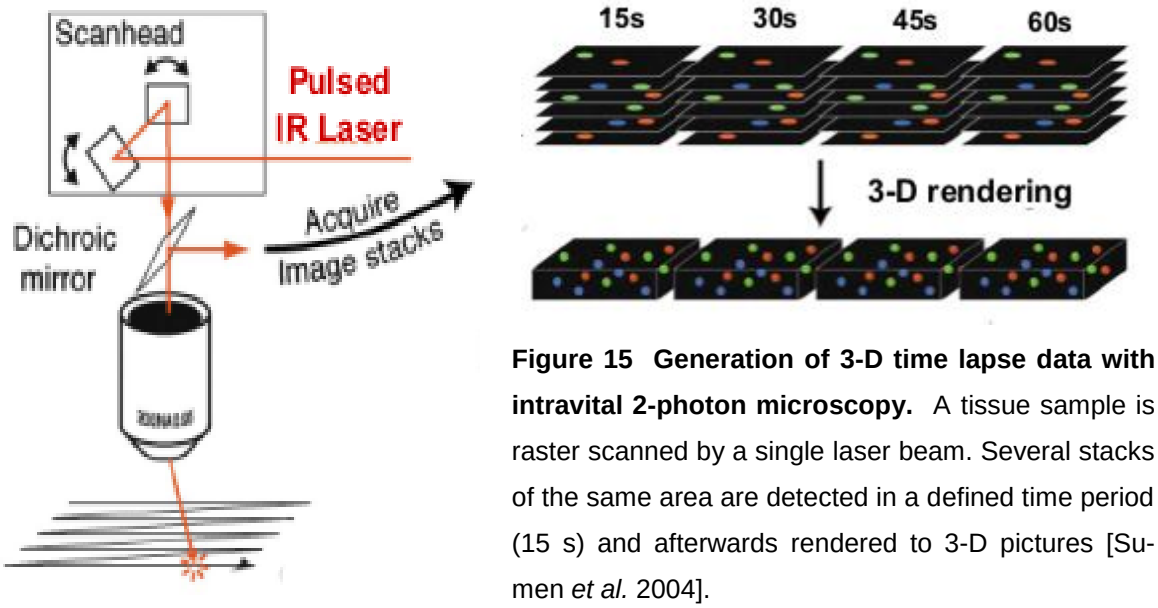

Figure 15 Generation of 3-D time lapse data with intravital 2-photon microscopy. A tissue sample is raster scanned by a single laser beam. Several stacks of the same area are detected in a defined time period (15 s) and afterwards rendered to 3-D pictures [Sumen *et al.* 2004].

Unfortunately, because of the low energy of a long wavelength one single photon is not able to excite a conventional fluorescent molecule. Two photons are needed to provide enough energy. But the probability that both photons are absorbed nearly simultaneously at the same fluorochrome is very low. To increase the possibility for such events, a femtosecond laser that pulses every 12.5 ns (80 MHz) which each pulse having a duration of just 100 fs is used generally to provide a high flux of photons. Normally, these lasers can emit a wavelength between 700 and 1000 nm [Williams B.Swaim 2010]. To increase the fluorescence the laser is limited on a beam waist of < 1 µm what results in a very compact focusing [Denk *et al.* 1990]. This leads to an excitation in only one single plane of the analyzed material. However, besides the long wavelength the extremely focused laser beam reduces photo bleaching and damage in the observed preparation which allows a relatively long microscopy period in the observed tissue [Williams B.Swaim 2010]. Additionally, besides the normal fluorescence also second harmonic generation is produced during 2-photon microscopy [P.A.Franken 1961]. This phenomenon occurs when an intense laser beam induces fluorescent radiation of the double frequency under distinct conditions, in this case during scanning special tissues like the collagen of muscles [Cox *et al.* 2003], bone [Kohler *et al.* 2009] or lung tissue [Bruns *et al.* 2010]. The wavelength of the second harmonic generation displays exactly the half wavelength of the incoming light and notably this kind of auto fluorescence does not lead to any photo bleaching. Second harmonic generation is a useful tool for a better orientation in the tissue where 2-photon microscopy is per-

formed [Friedl *et al.* 2007].

In the last years, several extremely interesting observations in the field of immunology have been made by using 2-photon microscopy. This was supported by the generation of various new fluorescent dyes for cell and tissue staining. Additionally, several transgenic mouse models were established that express fluorescent proteins under the control of distinct immune cells for example Lys-EGFP mice, that express enhanced GFP under the control of the lysosome M promoter, leading to green fluorescent neutrophils [Faust *et al.* 2000]. The tissues, mainly used for the 2-photon microscopy are the inguinal or popliteal lymph nodes and the bone marrow of the skull but in the last years with proceeding experience also other organs became feasible like the central nervous system (CNS), liver or spleen. With the unique possibility for very deep tissue penetration compared to single-photon excitation, depths of 450 µm in the lymph nodes and around 200 µm in the bone marrow can be reached. The further development of scan heads decreases the time that is needed to scan a single plane in an area observed by microscopy. This allows the acquisition of many planes in one preparation that can be rendered into 3-D stacks afterwards (Figure 15). Moreover, it is possible to detect multiple imaging stacks from the same area that enable the creation of 3-D time lapse movies [Sumen *et al.* 2004]. Different parameters can be measured within the recorded data for example cell-cell interactions or contact times between different cell types, mainly between T cells and antigen presenting cells (APCs) like dendritic cells [Mempel *et al.* 2004a] or B cells. Another possibility is to determine the interaction of cells with their environment like leukocyte adhesion to endothelial cells [Mempel *et al.* 2004c] or the interactions of hematopoietic stem cells with their niche [Mendez-Ferrer *et al.* 2010; Kohler *et al.* 2009]. Moreover, the motility and migration of cells is heavily studied. Examples are the homing and migration of T cells in the popliteal lymph note [Mempel *et al.* 2004a; von Andrian *et al.* 2003] and B cell behavior in germinal centers of lymph nodes [Hauser *et al.* 2007]. Furthermore, leukocyte migration in blood vessels and tissues [Mempel *et al.* 2004b] were analyzed.

2.10 Aim of the study

In the last years, intravital 2-photon microscopy became more and more important to answer longstanding unresolved questions in living animals. It enables the analysis of cell migration in time-lapse recordings of 3D tissue reconstructions [Cahalan *et al.* 2002].

The bone marrow supports intense traffic of blood cells in the extra vascular space and at the interface with the intravascular compartment. Also the special microenvironment provided by the bone marrow is critical for the regulation of hematopoietic cell behavior. For this reason the 2-photon microscopy is a very important approach to determine cell motility and interactions with the inner bone surface under different conditions. Unfortunately, the thickness of bone surrounding BM cavities in most anatomical locations renders these tissues inaccessible for in vivo imaging [Pannarale *et al.* 1997]. Until know there was just one model for bone marrow imaging available which visualizes the BM in the flat bones of murine skull. But for all *in vitro* studies with hematopoietic cells, these are isolated from murine long bones and also immunohistological stainings of bone marrow are performed on slices from long bones. To compare these data directly with results from 2-photon microscopy we concluded that the imaging should be performed in long bones. Moreover, it was recently shown, that skeletal progenitor cells from the calvaria are not able to form stem cell niches as efficiently as skeletal progenitor cells from fetal long bones [Chan *et al.* 2009]. For these reasons we established a completely new method for intravital 2-photon microscopy that allows the visualization of cells in the bone marrow of murine long bones.

With this new approach we first wanted to analyze the motility and localization of hematopoietic progenitor cells and early hematopoietic progenitor cells with respect to aging. Aged hematopoietic stem cells are impaired in supporting hematopoiesis and this is thought to be, at least in part, a consequence of the aging [Geiger *et al.* 2002; van Zant *et al.* 2003; Rando 2006]. Multiple cellular and molecular mechanisms have been implemented in hematopoietic stem cell aging. However, it was recently postulated that aged in contrast to young primitive hematopoietic cells present with altered, less favorable interactions with the niche, which might in part explain impaired hematopoiesis in aged individuals. This hypothesis should be clarified by intravital 2-photon microscopy, with the idea, that the reduced adhesion of HPCs and eHPCs might result in a larger distance of these cells to the

endosteal layer and maybe also in increased motility.

The second part of the study focused on neutrophil behavior after G-CSF treatment. This drug induces rapid neutrophil mobilization from the bone marrow into the circulation, but the underlying mechanisms are completely unknown. In the beginning the first view on neutrophils in the bone marrow of long bones under steady-state and G-CSF induced conditions should be realized. Afterwards the central question was how neutrophils react to G-CSF on the single-cell level directly after injection. Finally, the molecular mechanisms leading to the rapid release from bone marrow should be identified. Essentially, a detailed understanding of the role G-CSF plays in the process of neutrophil mobilization might deliver valuable new insights, how this process could be improved in neutropenic patients to further minimize their risk for different, severe infectious diseases.

3. Materials and Methods

3.1 Materials

3.1.1 Mice

Age- and sex-matched animals of 8 to 16 weeks of age were used for most experiments. Experiments with old animals were performed with mice of 20-22 months of age. They were derived from the animal barrier facility at Cincinnati Children's Hospital Medical Center (CCHMC) or obtained from aged rodent colonies of the National Institute on Aging (Harlan).

C57Bl/6 mice were purchased from Harlan Winkelmann (Borchen), Charles River (Sulzfeld) or The Jackson Laboratory and subsequently housed in the animal barrier facility at the Otto-von-Guericke University (OvGU, Magdeburg). Animals expressing an enhanced green fluorescent protein (EGFP) under the lysozyme-promoter (Lys-EGFP mice) were provided by Thomas Graf (The Albert Einstein College of Medicine, USA). Animals expressing EGFP under the fractalkine receptor CX3CR1 (CX3CR-EGFP mice) were provided by Steffen Jung (Weizmann Institute, Israel). c-mpl ko mice ($TPO^{-/-}$) were provided from Oliver Winter (Charitè Berlin). In these mice the receptor of TPO (c-mpl) is disrupted in embryonic stem cells by insertion of a neomycin resistance marker [Gurney *et al.* 1994].

All animals were housed in a specific pathogen free (SPF) environment at the CCHMC barrier facility or at the OvGU facilities.

3.1.2 Buffers and additives

- Fetal calf serum (FCS)

  FCS (Integro) was heat-inactivated for 30 minutes at 56 °C before use.

- PBS (Phosphate buffered saline)

  136.9 mM NaCl
  2.7 mM KCl
  8.1 mM $Na_2HPO_4 + 2\ H_2O$
  1.47 mM K_2HPO_4

  Dissolved in 1000 ml dist. H_2O, pH 7.4, autoclaved. PBS was used unmodified or supplemented with 1 % FCS.

- Erythrocyte lysis buffer

  0.15 mM NH_4Cl
  1 mM $KHCO_3$
  0.1 mM Na-EDTA

  Dissolved in 500 ml dist. H_2O, sterile filtered

- Iscove`s Modified Dulbecco`s Medium (IMDM)

  IMDM (Gibco) was supplemented with 2 % FCS or 10 % FCS.

- Hanks buffered salt solution (HBSS)

  HBSS (Gibco) was supplemented with 2 % FCS.

3.1.3 Antibodies and fluorescent markers

3.1.3.1 Antibodies for stem cell isolation (LIN-Cocktail)

Specificity	Source	Isotype	Clone	Final conc. in LIN cocktail
CD5 (Ly-1) Biotin	BD-Biosciences (Heidelberg, Deutschland	IgG2a, k	53-7.3	111.1 µg/ml
B220 (CD45R) Biotin	BD Biosciences	IgG2a, k	RA3-6B2	74.1 µg/ml
Mac-1 (CD11b) Biotin	BD Biosciences	IgG2b, k	M1/70	70 µg/ml
CD8a (Ly-2) Biotin	BD Biosciences	IgG2a, k	53-6.7	111.1 µg/ml
Gr-1 (Ly-6G/6C) Biotin	BD Biosciences	IgG2b, k	RB6-8C5	63.7 µg/ml
TER-119 (Ly-76) Biotin	BD Biosciences	IgG2b, k	TER-119	70 µg/ml

3.1.3.2 Antibodies for stem cell isolation (FACS)

Specificity	Source	Isotype	Clone	Final conc.
Streptavidin FITC Isotype control	BD Biosciences	--	--	6 µg/ml
Streptavidin PE Isotype control	BD Biosciences	--	--	3 µg/ml
Streptavidin APC Isotype control	BD Biosciences	--	--	6 µg/ml
Streptavidin FITC Stem cell staining	BD Biosciences			3.3 µg/ml
c-Kit (CD117) APC Stem cell staining	BD Biosciences	IgG2b, k	2B8	1.25 µg/ml
Sca-1 (Ly6A/E) PE Stem cell staining	BD Biosciences	IgG2a, k	E13-161.7	1.25 µg/ml
CD16/CD32	BD Biosciences	IgG2b, k	2.4G2	5 µg/ml
7-Aminoactinomycin (7-AAD)	Molecular Probes	--	--	5 µg/ml

3.1.3.3 Antibodies for FACS analysis

Specificity	Source	Isotype	Clone	Application	Final conc.
Gr-1 (Ly6G/6C) PE	BD Biosciences	IgG2b, k	RB6-8C5	FACS	200 µg/ml
F4/80 FITC	BD Biosciences	IgG2b, k	BM8	FACS	200 µg/ml

3.1.3.4 Antibodies for mouse injections

Specificity	Source	Isotype	Clone	Application	Final conc. per mouse (20g)
Anti KC antibody	R&D Systems	IgG2a	48415.111	FACS and 2-photon microscopy	50 µg
Anti MIP-2 antibody	R&D Systems	IgG2b	40605	FACS and 2-photon microscopy	20 µg
anti-Gr-1 antibody	Bioxcell	Rat IgG2b	RB6-8C5	FACS	823 µg
Rabbit CXCR2 antiserum	[Carlson *et al.* 2008b]	--	--	FACS and 2-photon microscopy	--
Normal rabbit serum	[Carlson *et al.* 2008b]	--	--	FACS and 2-photon microscopy	--
IgG2a Isotype control	BD Biosciences	--	--	FACS and 2-photon microscopy	50 µg
IgG2b Isotype control	BD Biosciences	--	--	FACS and 2-photon microscopy	20 µg
IgG Isotype control	Acris	--	-	FACS and 2-photon microscopy	100 µg/ml

3.1.3.5 Fluorescent dyes for *in vivo* imaging

Specificity	Source	Application
Carboxy Fluorescein Succinimidyl Ester (CFSE)	Molecular Probes	Cell staining
Cell Tracker Orange (CTO)	Molecular Probes	Cell staining

Specificity	Source	Application
Rhodamine-Dextran 40kD	Sigma-Aldrich	blood vessels staining

3.2 Methods

3.2.1 General Methods

3.2.1.1 Mouse handling

3.2.1.1.1 Intraperitoneal injection

For intraperitoneal (i.p.) injections the relevant compounds were dissolved and diluted in sterile PBS to the desired concentration. A maximal volume of 500 µl was injected into the peritoneum using a fine dosage syringe with an integrated 0.3 x 12 mm cannula (Braun Omnican F).

3.2.1.1.2 Retroorbital i.v. injection

Mice were slightly anaesthetized by isoflurane (CuraMed Pharma) inhalation. The antibodies, cells or dyes were injected into the retro-orbital sinus at a maximal volume of 200 µl sterile PBS using a fine dosage syringe with integrated 0.3 x 12 mm cannula (Braun Omnican F).

3.2.1.1.3 Ketamin-Rompun narcosis

For a mouse narcosis lasting up to 1 h, 1 ml Ketamin [50 mg/ml] and 0.5 ml Rompun [2 %] were mixed with 3.5 ml sterile NaCl and 100 µl per 10 g animal body weight were injected i.p.

3.2.1.1.4 Bleeding

Mice were slightly anesthetized by isoflurane inhalation and 75 µl blood were collected by retro-orbital puncture with a capillary tube into a 1.5 ml test tube containing 20 µl Heparin-Sodium (168 U/ml final concentration) to avoid coagulation.

3.2.1.2 Isolation of bone marrow cells

Mice were killed by cervical dislocation. The hind limbs were disinfected with 70 % ethanol and the skin was removed. The paws were clipped and the thigh was separated from the shank by a cut through the knee joint. Now the muscles were carefully removed from the thigh with scissors and the femur was taken out of the hip.

The tibial muscles were relieved by down-pulling with the scissors and the exposed bones were stored in PBS supplemented with 1 % FCS. Afterwards the bone marrow was flushed out of the bones with a 21G cannula connected to a 5 ml syringe into a 50 ml test tube filled with 10 ml PBS + 1 % FCS. To get a single cell suspension it was resuspended carefully and the suspension was filtered through a cell strainer (100 µm pore diameter).

To isolate bone marrow from old mice the fragile bones were pestled in 10 ml PBS + 1 % FCS. After grinding the suspension was removed and filtered through a 100 µm cell strainer (Falcon BD). In order to loose as little cells as possible the mortar was washed twice with 10 ml PBS + 1 % FCS and these fractions were pooled with the first filtrate. This alternative protocol was also used for some bone marrow isolations from young mice to increase the number of isolated cells.

3.2.1.3 Isolation of splenocytes

Mice were killed by cervical dislocation. The spleen was removed and stored in a 50 ml tube containing 10 ml PBS + 1 % FCS. To get a single cell suspension, the organ was ground through a 100 µl cell strainer with the piston of a 5 ml syringe into a cell culture plate. The cell suspension was centrifuged (5 min, 400 x g, RT) and the supernatant was discarded. To eliminate red blood cells, the precipitated cells were resuspended in 5 ml erythrocyte lysis buffer per spleen. The cells were agitated with a pipette for 1 min, and then incubated for 5 min at RT. Administration of 40 ml PBS + 1 % FCS stopped the lysis reaction and the cells were centrifuged (5 min, 400 x g, RT). After washing in 50 ml PBS (5 min, 400 x g, RT) cells were resuspended in 5 ml PBS and the cell number was calculated (view 3.2.3). $1 \cdot 10^7$ cells were transferred to a 96 well plate for antibody staining.

3.2.1.4 Estimation of cell numbers in a cell suspension

For calculating the cell number in a suspension, an aliquot of 10 µl cell suspension was mixed 1:1 with trypan blue (0.4%) and transferred into a Neubauer counting chamber. Trypan blue stained cells were regarded as dead and excluded from counting.

3.2.1.5 Fluorescence activated cell sorting (FACS) analysis

To analyze blood samples the total volume of 75 µl (see 3.2.1.1.4) was transferred

into a 96 well plate and 150 µl erythrocyte lysis buffer were added to eliminate red blood cells. The solution was agitated with a pipette for 1 min, and incubated for 5 min at room temperature (RT). After centrifugation (5 min, 400 x g, RT), the supernatant was discarded and the erythrocyte lysis repeated twice as described above. Then the cells were washed once with 200 µl sterile PBS and used for FACS analysis

For BM analysis the precipitated (5 min, 400 x g, RT) cells (view 3.2.1.2) were resuspended in 5 ml erythrocyte lysis buffer per two hind limbs. The suspension was agitated with a pipette for 1 min, and then stored for 5 min at RT. The reaction was stopped by administration of 40 ml PBS + 1% FCS. After a centrifugation step (5 min, 400 x g, RT) the cells were washed in 50 ml PBS (5 min, 400 x g, RT) and resuspended in 1 ml PBS. Then the cell number was estimated and $1 \cdot 10^7$ cells were transferred to a 96 well plate for antibody staining.

For antibody staining, the precipitated cells from different sources were resuspended in 80 µl of the relevant antibody solution (in sterile PBS) and incubated for 10 min at RT in the dark. Afterwards the cells were washed with 200 µl PBS (5 min, 400 x g, RT), the supernatant was discarded and the cell pellet resuspended in 500 µl PBS. FACS-analysis was performed on a BD FACSCalibur and analyzed using DAKO's "Summit" software.

3.2.2 Stem cell specific methods

3.2.2.1 Preparation of hematopoietic progenitor cells (HPCs) and early hematopoietic progenitor cells (eHPCs)

Before use Dynabeads (Dynal) must be washed carefully. In the first step the entire 5 ml of beads were transferred into a 15 ml test tube. Then 10 ml IMDM + 2 % FCS were added and the beads separated with a strong magnet (Dynal). After 3 minutes the medium was removed with a 5 ml pipette and the tube taken out of the separator. The beads were resuspended in 10 ml IMDM + 2 % FCS before the tube was again applied to the separator for 3 minutes. After this step the medium was carefully removed. This washing procedure was repeated twice and finally the beads were resuspended in 5 ml IMDM + 2 % FCS and stored at 4 °C. The whole procedure was performed under sterile conditions.

To isolate the HPCs and HSCs from a bone marrow derived cell suspension by FACS, most of the unwanted, mature cell types (LIN-positive cells) were eliminat-

ed by positive magnetic depletion. This step was based on an antibody cocktail, containing antibodies directed against the most common mature cell types, residing in the bone marrow (view 2.2.2).The isotype of all antibodies in this cocktail was rat immunoglobulin IgG2 and therefore the labeled cells were depleted by addition of sheep anti-rat IgG coated Dynabeads.

In detail, bone marrow of 10 C57Bl/6 mice was isolated as described above (view 3.2.1.2). After filtration the cells were centrifuged (5 min, 400 x g, RT), resuspended in 24 ml HBSS + 2 % FCS (RT) and the cell number was calculated (view 3.2.1.2). 16 ml of Ficoll (1083, Sigma) were put in a 50 ml tube and carefully overlayed with the cell suspension at room temperature. With the following centrifugation (25 min, 600 x g, RT, without brake) a gradient was formed, which separated leukocytes from erythrocytes (Figure 16). The leukocyte fraction was removed and transferred into a new 50 ml tube. All next steps were done at 4 °C. To get rid of the Ficoll, the cells were washed twice with cold IMDM + 2 % FCS, first with 50 ml, then with 25 ml (5 min, 400 x g, 4 °C). The precipitated cells were resuspended in 3 ml IMDM + 2 % FCS and counted again. Per $1x10^8$ cells, 112.4 µl LIN cocktail were added and agitated 25 min at 4 °C. Afterwards the cells were washed twice with 25 ml IMDM + 2 % FCS (5 min, 400 x g, 4 °C). Dynabeads were added to the cell suspension in a four beads per cell ratio (concentration of bead stock: $4x10^8$ beads/ml) and agitated 25 min at 4 °C. After this incubation step, the cells were transferred into a 15 ml test tube and filled up with IMDM + 2 % FCS to a total volume of 8 ml. With the aid of a magnetic separator the bead bound LIN positive cells were precipitated. The supernatant containing the LIN negative cells was removed, transferred to

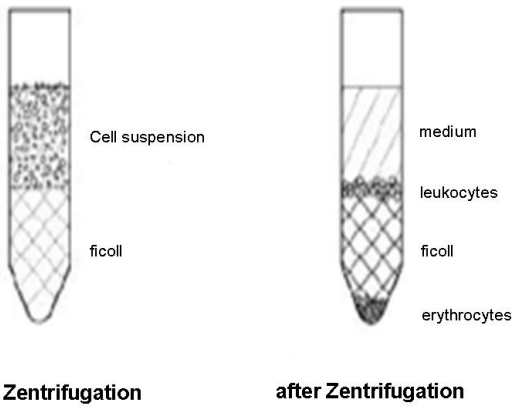

Figure 16 Enrichment of leukocytes. A Ficoll gradient centrifugation can separate leukocytes from other bone marrow cells. A suspension of whole bone marrow cells is placed on Ficoll very carefully. The density of the Ficoll has to be lower than the density of leucocytes but higher than the density of erythrocytes.

Adapted from http://edoc.hu-berlin.de/dissertationen/wentges-marek-2004-12-13/HTML/chapter2.html

a new 15 ml tube and the separation was repeated at least three times. Precipitated beads were washed in 7 ml IMDM + 2 % FCS afterwards to obtain all unbound cells in the supernatant and this fraction was also separated three times. Both suspensions were combined in a 50 ml test tube and spun for 5 min at 400 x g at 4 °C. Precipitated cells were then resuspended in 1 ml IMDM + 2 % FCS. After calculating the cell number, 10 µl of the FC-block antibody mixture CD16/CD32 were added to the cells in order to avoid unspecific binding of the monoclonal antibodies which were subsequently used for the fluorescent based stem cell sort. After incubation for 15 min at 4 °C with gentle shaking, three fluorescent dye coupled reagents were added:

Antibody	Stock concentration	Dilution	Amount
Strept.-FITC (fluorescein)	0.5 mg/ml	1:150	6.60 µl
c-Kit APC-(allophycocyanin)	0.2 mg/ml	1:160	6.25 µl
Sca-1-PE (phycoerythrin)	0.2 mg/ml	1:160	6.25 µl

As all antibodies of the LIN-cocktail were biotinylated the streptavidin-FITC staining could be used as indicator for contaminating LIN positive cells. Additionally the eHPCs and HPCs were stained for their specific receptors with the monoclonal anti-c-Kit and anti-Sca-1 antibodies. The cells were agitated 20 min at 4 °C and then washed for the last time (5 min, 400 x g, 4 °C) in 25 ml IMDM + 2 % FCS. For the cell sorting the cells were resuspended in 500 µl IMDM + 2 % FCS, supplemented with 7-Aminoactinomycin (7-AAD) [1 mg/ml]. This reagent specifically stained dead cells and thus allowed gating on living cells during the sort. In parallel, 5 single color control stainings (FITC, APC, PE, 7-AAD, unstained) were produced from 10 µl each of the bone marrow cell suspension to adjust the FACS compensation settings.

For the isolation of early progenitor and progenitor cells, a MoFlo cell sorter (DAKO) was used. A careful selection of the right cell populations was required to finally receive the correct cell types. In the first step a gating on living cells was realized using the 7-AAD signal (Figure 17 a)). Additionally this gate was combined with the established and expected forward scatter (FSC)/side scatter (SSC) morphology (Figure 17 b)). Subsequently HPCs and eHPCs were indicated by the

fact, that eHPCs express the receptor c-Kit as well as the receptor Sca-1. In contrast, HPCs were positive for the c-Kit receptor but negative for Sca-1. This allowed a separation of these two cell populations (Figure 17 c)). eHPCs and HPCs were sorted into 15 ml tubes filled with 1 ml IMDM + 10 % FCS respectively. After sorting both isolated cell populations were tested for their purity by FACS (Figure 18).

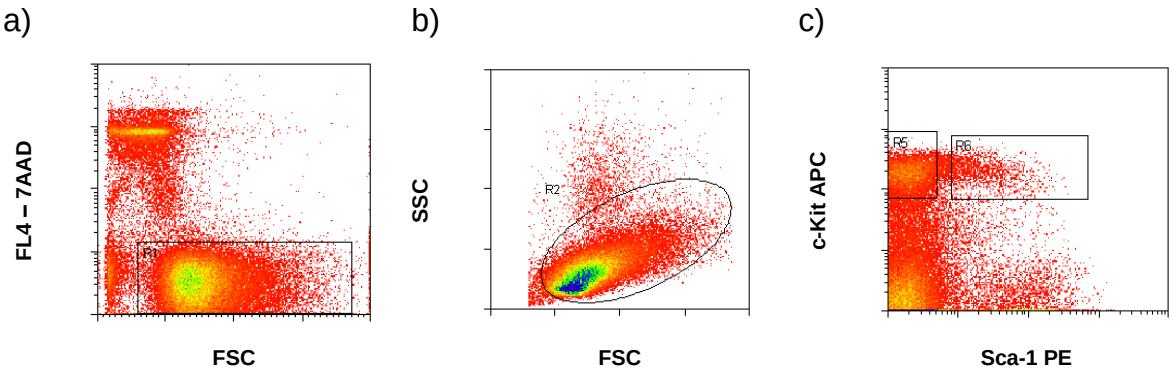

Figure 17 Example of an early hematopoietic progenitor cells and hematopoietic progenitor cell isolation via cell sorting. a) The first step was to eliminate dead cells by the 7-AAD signal. b) Secondly it was gated on cells with the right FSC/SSC morphology. c) Both desired cell populations were separated by their different expression of the surface receptors c-Kit and Sca-1 (R5: HPC, R6: eHPC).

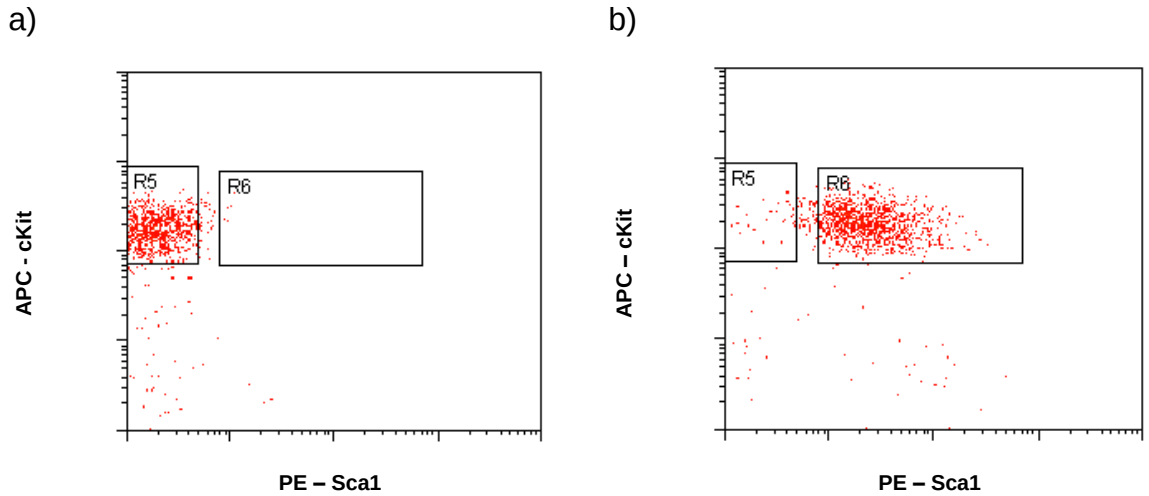

Figure 18 Purity test of the isolated early hematopoietic progenitor cells and hematopoietic progenitor cell. Clear populations of either a) HPCs (c-Kit^{+}, Sca-1^{-}) or b) eHPCs (c-Kit^{+}, Sca-1^{+}) were obtained.

3.2.3 Neutrophil specific methods

3.2.3.1 Neutrophil mobilization with G-CSF

The entire volume of a Neupogen® syringe (Amgen GmbH, 300 µg/0.5 ml or 480 µg/0.5 ml) was flushed into a 1.5 ml test tube and stored at 4 °C. For neutrophil mobilization 100 µg G-CSF per kg animal weight, diluted in a volume of 100 µl sterile PBS was injected i.v. into the retro-orbital plexus. Control animals received 100 µl pure PBS. Samples of blood or other organs were collected 2 h after mobilization.

3.2.3.2 Neutrophil mobilization with AMD3100

To mobilize cells with AMD3100 (Sigma-Aldrich) 100 µl of a 1 mg/ml solution in H_2O/PBS (1:4 v/v) were injected i.v. into the retro-orbital plexus. 2 h later 75 µl of peripheral blood were analyzed for neutrophil counts. Control animals received 100 µl H_2O/PBS.

3.2.3.3 Neutrophil mobilization with thrombopoietin

100 µl of 10 µg/ml murine thrombopoietin (R&D Systems) solution in PBS were injected i.v. into the retro-orbital plexus. 2 h later 75 µl of peripheral blood were analyzed for neutrophil counts. Control animals received 100 µl PBS.

3.2.3.4 Anti KC and anti MIP-2 treatment for inhibition of neutrophil mobilization

For Inhibition of the chemokines KC and MIP-2 50 µg monoclonal anti-KC and 20 µg anti-MIP-2 antibodies, diluted in PBS were administered in a total volume of 100 µl per animal simultaneous. The injection route was either i.v. or i.p. at different time points. Likewise, control animals received equivalent concentrations of IgG2a and IgG2b isotype controls the same way.

3.2.3.5 Inhibition of neutrophil mobilization by blocking CXCR2

To block CXCR2 *in vivo*, 100 µl of rabbit anti-CXCR2 antiserum were injected i.p. 48 h before mobilization with G-CSF. Control animals received equal amounts of normal rabbit serum (NRS). For some experiments the antibody was titrated down to 10 µl, always diluted in sterile PBS to a total volume of 100 µl.

3.2.3.6 Antibody mediated neutrophil depletion

For depletion of neutrophils, 100 µg of an anti-Gr-1 antibody (RB6-8C5, Bio X Cell, USA) were injected intraperitoneally in a total volume of 100 µl 48 h before onset of the experiment. Control animals were likewise treated with 100 µg of a control rat IgG.

3.2.3.7 Acute peritonitis model

An acute peritonitis was induced by injection of 500 µl 3 % thioglycollate broth (Sigma Aldrich) i.p. Control animals were treated with 500 µl PBS following the same protocol. After 2 h a peritoneal lavage was performed. Therefore mice were killed by cervical dislocation. 5 ml PBS + EDTA were injected into the peritoneum with a 20 G cannula attached to a 5 ml syringe. After one minute of belly massage the maximal possible volume of PBS cell suspension was drawn out of the peritoneum using the same syringe. The cells were analyzed by FACS for the amount of Gr-1 positive cells. Additionally, bone marrow and peripheral blood were collected and analyzed for the occurrence of neutrophils.

To inhibit the formation of an acute peritonitis 50 µg anti-KC and 20 µg anti-MIP-2 antibodies were injected simultaneously in a total volume of 500 µl PBS i.p. 20 minutes before induction of the peritonitis. Control animals received equivalent concentrations of anti-IgG2a and IgG2b-isotype controls in 500 µl PBS likewise.

3.2.4 Intravital 2-photon microscopy

3.2.4.1 Cell staining for 2-photon microscopy

Cells were stained for *in vivo* microscopy either with CFSE [5 µM] or CTO [25 µM] in 1 ml PBS. After incubation at room temperature for 10 minutes in the dark, the staining was stopped by administration of 15 ml PBS + 1 % FCS. Before injection into mice, cells were washed once with PBS (5 min, 300 x g, RT).

3.2.4.2 Blood vessel staining for 2-photon microscopy

To visualize the blood vessels and blood flow during *in vivo* microscopy, 200 µl of Rhodamine-B-Isothiocyanate labeled 40kD dextran ([2 mg/ml], Sigma) in sterile PBS were injected retro-orbitally right before onset of the imaging.

3.2.4.3 Mouse narcosis and bone preparation

The *in vivo* 2-photon microscopy was performed up to 12 h and so for the whole time period mice needed to be narcotized. To assure a deep narcosis, an intubation anesthesia with oxygen + 1 % isoflurane was chosen. In the beginning the mice were slightly anesthetized by a Ketamin-Rompun injection (view 3.2.1.1.3) to allow the intubation procedure. Then the animals were fixed with an elastic band at their teeth on a bevel (Figure 19 a) and b)). With a forceps the tongue was pulled to one side and a tracheal tubus was inserted very carefully into the trachea which was clearly detectable by the illumination with a goose neck lamp. Through the tubus animals were mechanically ventilated by a small animal respirator (MiniVent, Hugo Sachs, Germany) with a breathing rate of 250 per minute. Oxygen + Isoflurane were mixed with a vaporizer (Univentor, Uno, Netherlands) and a volume of 250 µl per breath was inhaled by the animal (Figure 19 c)).

a)

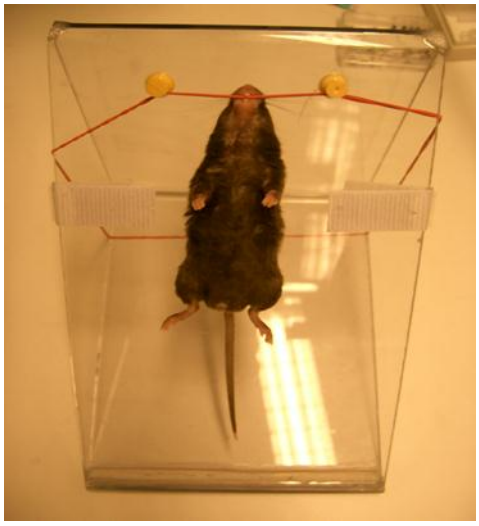

b)

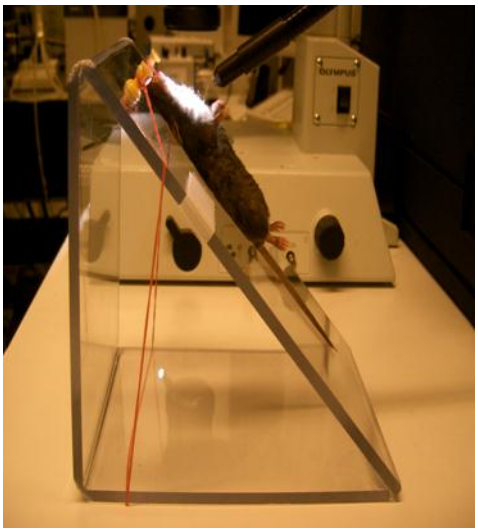

c)

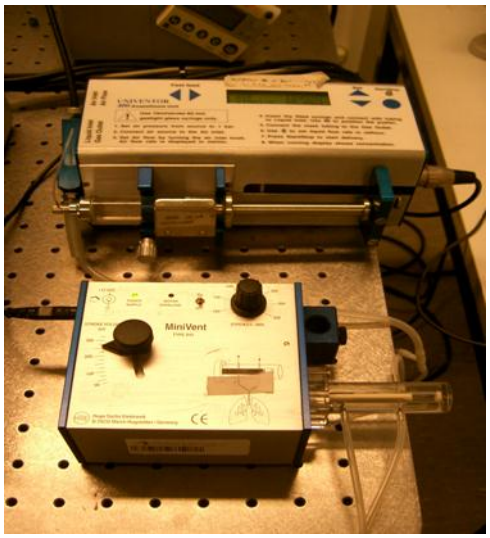

Figure 19 Mouse fixation for intubation and narcosis. a) The animal was fixed with its front teeth on a bevel. b) The throat was illuminated to facilitate the finding of the trachea, which was detectable as a small bright whole in the deeper part of the mouth. c) Setup for mouse narcosis. In the upper part of the picture the vaporizer can be seen, which mixed the isoflurane with pure oxygen. This anesthetic gas was transferred to a respirator (foreground) by which a defined gas volume and the breathing rate could be adjusted.

To allow 2-photon microscopy in the lower legs of mice these bones had to be exposed and moreover, their surface structure had to be thinned to allow microscopic imaging in the marrow. Therefore the skin was cut carefully directly along the bone. The overlaying muscles were removed with a scalpel, thereby especially avoiding bigger blood vessel injury. By using an electric drill (Dremel) with a sulfoxide grindstone (model 997, Dremel) the bone was thinned, constantly observed with a stereo microscope to not totally remove the covering bone layer. The residual bone surface was kept at 30-50 µm thickness (Figure 20 E)). While drilling the

procedure was interrupted about every 10 seconds and the bone was cooled and washed with PBS to avoid an overheating of the treated area.

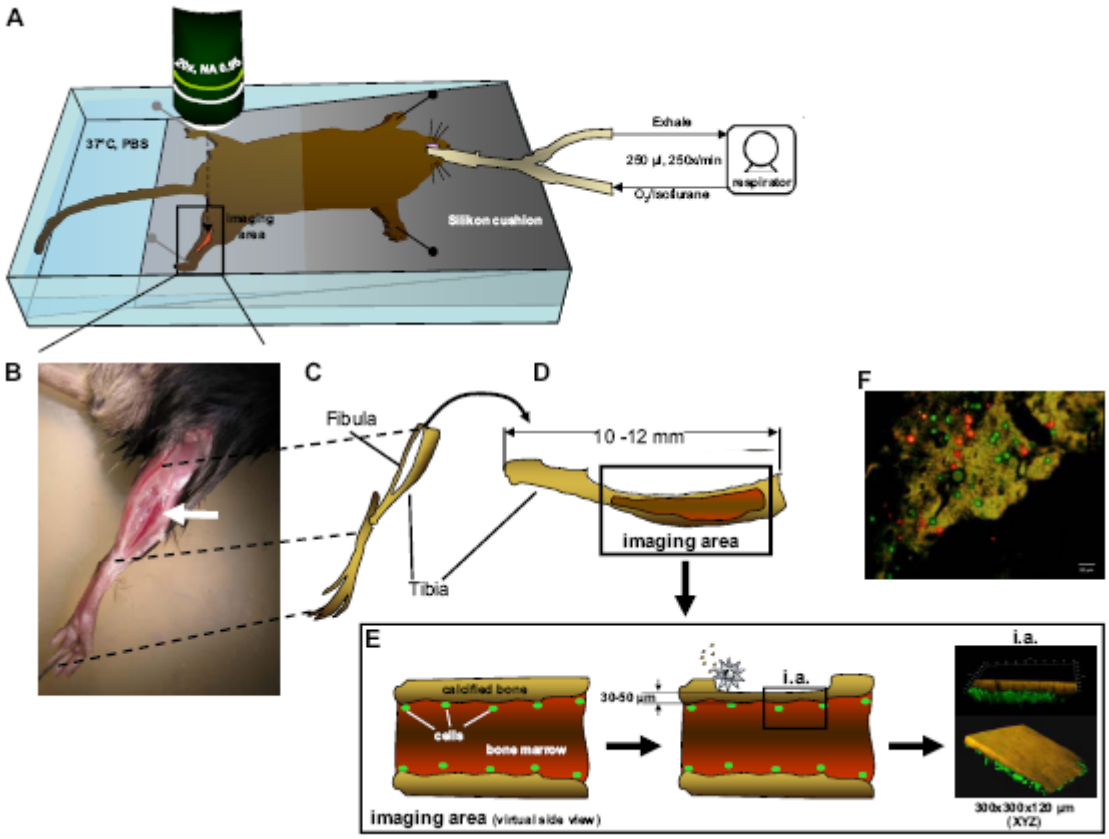

Figure 20 Overview of the mouse treatment and long bone preparation for intravital 2-photon microscopy. A) Fixation of the mouse in the imaging chamber. The animal is ventilated and thereby anesthetized through a tracheal tubus with a mechanical small animal respirator at depicted rates and volumes. The gross area of bone thinning and imaging is boxed and the approximate position of the microscope lens is indicated with a dashed arrow. Imaging can be performed anywhere within the red (thinned) area of the tibia. All fluorescently marked cells detectable within this area are recorded by individual Z-stacks. B) A close-up micrograph of a mouse fixed for imaging with the position of the tibia indicated (white arrow). C) Schematic overview how the hind leg bones are positioned in the animal shown in panel B). D) Enlargement of the tibial bone rotated 90°clockwise with the area of preparation indicated by the red color. E) Virtual side view of the tibial bone in the area of imaging to demonstrate the process of careful bone thinning by an electric drill. The residual bone surface is kept at 30 to 50 µm of thickness. The figure on the right shows rendered images of a bone with fluorescently labeled (green) cells below the bone surface. The typical XYZ dimensions of the area of imaging are depicted. F) To demonstrate the practicability of the transplantation/visualization technique, BM cells were stained with CFSE (green) or CTO (red) and transplanted together in equal numbers in recipient animals. Cells were visualized by 2-photon intravital microscopy in the region close to the endosteum in the tibia (brown auto fluorescence signal of the calcified bone) 16 hours post injection.

3.2.4.4 Two-Photon microscopy

After preparation of the bone, the anesthetized animals were transferred into a laboratory made imaging chamber. This chamber was lined with silicon, in which the mice were fixed with needles (Figure 21). Additionally, the chamber was heated by an external water bath to keep the animals at a temperature of 37 °C. During microscopy, pre-warmed PBS was filled into the chamber until the legs were covered with the buffer. Besides the warming of the animal, the fluid acted as an immersion medium for the water dipping objective.

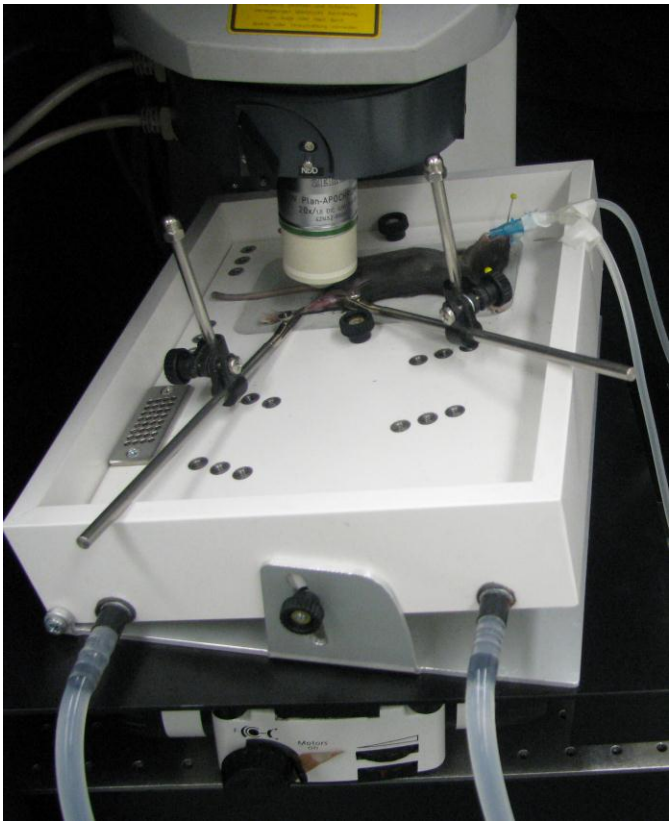

Figure 21 Intubated animal under the 2-photon microscope. The Imaging chamber with an intubated and fixed mouse was placed under the 2-photon microscope**.** Pre-warmed PBS was added afterwards.

2-photon microscopy of stem cells was mainly performed using a customized 2-photon microscope (TrimScope; LaVision BioTec) with detection either by a charge-coupled device (CCD) camera (multifocal illumination) or an array of independent photo-multiplier tubes (PMTs) detectors (single-point illumination). Bone tissue was identified due to its strong auto fluorescence (with CCD camera) under unfiltered light conditions or using its second-harmonic (SHG) signal (with PMT).

Two-photon microscopy of neutrophils was performed using a Zeiss LSM-710 microscope with simultaneous detection via external non-descanned-detectors (NDDs). Neutrophils were detected via GFP-fluorescence, blood vessels by injection of Rhodamine-B-Isothiocyanate labeled 40 kD dextran (Sigma) and bone by its second harmonic generation (SHG)-signal. Movies were recorded during 1 - 3 h after injection of stimuli for 60 minutes each. Several experiments were done in individual animals for up to 6 h.

For imaging, a 300 x 300 µm area (LaVision BioTec) or a 423 x 423 µm area

(Zeiss) was scanned in 31 steps of 4 µm down to 120 µm depth using an illumination wavelength of either 800 or 880 nm (MaiTai TiSa-laser) detecting green (530 nm) and red (580 nm) fluorescence, as well as unfiltered light or SHG (480-nm emission). This sequence was repeated every 60 seconds for a total of up to 60 minutes.

3.2.4.5 Data analysis

3.2.4.5.1 Processing of data with the rendering software "Volocity ®"

After recording sequences with the 2-photon microscope, the image raw data were imported into the 3D rendering software Volocity (Improvision, Perkin Elmer, UK). By use of this software suite brightness and contrast of the different channels were optimized. Afterwards the movies were exported as video sequences in a compressed avi format for further analysis.

3.2.4.5.2 Cell tracking

The motility of cells inside the bone marrow was determined using the laboratory made "cell-tracker" software [Reichardt *et al.* 2007]. By following single cells with the mouse cursor over the complete movie sequence the software recorded different parameters of cell motility, which could be further analyzed. If possible, three independent areas with 25-30 cells respectively were determined per microscopic experiment.

3.2.4.5.3 Generation of "Kinetic overlays"

Kinetic overlays were used as a helpful tool to display cell motility at different time points in one picture. Three sequenced pictures from an avi file were imported into Corel Photo-Paint X3. Each picture was divided into the three single RGB channels that were recorded during microscopy. Just the channel, representing the cells was maintained, the other channels were deleted. Then the three sequenced pictures were combined.

3.2.4.5.4 Calculation of cell distance to the endothelial layer

The measurement of cell distances to the endosteal layer (inner bone surface) was performed with the help of the Volocity software. The black levels of the SHG channel (bone) of a respective picture were reduced, so that the bone structure

was just detectable and appeared as thin layer. Then an x,y,z-calibrated grid was blend in this picture from which the distances of a cell to the endosteal wall could be estimated.

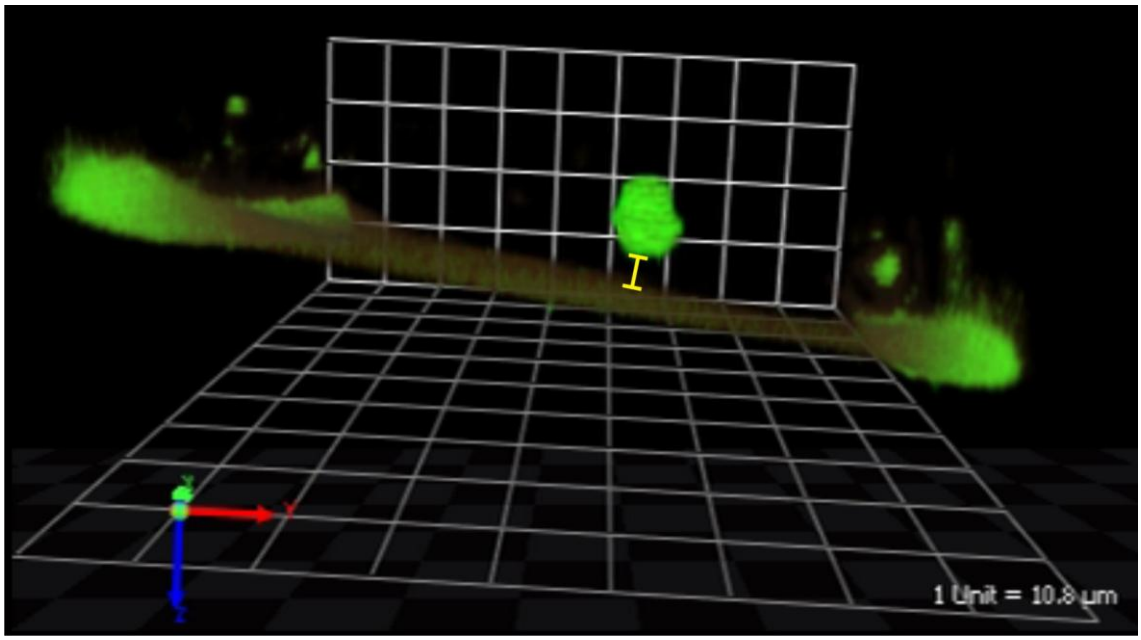

Figure 22 Distance measurement between cell and bone. A CFSE stained cell and the brownish bone structure were displayed within a calibrated grid of small units. The bone signal was reduced until it was barely visible. This allowed the calculation of the distance between bone and cell. The yellow bar demonstrates a representative distance of 9 µm.

3.2.4.5.5 Statistical analysis

Data are shown as mean +/- SEM or median (in column scatter plots). Data were analyzed using GraphPad Prism software using the unpaired Student's t test. Differences were significant when $p < 0.05$ ($p < 0.05$ * , $p < 0.01$ ** and $p < 0.001$ ***).

4. Results

4.1 Part I: Localization and dynamics of young and aged hematopoietic progenitor cells and early hematopoietic progenitor cells in the murine bone marrow revealed by intravital 2-photon microscopy

The aim of the first part of this thesis was to visualize hematopoietic progenitor cells and early hematopoietic progenitor cells in the bone marrow of murine long bones by intravital 2-photon microscopy and to analyze their behavior under different conditions. These observations were of great interest as stem cells of this origin are regularly taken for different immunological assays (i.e. *in vitro* generation of dendritic cells from bone marrow progenitors) but a clear characterization of these cells was still lacking. Until now, all microscopic approaches to characterize hematopoietic progenitors were done in the calvarium of mice, where a small spot of bone marrow is located. In different publications these microscopic data were combined with immunohistological stainings taken from bone marrow slices of the murine femur and tibia. Recent studies [Lo *et al.* 2009] revealed that both sources of bone marrow display a unique and distinguishable hematopoietic activity.

Based on this innovative work we believed that it was necessary to study hematopoietic cell behavior *in vivo* at the same place from where cells for *in vitro* approaches are normally isolated. To realize the *in vivo* observation of early hematopoietic progenitor cells in long bones of mice, a completely new method for 2-photon microscopy was established.

4.1.1 Visualization of hematopoietic progenitor cells and early hematopoietic progenitor cells in long bones of mice

To study the behavior of hematopoietic progenitor cells (HPC, $L^-S^-K^+$, Lineage$^-$ Sca-1$^-$ c-Kit$^+$) and early hematopoietic progenitor cells (eHPC, $L^-S^+K^+$, Lineage$^-$ Sca-1$^+$ c-Kit$^+$) in the bone marrow, eHPCs and HPCs cells were isolated by cell sorting, stained with either CFSE or CTO and adoptively transferred into untreated recipients (view 3.2.1.1.2). The intravital cell imaging in the tibiae of anesthetized animals was performed between 18 – 36 h after transfer by use of our newly developed imaging technique (view 3.2.4.4).

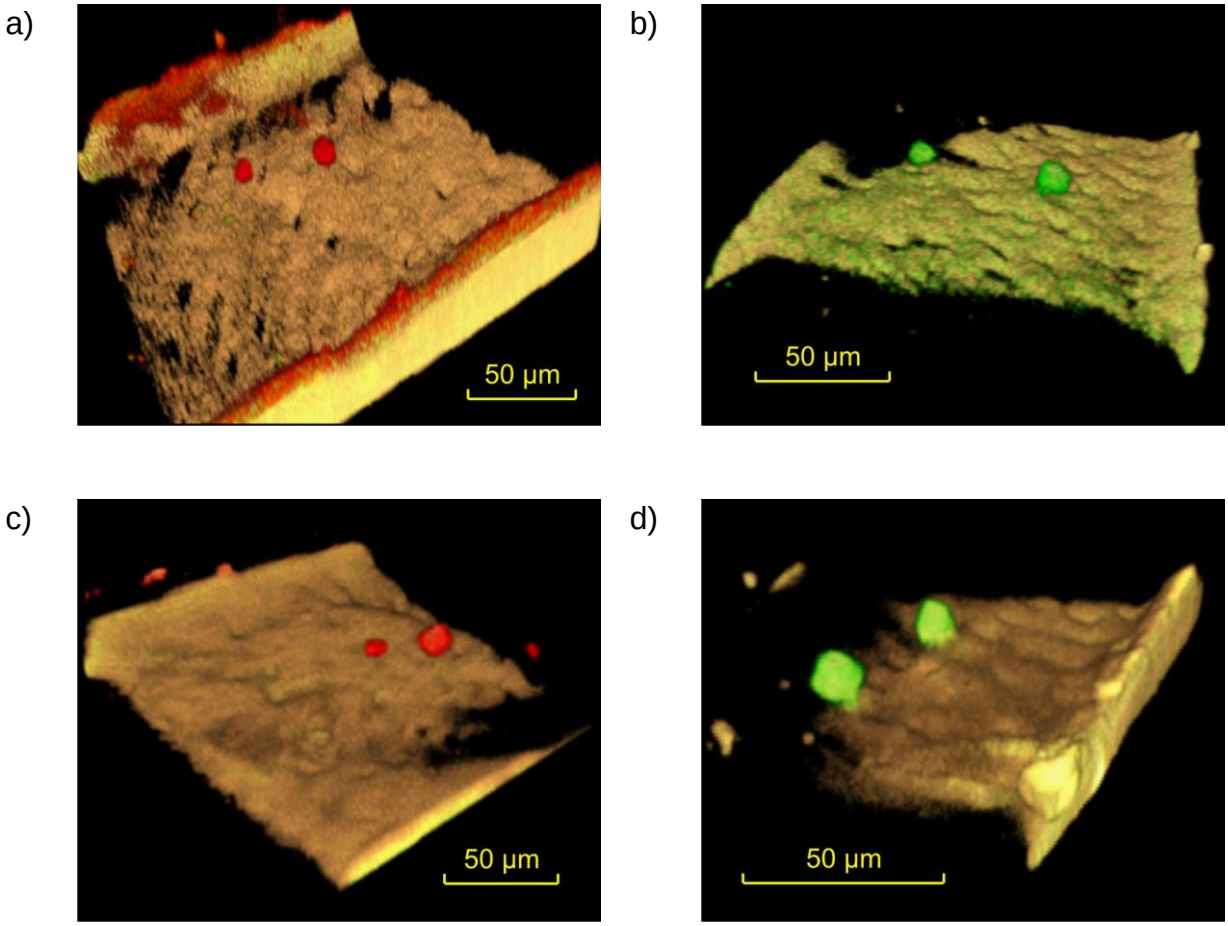

Figure 23 3-D rendering of eHPCs. The cells were isolated from 8 weeks old C57Bl/6 mice, adoptively transferred into untreated WT recipients and visualized by intravital 2-photon microscopy in the bone marrow of the anesthetized recipient animals 24 h after transfer. Cells were stained with either CTO (red) or CFSE (green). The bone structure was recorded by its auto fluorescence and delineated in a brown color. The pictures a) - d) represent characteristic images from 4 independent experiments. All pictures were recorded with a magnification of 200x. View also supplemental movies 1 – 4.

4.1.2 Localization and dynamics of hematopoietic progenitor cells in long bones of mice

This self-established intravital 2-photon model allowed us to further describe the localization of HPC cells and eHPCs in the tibial bone marrow. A small number of these cells were found in direct contact with the inner bone surface (Figure 25) whereas most cells were located farther away (Figure 24 and Table 1).

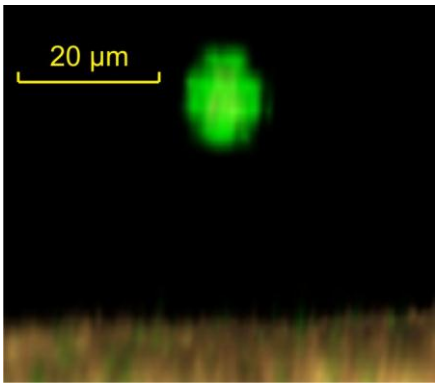

Figure 24 eHPCs (CFSE stained) with a certain distance to the brown structure of the inner bone surface. 3D rendering, of an intravital 2-photon image, detected with a magnification of 200x.

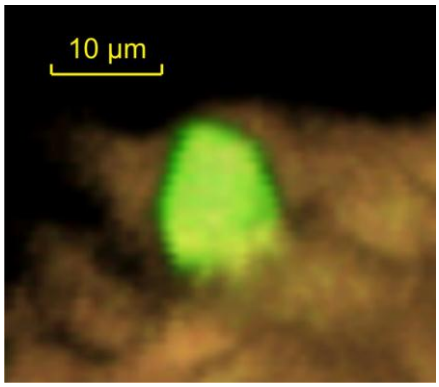

Figure 25 eHPCs (CFSE stained) in direct contact to the brown structure of the inner bone surface. 3D rendering, of an intravital 2-photon image, detected with a magnification of 200x.

After performing a more detailed analysis of cell distances we found that 11 % of transplanted eHPCs had direct contact to the endosteum in the tibia, whereas just 4 % of HPCs were in direct contact to the endosteal layer (Table 1). In addition, eHPCs resided closer to the endosteum compared to HPCs (11 µm vs. 19 µm; Table 1).

Table 1 Overview over all detected HPCs and eHPCs, isolated from young mice in the bone marrow of C57Bl/6 recipients. Two populations were detected, one smaller part in direct contact to the endosteum, the bigger part still in close vicinity, but not in contact. In the right lane the mean distance of all analyzed cells to the endosteum was calculated. n = number of experiments

	Number of all analyzed cells	Percentage of cells with distance to the endosteum	Percentage of cells in direct contact to the endosteum	Mean distance to the endosteum in µm
eHPCs ($L^-S^+K^+$) from young mice	44 n = 6	88.6	11.4	10.72
HPCs ($L^-S^-K^+$) from young mice	93 n = 6	95.7	4.3	18.94

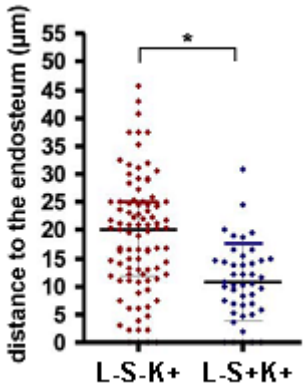

Figure 26 Localization of HPCs (L-S-K+) and eHPCs (L-S+K+), isolated from young mice, to the endosteal layer. Distance of HPCs and eHPCs from the endosteum; each dot represents a single cell; black horizontal bars depict the average distance; and red/blue horizontal bars depict the standard deviation. eHPCs are located significantly closer to the endosteum, compared to HPCs. *p < .05.

Regarding the cell motility of both progenitor cell types we found that they did not show any displacement. Instead, all observed cells displayed a "running on the spot" behavior and just a proceeding protrusion movement in the cell periphery was detectable. To exclude that the staining and transfer procedure was responsible for the resting behavior of eHPCs and HPCs, also whole bone marrow cells were isolated and stained with CFSE and CTO. 16 h after adoptive transfer a valid number of these cells displayed a clearly detectable motility in the bone marrow (data not shown). Dye exchange experiments were performed, to exclude label specific influences and no influences of the dye could be detected with respect to cell localization in the bone marrow.

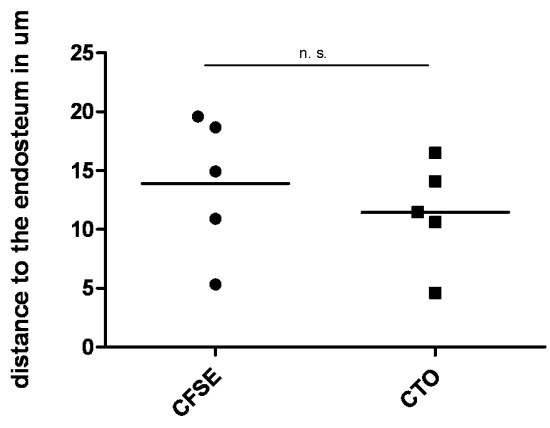

Figure 27 Comparison of eHPCs, stained with either CFSE or CTO. To exclude an influence of the cell staining referring to the cell distance to the endosteal layer, five random cells from every staining were chosen. No difference in the cell localization was detectable.

To describe the "running on the spot" behavior of HPCs und eHPCs, we mathematically quantified the extent of cell protrusion movement over time with the help of our cooperation partners from the CCHMC. New algorithms were developed to calculate both the change in volume and the surface area of the observed cells

over time. This analysis was based on data obtained from 2-photon microscopy. It revealed that HPCs as well as eHPCs presented an active cell protrusion movement indicated by absolute changes in cell volume between time points (Figure 28 a)) as well as by the variance in change of the cell volume (Figure 28 b)) and the variance in the change of the cell surface area (Figure 28 c)). The variance is a measure of variability, representing the extent of the changes in volume or cell surface area per 1 minute. By this analysis a trend was uncovered for HPCs being more active with respect to changes in the cell surface area compared to eHPCs.

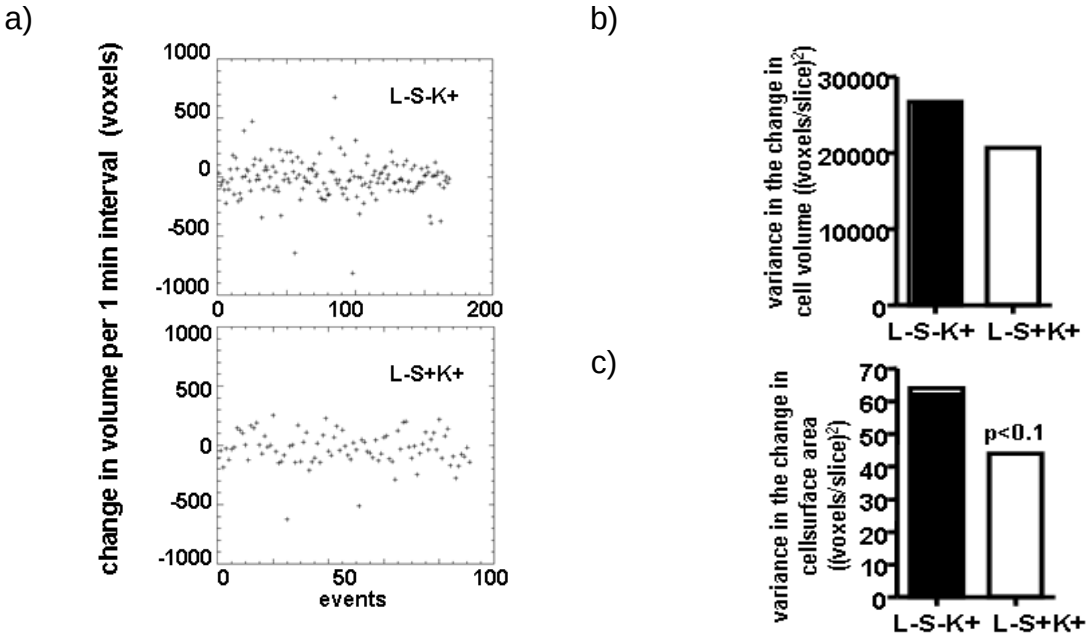

Figure 28 CFSE-labeled HPCs ($L^-S^-K^+$) or eHPCs ($L^-S^+K^+$) after transplantation into recipient animals. Tibiae from recipient animals were analyzed between 16 and 40 hours after transplantation. a) Quantification of cell protrusion movement, determined as the change in volume over time (interval of 1 minute) of transplanted HPCs and eHPCs. b) Average variance in the change in cell volume in a 1 minute time interval of HPCs and eHPCs. c) Average variance in the change of cell surface area in a 1 minute time interval of HPCs and eHPCs cells. All data were calculated for n = 169 changes for HPCs and n = 92 changes for eHPCs, based on at least 3 independent experiments for each cell population.

4.1.3 Dynamics of differentiated hematopoietic cells in the bone marrow

Since we did not detect profound motility of HPC and eHPC *in vivo* it was necessary to put this behavior into the perspective of other bone marrow-resident cells. To describe the motile behavior of differentiated hematopoietic cells in the bone

marrow a well established transgenic mouse model was used, in which macrophages and dendritic cells express a green fluorescent protein (GFP) under control of the fractalkine receptor CX3CR. Tibiae of the transgenic mice were prepared and intravital 2-photon microscopy was immediately started. In the microscopic pictures both cell types could be differentiated from each other by their cell morphology. Macrophages (Figure 29 a), white arrows) were round shaped and markedly smaller than dendritic cells which, in contrast, formed distinct cell clusters and displayed the typical dendritic morphology (Figure 29 a), red arrows) with the typical veiled protrusions.

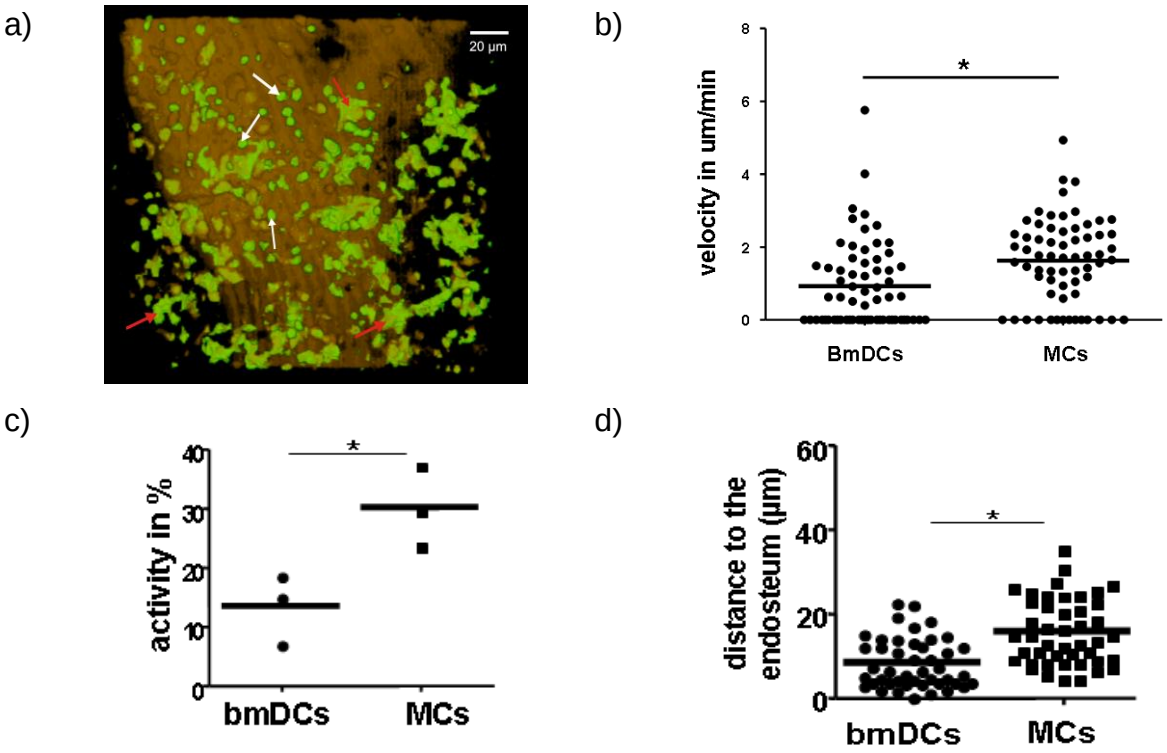

Figure 29 Time-lapse intravital microscopy of BMDCs and macrophages in the tibia. a) Visualization of dendritic cells (red arrows) and macrophages (MCs, white arrows) in the vicinity of the endosteum *in vivo* using the CX3CR-GFP mouse model, in which these cell types are green. The brown color delineates the SHG signal of the calcified bone. b) Quantification of the velocity of dendritic cells and MCs in the BM (n = 65 cells per cell type, based on 3 independent experiments).
c) Activity (meaning the percentage of cells that present with cell position changing migration) of dendritic cells and MCs in the BM, based on 3 independent experiments. d) Distance of BMDCs and MCs to the endosteum (vertical bars representing average). n = 65 cells per cell type, based on 3 independent experiments.

By analyzing the motility of the fluorescent cells, macrophages displayed a significantly elevated cell velocity of 1.6 µl/min compared to dendritic cells showing a

velocity of just 0.9 µm/min (Figure 29 b)). Also activity was markedly higher in macrophages in comparism to DCs (Figure 29 c)). Moreover the distance of both cell types to the endosteal layer was evaluated. The distance was measured between the lower surface of the cell and the SHG-channel of the bone tissue, displayed with a yellow scale bar (view 3.2.4.5.4). All cells were found close to the endosteum, but rarely in direct contact. Notably, dendritic cells were found markedly closer to the inner bone surface than macrophages (8.2 µm to 15.6 µm, Figure 29 d)), suggesting a correlation between close contact to the endosteal layer and cell motility.

4.1.4 Altered localization and elevated dynamics of aged eHPCs

Multiple cellular and molecular mechanisms have been suggested to describe hematopoietic stem cell aging. In this context is was recently postulated that aged stem cells compared to young ones present an altered, less favorable interaction with their stem cell niche [Xing *et al.* 2006]. This finding could in part explain impaired hematopoiesis in aged individuals, because there are hints, that the close interaction of stem cells to their niche is essential for normal hematopoiesis [Geiger *et al.* 2007]. By using an intravital 2-photon microscopy approach we aimed at directly testing this hypothesis.

Table 2 Overview over all detected HPCs and eHPCs, isolated from aged mice in the bone marrow of C57Bl/6 recipients. Two populations were detected, one smaller part in direct contact with the endosteum, the bigger part still in close vicinity, but not in contact. In the right lane the mean distance of all analyzed cells to the endosteum was calculated. n = number of individual animals analyzed.

	Number of all analyzed cells	Percentage of cells with distance to the endosteum	Percentage of cells in direct contact to the endosteum	Mean distance to the endosteum in µm
eHPCs ($L^-S^+K^+$) from aged mice	50 n = 3	88	12	18.05
HPCs ($L^-S^-K^+$) from aged mice	109 n = 3	79.8	20.2	12.38

Interestingly, after transplantation of eHPCs and HPCs from aged mice into naïve

recipients, we found HPCs to be significantly closer located to the endosteal layer compared to eHPCs (12 µm compared to 18 µm). This was exactly opposite to the situation which we had observed in young mice before (19 µm compared to 11 µm). Here the eHPCs were found in smaller distance to the endosteum. Furthermore, comparing the number of HPCs and eHPCs with direct contact to the endosteal layer from young and aged mice, we found that both cell types from older animals were located closer to the endosteum than cells from young mice (table 1 and table 2).

Upon transfer, aged eHPCs, similar to young ones, were detected at solitary spots along the endosteum and were completely immobile (data not shown). Compared to young eHPCs, aged eHPCs were located at sites more distant from the endosteum. They displayed an average distance to the endosteum of 18.1 µm (Table 2) compared with 10.7 µm for young cells; Table 1 and Figure 26 a)). The maximum distance we observed for aged eHPCs was even over 50 µm.

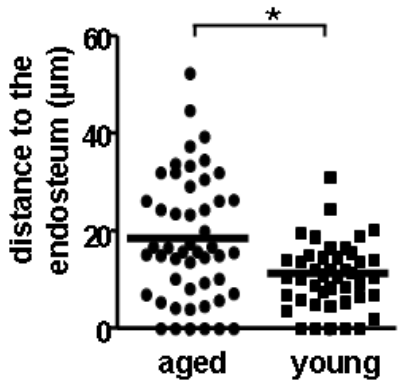

Figure 30 Distance comparison of eHPCs (L-S+K+) isolated from aged versus young mice to the endosteal layer. eHPCs were isolated either from young or aged mice and the distance to the endosteal layer was calculated. Each dot represents a single cell; black horizontal bars depict the average distance. eHPCs from young mice are located significantly closer to the endosteum, compared to eHPCs from aged mice. *p < .05.

Moreover, interestingly, aged eHPCs presented a significantly increased protrusion movement compared to young eHPCS, indicated by increased changes in cell volume between time points (Figure 31 a)), a clearly increased average variance in cell volume change and also an elevated average of the cell surface area (Figure 31 b)).

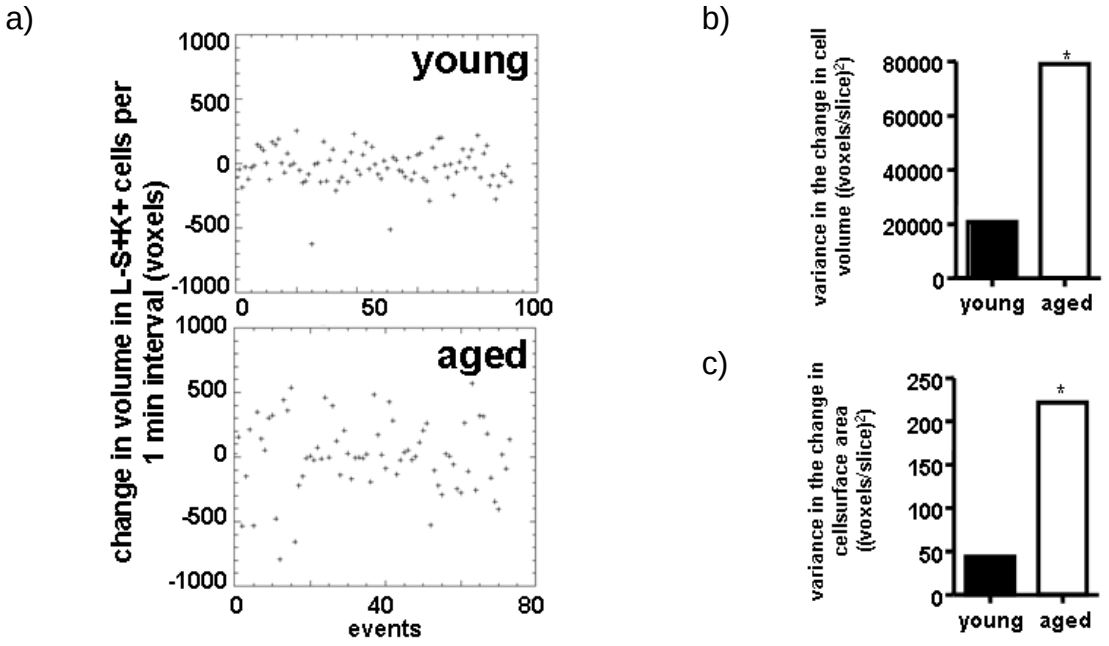

Figure 31 HSCs from aged mice (20- to 24-month-old animals) were fluorescently labeled (CFSE or CTO) and transplanted into young recipient animals. Tibiae from recipient animals were analyzed between 16 and 40 hours after transplantation. a) Quantification of cell protrusion movement, determined as the change in volume over time (interval of 1 minute) of transplanted $L^-S^-K^+$ and $L^-S^+K^+$ cells. b) Average variance in the change in cell volume in a 1 minute time interval of $L^-S^-K^+$ and $L^-S^+K^+$ cells. c) Average variance in the change of the cell surface area in a 1 minute time interval of $L^-S^-K^+$ and $L^-S^+K^+$ cells. All data were calculated for n = 44 for young $L^-S^-K^+$ cells and n = 50 for aged $L^-S^+K^+$ cells, based on at least 3 independent experiments for each cell population.

To further characterize the localization of eHPCs we transplanted young and aged cells into animals with YFP labeled osteoblasts (Col1a1-GFP) [Kalajzic *et al.* 2002]. By analysis of the microscopic data in this model we found that neither young nor aged eHPCs (n = 20 for both cell types) were directly associated with osteoblasts which are located along the endosteal layer of long bones.

4.1.5 Summary - Part I

Our novel approach of intravital 2-photon microscopy allows the first view on cells residing in the bone marrow of murine long bones. We were able to visualize adoptively transferred HPCs and eHPCs in close vicinity to the endosteal layer. Some cells were found in direct contact to the endosteum and they displayed active interactions with their microenvironment but we could not clarify, to which specific cells of the endosteum they establish the close contact. However, most cells

were located farther away from the inner bone surface. No HPC or eHPC show any motility although we could demonstrate by intravital microscopy that other more mature hematopoietic cells like dendritic cells or macrophages are motile in the same microenvironment. Instead of motility, all cells displayed an active protrusion movement that we determined with new algorisms that could analyze the changes in cell volume and cell surface area. On the basis of these calculations we found a tendency of HPCs to be more active than eHPCs. Then we focused on the differences between eHPCs from aged and young mice. We found eHPCs to be located more distantly from the endosteal layer compared to eHPCs from young animals. Moreover, cells from old animals revealed a significantly increased protrusion activity. These data suggest that cells in close contact to the inner bone surface are more quiescent than cells with more distance to the endosteum.
This part of the work was published in Blood 2009 [Kohler *et al.* 2009].

4.2 Part II: Analysis of G-CSF mediated neutrophil emergency release from the bone marrow of murine long bones

In many infection models, neutrophils are rapidly mobilized from the bone marrow into the peripheral blood from where they are then recruited to sites of acute infection. At these places they play an important role in the immunological fight against invading pathogens. In many different studies it has been shown that G-CSF is crucial for this emergency release [Metcalf *et al.* 1996; Shahbazian *et al.* 2004; Knapp *et al.* 2004; Cataisson *et al.* 2006; Gregory *et al.* 2007] but the underlying mechanisms how G-CSF induces acute neutrophil mobilization still remain largely unknown. This lack of knowledge is highly noteworthy because of the fact that the mobilizing features of G-CSF have been used in clinical applications for more than 20 years to reconstitute neutropenic patients.
In order to clarify how neutrophils react in response to a systemic G-CSF trigger on the single cell level *in vivo* and to investigate the immediate cell-intrinsic processes induced by this treatment we used our established technical approach of intravital 2-photon microscopy in the long bones of mice.

4.2.1 Visualization of the inner bone surface and blood staining for 2-photon microscopy

In the beginning of this project we expanded our method of intravital 2-photon microscopy in murine long bones. After the preparation a remaining bone layer of about 30 - 50 µm was maintained to ensure a closed bone marrow cavity, unaffected by external influences (Figure 32 b)). By the use of new advanced microscopy hardware, a much more detailed view into the bone marrow cavity with a drastically increased optical resolution was possible. For the first time the remarkably structured endosteal surface of the tibia was visible, with a lot of indentations (Figure 32 a)). This structure could also be much better presented in an angular perspective and it was reminiscent of a crisp bread slice (Figure 32 b)). A closer look on the invaginations revealed, that they formed small craters and some of them ended up in tiny canals which completely crossed the remaining bone layer (Figure 32 c) – f)).

Additionally, a blood vessel staining with rhodamine-dextran was included in all imaging approaches. This was important to determine the expected release of neutrophils from the bone marrow into the blood flow. Immediately after retro-orbital injection of the dye the vessels could be seen during 2-photon acquisition with a filter detecting wavelengths between 565 – 610 nm. This fact also served to demonstrate an intact blood supply of the bones during our investigations. Bigger vessels were found in deeper regions of the marrow. With closer distance to the endosteum the vessels became thinner and just beneath the inner bone surface they strongly branched into a filamentous network and lined the entire bone structure (Figure 32 g)). Moreover, it was conspicuous that blood vessels crossed the bones through the observed canals, indicating a consistent blood exchange with the environmental tissue (Figure 32 h)).

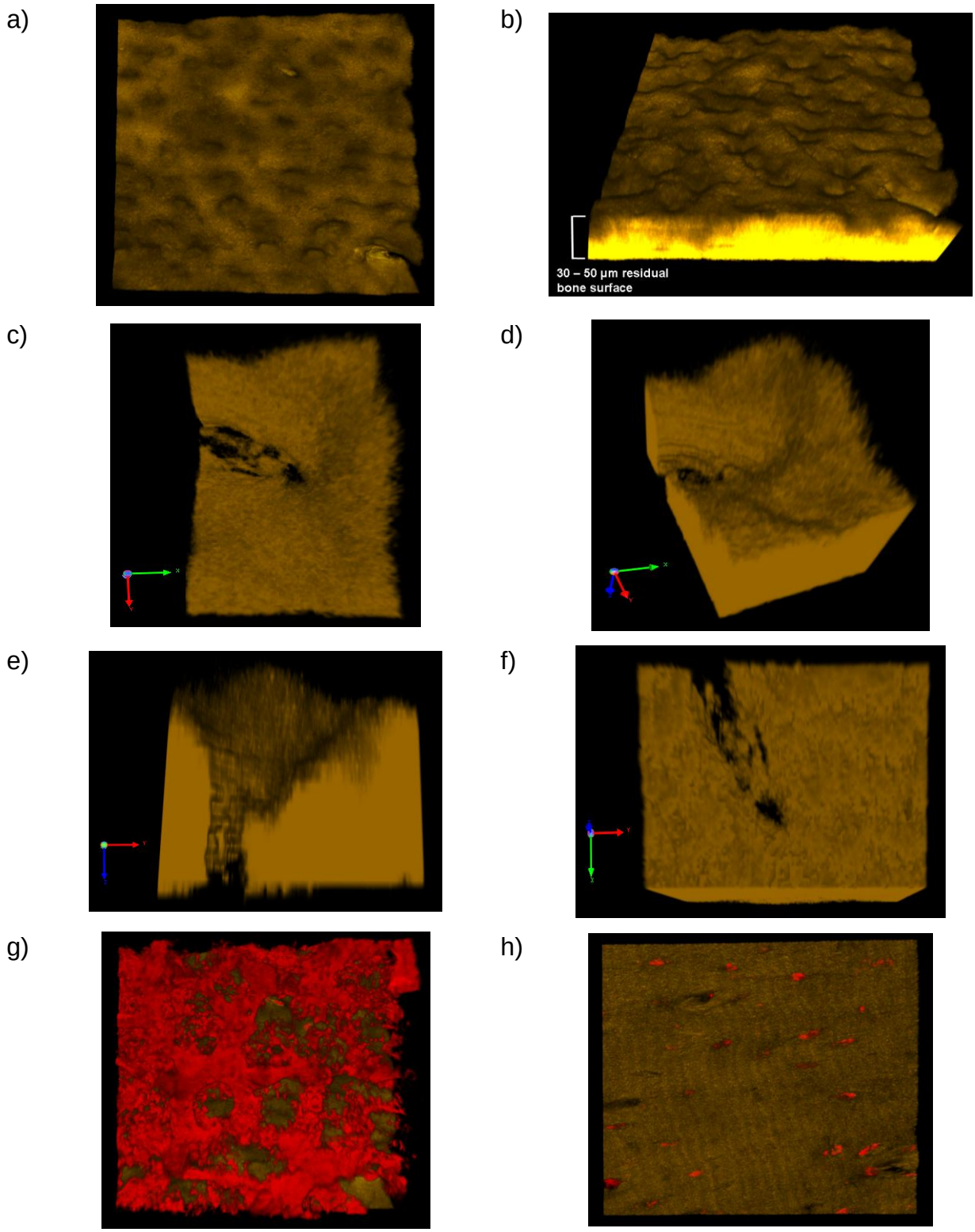

Figure 32 Visualization of bone structure and blood vessels. a) Top view on the inner bone surface of murine long bones, detected by its SHG signal. b) An angular view revealed a crisp bread-like structure of the inner bone surface, with lots of indentations. c) – f) A closer look on the small invaginations revealed that some end up in small channels which cross the entire bone layer g) A blood vessel staining with rhodamine-dextran showed an intimately connected network of vessels close to the endosteal layer. h) A view from the outside on the bone surface after blood vessel staining demonstrated, that many pores constitute channels for blood vessels. View supplemental movie 5.

4.2.2 G-CSF treatment induces rapid neutrophil mobilization into the peripheral blood

In order to specify the kinetics of neutrophil mobilization for further analysis we started with assessing the neutrophil number in the peripheral blood after a single, retro orbital injection of G-CSF. A volume of 75 µl blood was taken repetitively from the same animals by retro-orbital puncture at different time points after G-CSF injection (4 h, 8 h, 12 h, 16 h, 25 h). These blood aliquots were analyzed by FACS for the percentage of Gr-1 positive cells. 0 h reflected a first sample collection immediately before the injection. A constant increase of neutrophils in the peripheral blood from around 15 % up to over 40 % was measured in the samples taken within the first 12 h. At later time points (25 h after injection) the cell number slightly decreased to about 28 %. Unfortunately, there was no significant difference between G-CSF and PBS treated animals (Figure 33 a)). One explanation for this observation could be that the repeated bleeding procedure as such was responsible for neutrophil mobilization also in the control animals. To exclude this effect the number of blood drawings was reduced to only two collections right before G-CSF or PBS injection and 12 h after the treatment (Figure 33 b)). Again, there was no significant difference in the measured numbers of Gr-1 positive cells, comparing G-CSF and PBS injected mice. The measured percentages at the two time points assembled around 20 % and the highest neutrophil number was even found in the blood sample which was taken before G-CSF treatment. Moreover, there was a high standard deviation in the samples which were collected before injection of either agent. It was known from the literature that female, 8 weeks old C57Bl/6 mice which were used for the experiments should constantly carry 7.35 % (percent of total white blood cells) circulating neutrophils in their peripheral blood under unstimulated conditions [http://phenome.jax.org]. By this number it became clear that neutrophils in the analyzed animals were already pre-mobilized by the blood drawing procedure and that this protocol had to be optimized.

a) b)

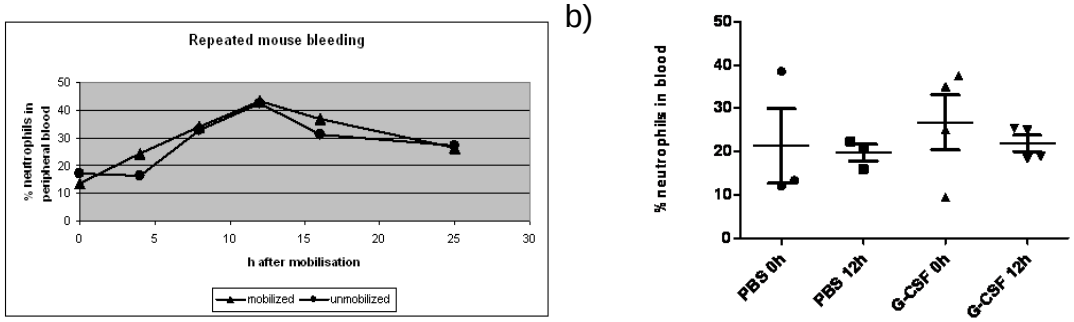

Figure 33 Neutrophil mobilization into peripheral blood after a single i.v. injection of G-CSF. a) Kinetics of the increase in neutrophil cell number in the peripheral blood upon mobilization with G-CSF or with PBS as unmobilized control after repetitive bleeding. b) To reduce repetitive blood drawing and thereby minimizing the pre-mobilizating effect of this procedure just 2 time points per injected animal were considered. n = 3 – 4 animals were analyzed for each time point.

From now on the animals were housed as calmly as possible and all unnecessary transports were avoided to exclude any side effects of mouse treatment on the neutrophil behavior. To completely avoid repetitive bleeding we decided to focus on a time point 2 h after administration of the mobilizing agent for blood withdrawal. This time point was chosen according to published reports [Wengner *et al.* 2008] showing that 2 h after triggering neutrophils with G-CSF a first peak of mobilized cells in the blood should be detectable.

To clarify the impact of an injection on neutrophil mobilization into the blood we then tested different injection routes. Double retro orbital injections (i.v.) with PBS followed by G-CSF led to a strong neutrophil mobilization into the blood flow after 2 h. Interestingly we found that a double injection of only PBS mobilized the cells just as well as a single treatment with G-CSF. A single i.v. injection of PBS led to the lowest increase of Gr-1 positive cells in the blood, but also this single control injection recruited neutrophils compared to a completely untreated animal (Figure 34 a)). These same four injection conditions were then repeated for an i.p. route and an i.v. administration into the tail vein. Strong neutrophil mobilization into the peripheral blood could be observed ranging from 40 % to 70 % (Figure 34 b) and c)) in all settings. In a last experiment retro orbital and i.p., single or double injections of PBS were compared. An additional mouse group was only pricked on the two injection time points without any injection. This should clarify how sensitive the cells reacted on external interferences unavoidable in conjunction with the planned experiments. The analysis of this prick-test clearly demonstrated, that all kinds of

repeated mouse treatment activated neutrophils and led to their recruitment into the peripheral blood (Figure 34 d)).

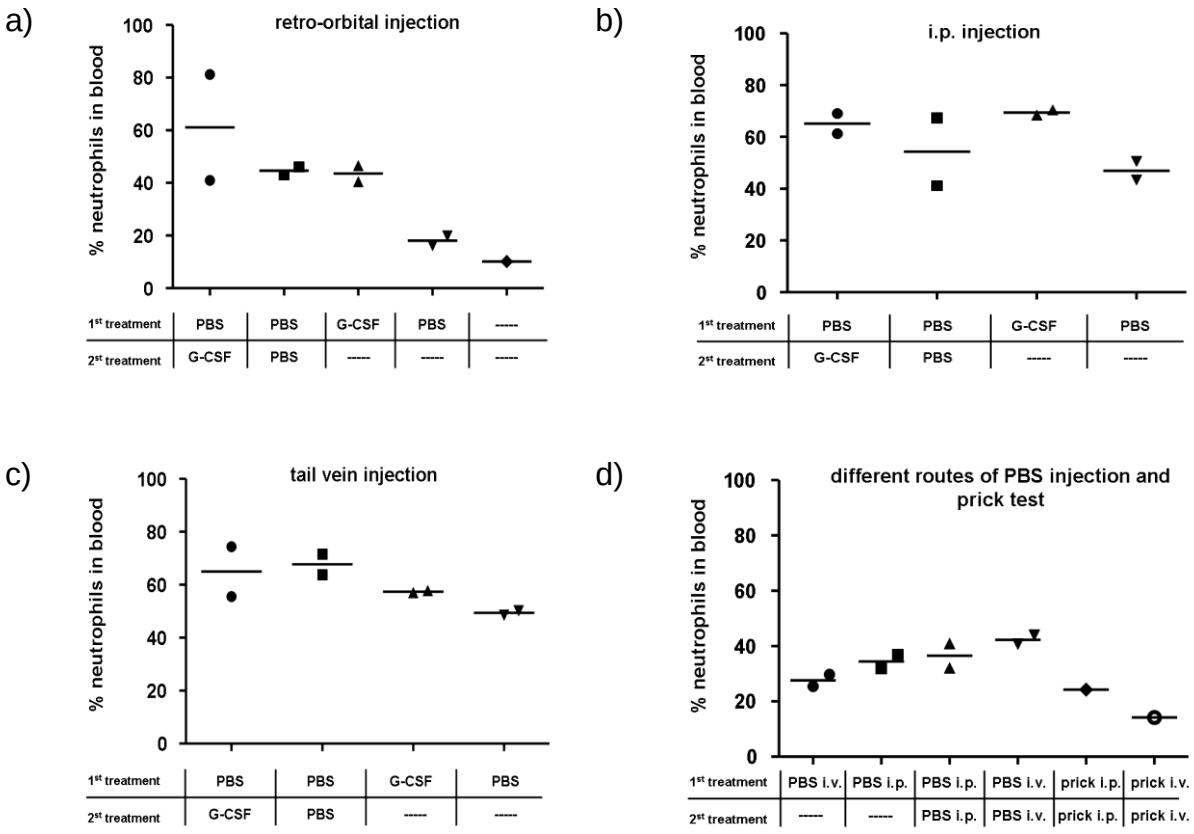

Figure 34 Neutrophil mobilization caused by different injection methods. Different application routes led to an unspecific mobilization of neutrophils. The 2nd treatment was performed 20 minutes after the 1st one. Upon a) retro orbital i.v. injection, b) i.p. injection or c) i.v. injection into the tail vein of different PBS/G-CSF combinations the recruitment of neutrophils into the peripheral blood was assessed. d) For the prick test a 27 G cannula was pierced into either the peritoneum or behind the eye without any injection. 2 h after the last treatment 75 µl blood were drawn from each animal and analyzed for the number of circulating neutrophils by Gr-1 specific FACS analysis. n = 1 – 2 animals were analyzed for each condition.

By comparing the different injections and combinations it became obvious that the injection route and the frequency of treatments had a strong influence on the number of peripheral blood neutrophils. Based on these results we redefined our neutrophil mobilization protocol for G-CSF.

First of all the animals were handled much more carefully now throughout all procedures. The retro orbital injection was chosen as optimal protocol, because it induced the lowest mobilization of neutrophils with PBS as a “trigger”. Furthermore

G-CSF was injected once, 2 h before investigation of the mobilization status and blood withdrawal was reduced to one terminal time point. With these changes implemented the results became much more consistent (Figure 35 a) and c)) and a very reproducible and clear mobilization of neutrophils into peripheral blood was measureable. Besides the neutrophil Gr-1 high positive cell population, a second, Gr-1 intermediate cell type was detected by FACS analysis. This population was identified as macrophage type by an anti-F4/80 antibody staining (Figure 35 b)). Also the number of these cells was strongly increased after G-CSF mobilization (Figure 35 d)).

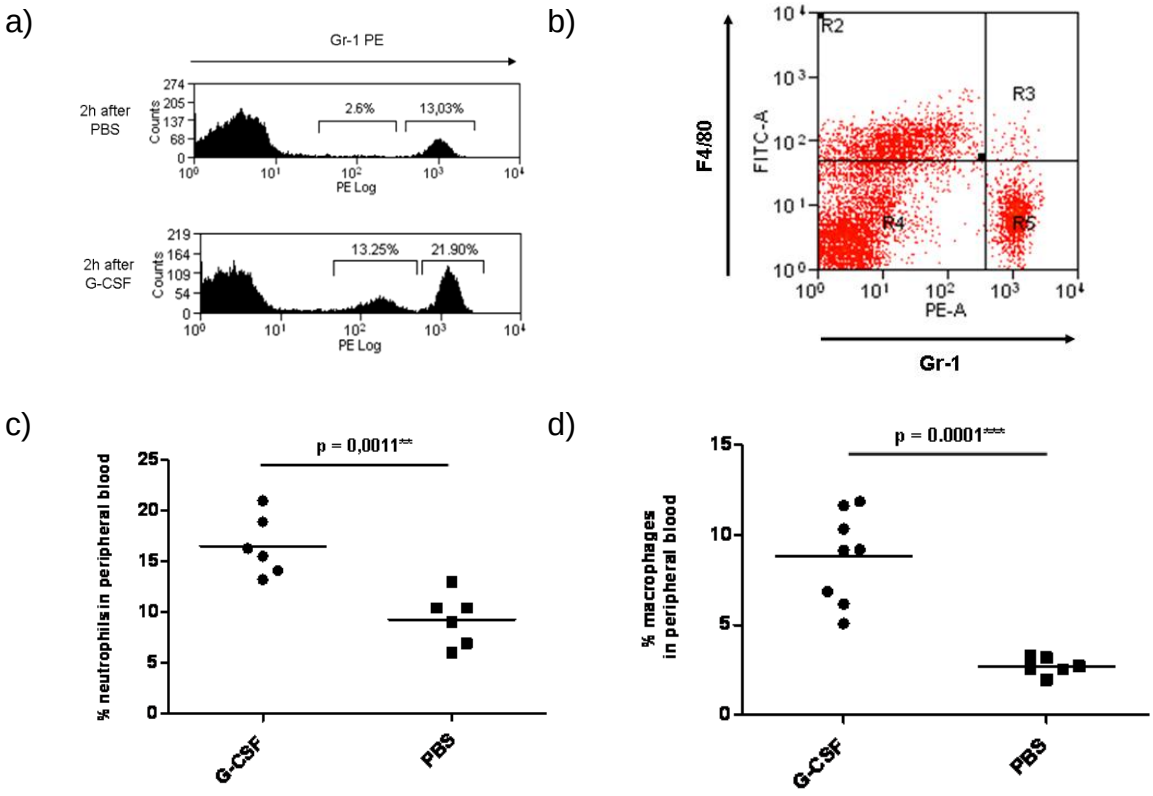

Figure 35 Neutrophil mobilization into peripheral blood upon G-CSF injection. a) 2 h after retro orbital G-CSF injection blood was collected and analyzed for the percentage of Gr-1 high neutrophils and Gr-1 intermediate cells that were recruited into the peripheral blood. Control animals received an equal volume of PBS. b) The Gr-1 low cells were identified to be macrophages by antibody staining with F4/80 c) Statistical analysis of neutrophil recruitment. The mobilization experiment was repeated in 6 unrelated animals. d) Statistical analysis of macrophage recruitment. N = 6 animals were analyzed in this experiment. The result was representative for three independently performed experiments.

4.2.3 Dramatic increase of neutrophil motility in the bone marrow after G-CSF injection

The strong and rapid mobilization of neutrophils into peripheral blood suggested that this phenomenon could also have a detectable impact on the single cell behavior in the bone marrow, which is known as the main reservoir for mature neutrophils. To test this hypothesis our well established protocol for intravital 2-photon microscopy in murine long bones was used. The visualization of neutrophils was realized by using a transgenic mouse model, in which EGFP was expressed under control of the neutrophil specific lysozyme M promoter (LYS-EGFP mice) [Faust *et al.* 2000]. Therefore most of the mature neutrophils were fluorescently tagged in these animals. Rhodamine-dextran and likewise G-CSF were injected i.v. right before start of the preparation procedure to ensure that both substances reach the vasculature of the bone marrow simultaneously shortly before the onset of imaging. The fluorescently labeled dextran was used to visualize blood flow in the animals and thereby to provide an internal life status control. Control animals received PBS instead of G-CSF. After about 30 minutes of preparation the image acquisition was started to record three time sequences of about 30 minutes at three different areas. So in total a time period of 1-3 h after G-CSF administration was investigated. 20-30 cells per sequence were then analyzed for their velocity and activity.

In the PBS injected mice around 35 % of neutrophils were motile, denoted in activity. The velocity was measured to be at a population mean of 1.8 µm/min. However, after systemic G-CSF administration a dramatic increase in the overall motility of neutrophils was observed. Their velocity rose to a mean of 3.6 µm/min with some cells migrating at velocities >15 µm/min (Figure 36 a)). The migratory activity of the neutrophil population escalated to a mean of almost 60 % of living cells reaching almost 80% in some animals (Figure 36 b)). This observation was underlined by performing a kinetic overlay of three pictures of a movie sequence where localization changes are marked in color (Figure 36 c)). With this analysis it could be seen very easily that cells displayed a clearly higher motility after G-CSF treatment than cells from mice treated with PBS.

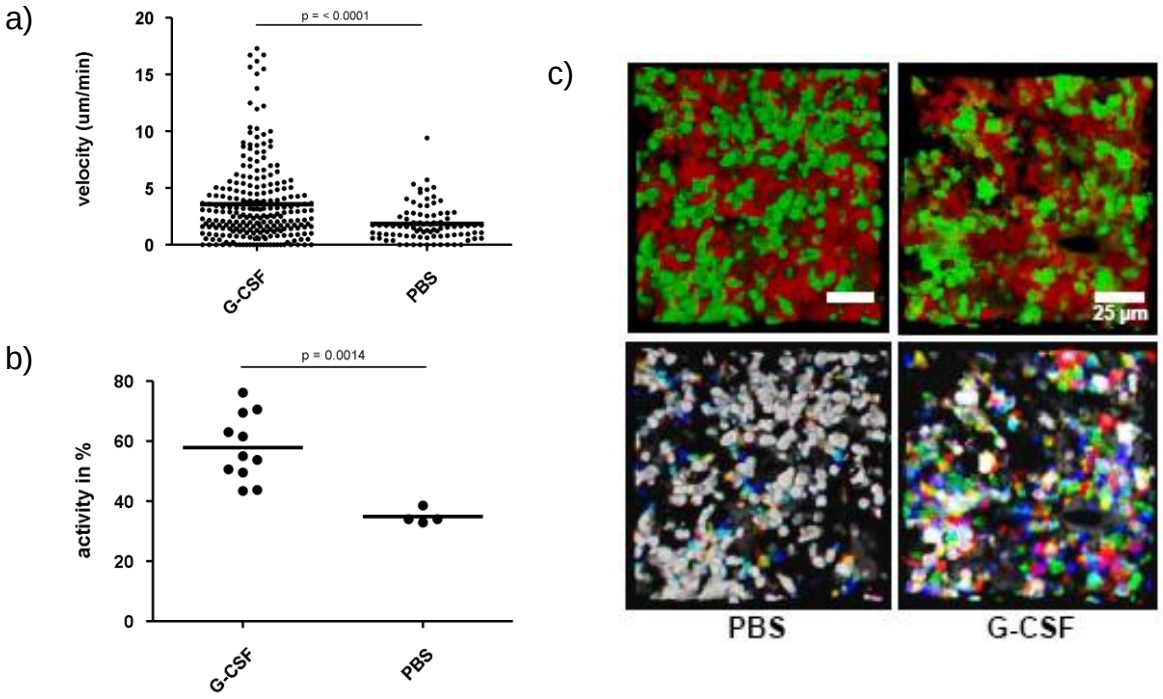

Figure 36 Influence of G-CSF injection on the migratory behavior of individual neutrophils in the bone marrow. a) and b) The overall cell velocity and activity of neutrophils significantly increased in the tibial BM 1-3 h after triggering with G-CSF. n = 11 animals were analyzed after G-CSF administration, n = 4 animals were analyzed after PBS treatment. c) A kinetic overlay of three sequential pictures also demonstrated a higher motility of neutrophils in mice which were treated i.v. with G-CSF. The changes of cell localization from picture to picture were marked with different colors. View supplemental movie 5 (2 h after PBS treatment) and 6 (2 h after G-CSF treatment). View supplemental movie 6 and 7.

Additionally we found a stronger tendency of neutrophils to leave the BM via blood vessels upon stimulation with G-CSF compared to PBS controls. The vessels of G-CSF treated animals appeared somehow destroyed, which could be caused by a massive influx of mobilized cells (Figure 36 c)). This invasion process of the vasculature by neutrophils could be observed in our intravital microscopy set-up. Cells entering the vasculature appear yellow because of the spectral overlap of green fluorescent cell bodies and the blood vessels stained in red (Figure 37). After administration of G-CSF an accumulation of neutrophils was observed in several distinct areas of the image. Regarding these observations we speculated that the cells swarm to defined vascular egression sites along the vessels, where a bottleneck arises. This could result in such an accumulation because not all cells were able to leave the marrow at the distinct exits coincidentally (Figure 37).

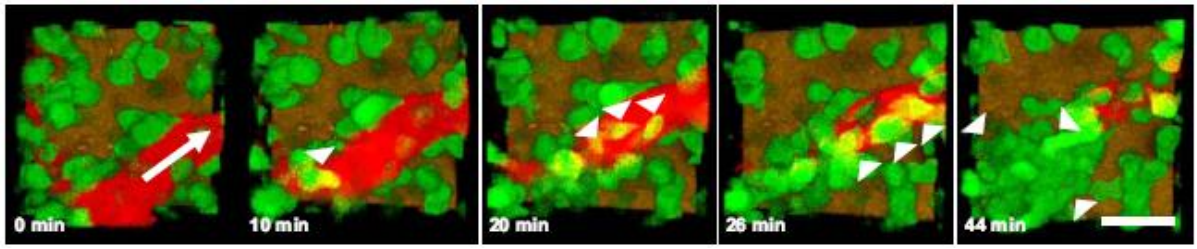

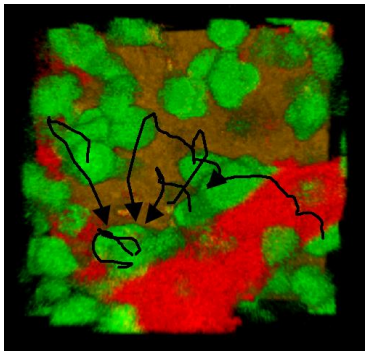

Figure 37 Neutrophils leave the BM into the vasculature upon stimulation with G-CSF. White arrowheads indicate single egression events. More or less all cells when motile showed a trend to migrate to distinct bottlenecks, where a swarm formation could be observed indicated by black arrows. View supplemental movie 8.

4.2.4 Long term behavior of neutrophils upon G-CSF stimulation

After characterization of the immediate early cell response towards G-CSF triggering we went on to analyze neutrophil activity and velocity over a time span of 6 h upon a single G-CSF injection in the same animals. 0 h after G-CSF administration the cell velocity remained at a level of unmobilized animals (1.7 µm/min) but already 1 h after mobilization the neutrophil velocity suddenly peaked at 4.5 µm/min. After 2 h the velocity started to slightly decrease to 3 µm/min after 4 h. Then a second peak of increasing cell velocity could be observed at around 5 h (Figure 38) after which the velocity constantly decreased until all cells stopped moving at around 12 h after experimental onset, probably due to the very long narcosis of the animals (data not shown).

As a control, one mouse was injected with G-CSF and directly killed by cervical dislocation. In the first 2 h hours the neutrophil velocity was comparable to a living animal but then it strongly decreased and after 4-5 h there was no cell motility detectable anymore (Figure 38, red dots). This observation proofed, that the other animals were definitely alive during the imaging procedure and that cells were obviously provided with all substances they needed for survival and motility. But there was still the question, how long neutrophils in a prepared and narcotized animal were able to exhibit their normal cell behavior like in an unopened mouse. A decrease in cell motility after several hours was expected, due to the narcosis, the cooling of the animal and the diminished blood pressure and blood glucose level because of a lacking nutrient supply. To answer this question, we injected animals

once with G-CSF but started the preparation and imaging 6 h, 12 h and 16 h after the treatment in individual mice. We found a constant level of 2 - 2.5 µm/min velocity at the indicated time points, showing that neutrophils stay in an activated status up to 16 h after a single G-CSF injection (Figure 38).

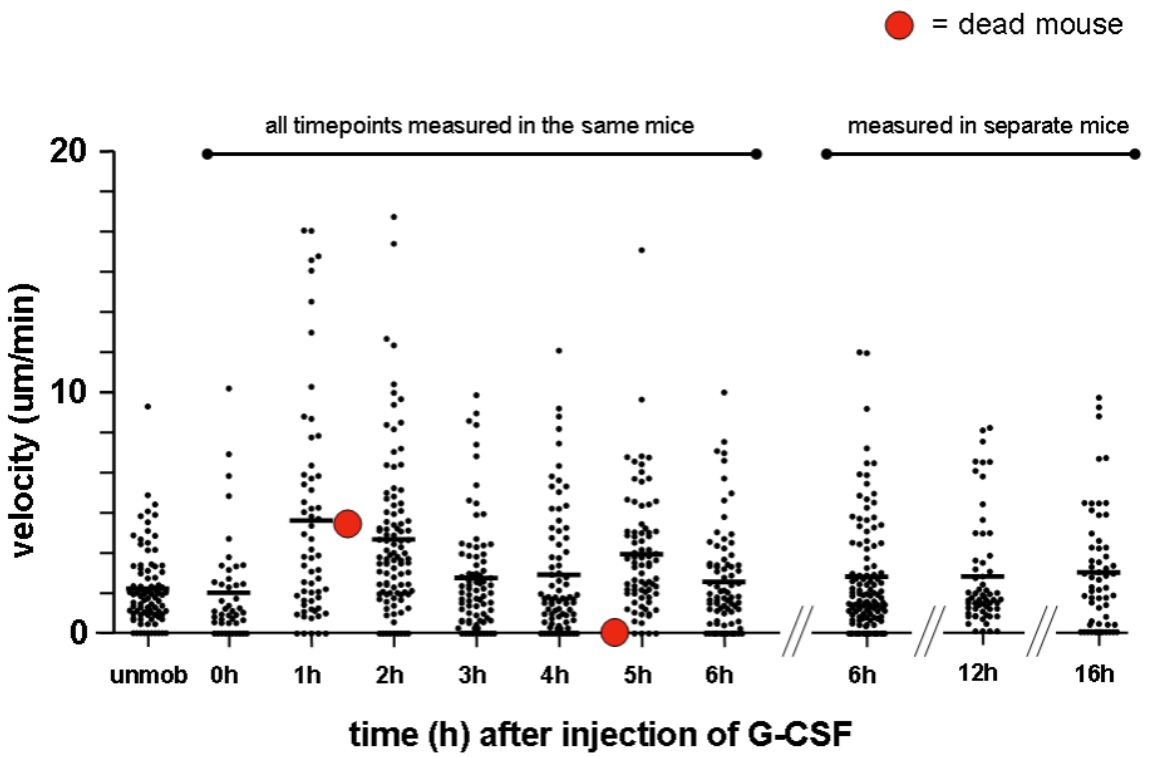

Figure 38 Long term development of neutrophil velocity upon stimulation with G-CSF. 2-photon acquisition was performed on BM neutrophils upon a single injection of G-CSF where on the left side of the graph individual animals were observed over 6 h. For comparison the 6 h, 12 h and 16 h time point was also investigated in animals which were freshly prepared after each time interval (right hand side). n = 4 mice unrelated were analyzed over 6 h, at time point 0 h just two animals and at time point 1 h just three animals could be measured for technical reasons. The red dots revealed the cell velocity in mice which received one G-CSF injection and where then killed immediately. n = 6 unrelated animals were prepared and analyzed 6 h after G-CSF injection, n = 3 unrelated animals were prepared and analyzed 12 h and 16 h after G-CSF injection.

Comparable results were obtained by analyzing the cell activity. This value peaked 1 - 2 h after G-CSF administration and like seen with the velocity, also again after 5 h. Comparable to the velocity, the activity almost doubled from 35 % in unmobilized animals to over 60 % in G-CSF treated mice after 1 h (Figure 39). Interestingly in contrast to the velocity the activity directly increased after mobilization at time point 0 h, suggesting that an elevated activity might be a hallmark of cells which have been disassociated from their stromal connections usually holding them back

in the bone marrow. In the control groups with individual mice for every time point also the activity stayed increased but, surprisingly, there was a third peak of neutrophil activity present after 12 h (Figure 39).

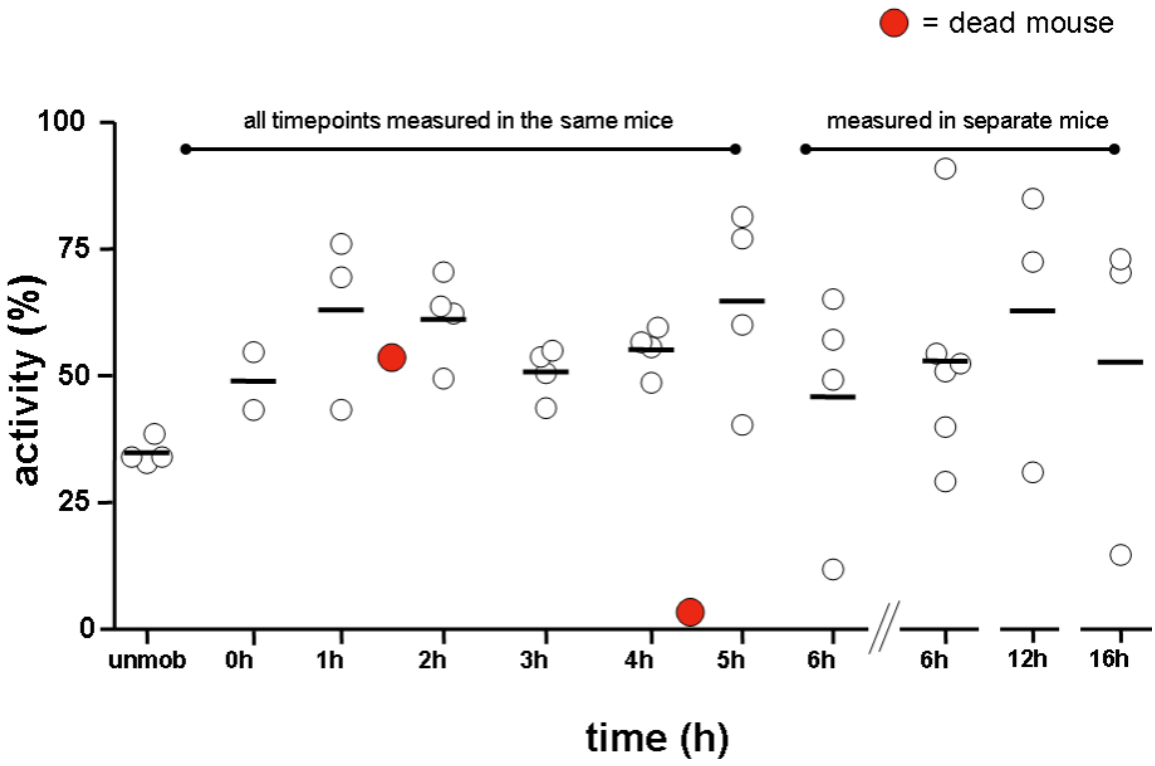

Figure 39 Long term development of neutrophil activity upon stimulation with G-CSF. Intravital 2-photon microscopy was performed on BM neutrophils following a single injection of G-CSF where on the left side of the graph individual animals were observed over 6 h. In comparison the 6, 12 and 16 hour time point was also investigated in animals which were freshly prepared after each time interval (right hand side). n = 4 mice were analyzed over 6 h, at time point 0 h just two animals and at time point 1 h just three animals could be measured for technical reasons. The red dots revealed the cell activity in mice which received one G-CSF injection and where then killed immediately. n = 6 unrelated animals were prepared and analyzed 6 h after G-CSF injection, n = 3 unrelated animals were prepared and analyzed 12 h and 16 h after G-CSF injection.

Taken together the acquired activity and velocity data suggested that it was possible to investigate a prepared and anesthetized animal for a maximum of 6 h in a constantly running 2-photon experiment. After this time interval the neutrophil motility dramatically went down and did not show normal activated cell behavior anymore like in freshly prepared animals.

4.2.5 Monocyte mobilization with G-CSF in CX3CR-EGFP mice

To verify if G-CSF only leads to an increased neutrophil motility in the bone marrow or if also other cell types like macrophages are affected we performed 2-photon microscopy in the long bones of a transgenic mouse line which expressed EGFP under control of the fractalkine receptor CX3CR1 (CX3CR-EGFP mice). These animals possess green fluorescent macrophages and dendritic cells [Jung *et al.* 2000]. Both cell types could be clearly divided from each other by their very different cell morphology. A kinetic overlay after movie acquisition already strongly suggested that compared to an unmobilized mouse (Figure 40 b)), no increase in cell motility of CX3CR-expressing cells was detectable upon G-CSF treatment of the animals (Figure 40 a)). For technical reasons it was not possible to detect the bone signal in the control animal which received PBS (Figure 40 b)).

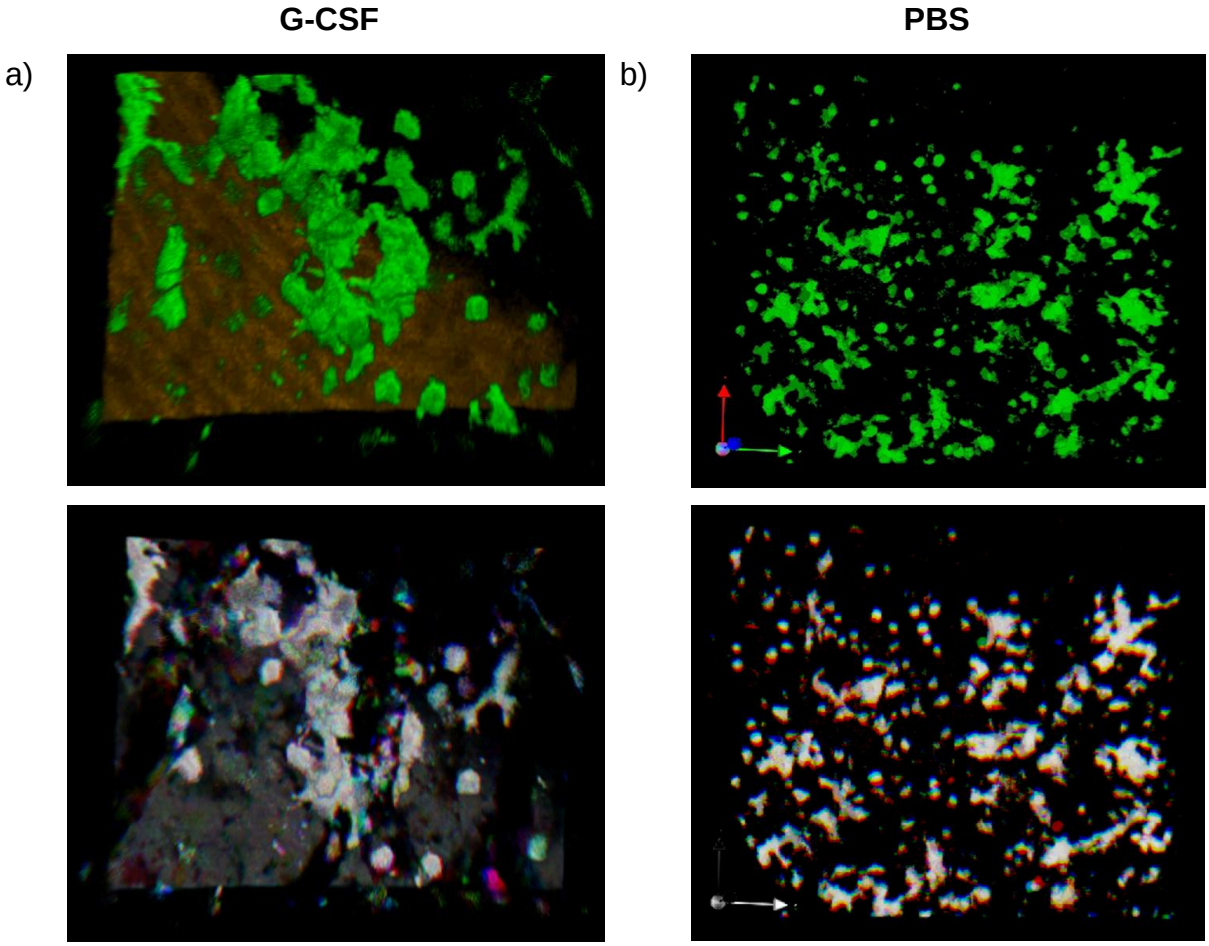

Figure 40 Macrophages and dendritic cells did not display altered cell motility upon stimulation with G-CSF. CX3CR-EGFP mice were injected either with G-CSF or PBS. Intravital 2-photon microscopy was performed 1-3 h after injection. A kinetic overlay of three sequenced pictures displayed no increase in cell motility of both morphotypes (DCs and macrophages) after a) G-CSF treatment compared to b) PBS injection. View supplemental movie 9.

These findings were then validated by measuring the velocity and activity of macrophages 2 h after G-CSF treatment. Interestingly we found that the velocity of macrophages was decreased 2-fold from 1.6 µm/min to 0.8 µm/min after stimulation with G-CSF. The same tendency could be observed for the activity of these cells, although not reaching the level of statistical significance (Figure 41).

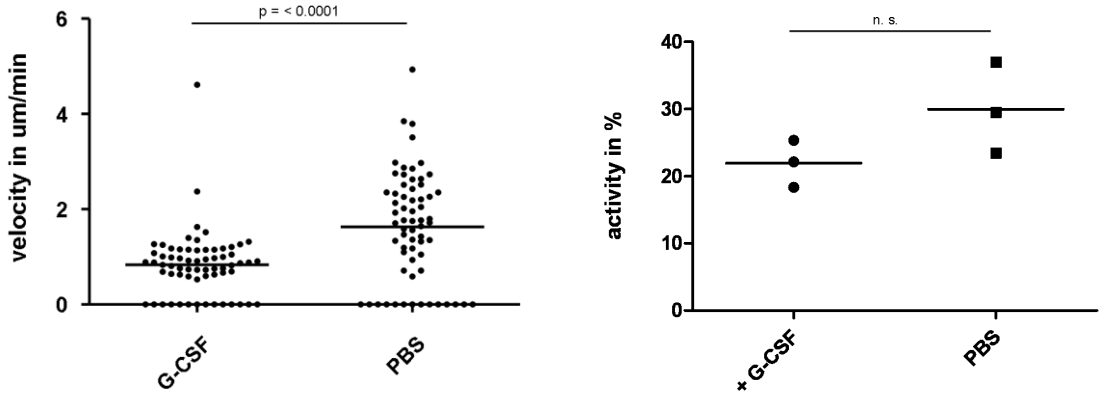

Figure 41 Analysis of macrophage motility with intravital 2-photon microscopy. Macrophages show no mobilization after an injection of G-CSF when analyzed for a) cell velocity and b) cell activity. The movies were recorded 1-3 h after G-CSF injection or after treatment with PBS control. n = 3 animals were analyzed independently for each condition.

4.2.6 Inhibition of G-CSF-induced neutrophil mobilization

In the next step we aimed at clarifying the molecular mechanisms which were crucial for the observed rapid neutrophil mobilization in response to a systemic G-CSF application. It is well known from several inflammation models [Kobayashi 2006; McColl *et al.* 1999; Gordon *et al.* 2005; Lally *et al.* 2005], that the proinflammatory chemokines KC (CXCL1) and MIP-2 (CXCL2) mediate a remarkable recruitment of neutrophils to sites of inflammation. To find out if KC or MIP-2 were also relevant mediators in case of a G-CSF induced neutrophil mobilization, monoclonal anti-KC and anti-MIP-2 antibodies were used to block neutrophil release from the bone marrow into the peripheral blood.

To demonstrate that the anti-KC and anti-MIP-2 antibodies worked in terms of blocking a neutrophil recruitment, a recently published model of acute peritonitis was used [Wengner *et al.* 2008]. The combined administration of both antibodies upon induction of the peritonitis led to a significant reduction of neutrophil counts in the peripheral blood and there was also a considerable but not significant neutrophil decrease in the peritoneal lavage detectable (Figure 42 a) and b)).

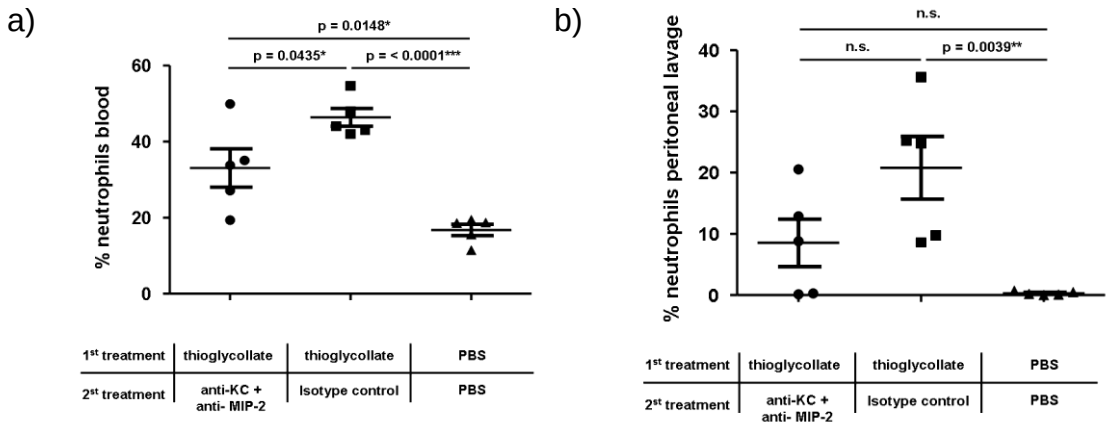

Figure 42 Administration of anti-KC and anti-Mip-2 antibodies blocked neutrophil mobilization in a mouse model of acute peritonitis. Anti-KC and anti-MIP-2 antibodies were injected 20 minutes before thioglycollate treatment. Neutrophil counts in either a) the blood or b) peritoneal lavage were assessed 2 h after induction. Control mice received PBS twice in the same time period instead. n = 5 animals were analyzed for every condition.

Afterwards we used these antibodies in our model of G-CSF mediated neutrophil mobilization. Both antibodies were injected simultaneously i.p. 18 h - 48 h before G-CSF administration to avoid a pre-stimulation of neutrophils (Figure 33 and 34). 2 h later peripheral blood was collected and analyzed for the percentage of circulating neutrophils. Control animals received unspecific antibodies of the same isotype and PBS after 48 h as vehicle control for G-CSF. However, FACS analysis showed no significant reduction of circulating neutrophils 2 h after treatment with anti KC/MIP-2 in the blood of mice (Figure 43).

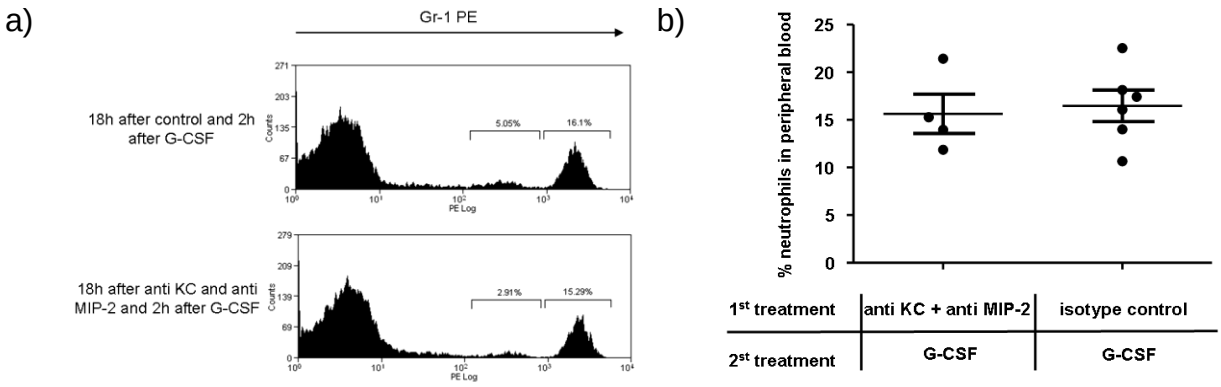

Figure 43 No reduction of G-CSF induced neutrophil mobilization after anti-KC and anti-MIP-2 treatment. Mice were injected i.p. with anti-KC and anti MIP-2 antibodies 16 h or 46 h before G-CSF treatment. 2 h later blood was collected and the FACS analysis was performed. n = 4 – 6 animals were analyzed for every condition.

In addition to the FACS analysis the antibodies were also tested in a 2-photon microscopy approach. Animals were treated with anti KC and anti MIP-2 in the same way as for the recruitment experiments and the *in vivo* behavior of cells was observed in the tibial BM. The development of neutrophil motility in response to systemic G-CSF matched the FACS results. Despite the antibody treatment there was only a very slight decrease in the activity of cells, which was not statistically significant and also the neutrophil velocity remained at almost the same level as compared to control-treated animals (Figure 44).

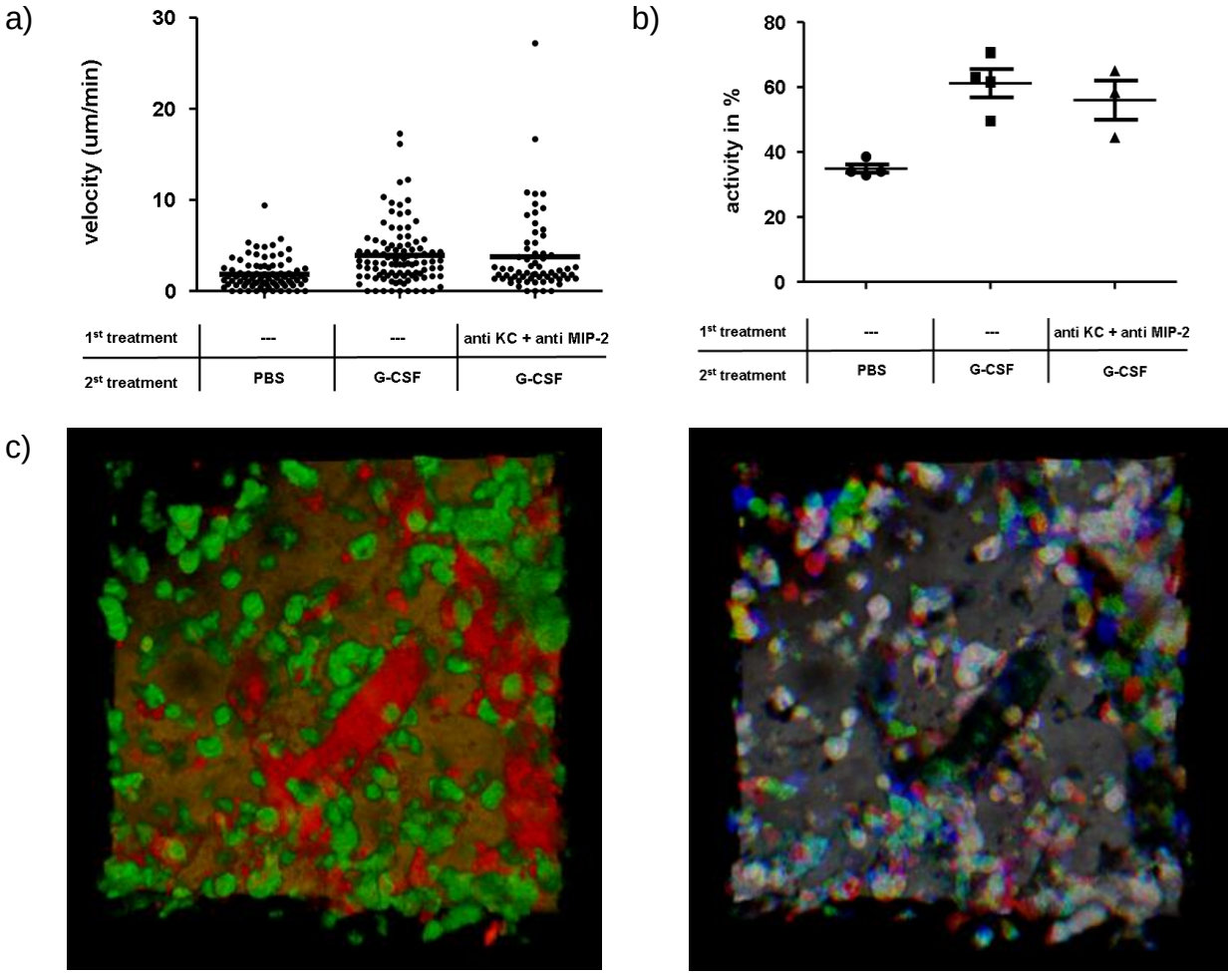

Figure 44 Intravenous treatment of mice with anti-KC and anti-Mip2 antibodies does not alter neutrophil mobilization on a single cell level. 18 h after before G-CSF mobilization anti-KC and anti-MIP-2 antibodies were injected. Despite antibody administration neither a) the velocity nor b) the neutrophil activity was significantly reduced. c) This result was also confirmed by a kinetic overlay. n = 3 - 4 animals were analyzed independently. View supplemental movie 10.

Although we were not able to inhibit neutrophil mobilization from the BM by application of anti-KC and anti Mip-2 antibodies our cooperation partner (Nancy Hogg,

London, UK) was able to detect a peak of KC appearance in the peripheral blood 45 min. after G-CSF injection by an enzyme-linked immunosorbent assay (ELISA, data not shown). This suggested that at least KC was released as a consequence of G-CSF treatment and thus might play a role in neutrophil mobilization.

4.2.7 Inhibition of neutrophil recruitment into the peripheral blood after CXCR2 antiserum treatment

As an alternative to inhibit the chemo-attractive action of KC and Mip-2 we then focused on blocking the surface receptor for both chemokines, the CXC receptor 2 which is highly expressed on neutrophil granulocytes [Bozic *et al.* 1994]. For the experiments a polyclonal CXCR2 antiserum was employed which had been shown before to potently inhibit neutrophil recruitment to an inflamed central nervous system (CNS) [Carlson *et al.* 2008a; Hosking *et al.* 2009]. 100 µl CXCR2 antiserum were injected i.p. 48 h before G-CSF administration and blood was taken for analysis another 2 h later. Control animals received the same volume of normal rabbit serum (NRS).

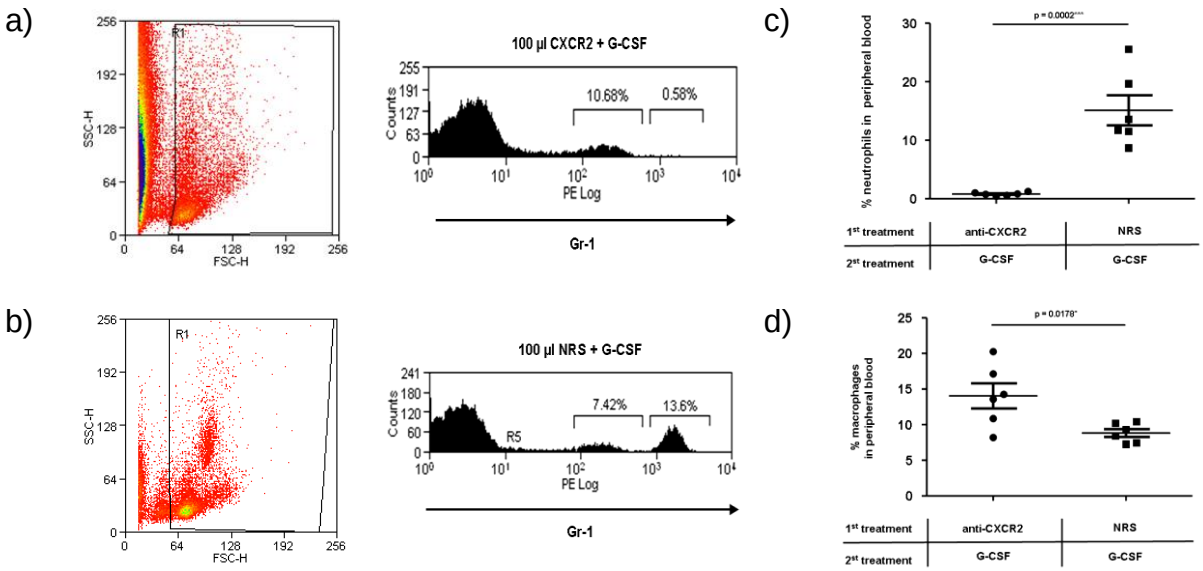

Figure 45 Administration of an anti-CXCR2 antiserum entirely blocks neutrophil recruitment to the peripheral blood. a) Antiserum treatment of mice 48 h before G-CSF injection dramatically decreased neutrophil counts in the blood b) compared to the administration of an unspecific immune serum (NRS). c) A statistical analysis revealed the strong significance. d) The mobilization of macrophages is not inhibited by anti-CXCR2, rather it slightly increase their number. n = 6 animals were analyzed for each condition. The result was representative for three independently performed experiments.

Following this protocol we observed an almost complete inhibition of neutrophil entry into the blood flow upon G-CSF stimulation by FACS analyses (Figure 45 a) and b)). A statistical analysis of these data also revealed a dramatic decrease of neutrophil numbers in the circulation after CXCR2 antiserum treatment in contrast to control animals which received NRS (Figure 45 c)). Additionally it was conspicuous that the number of macrophages expressing intermediate levels of Gr-1 was not affected by the antiserum treatment.

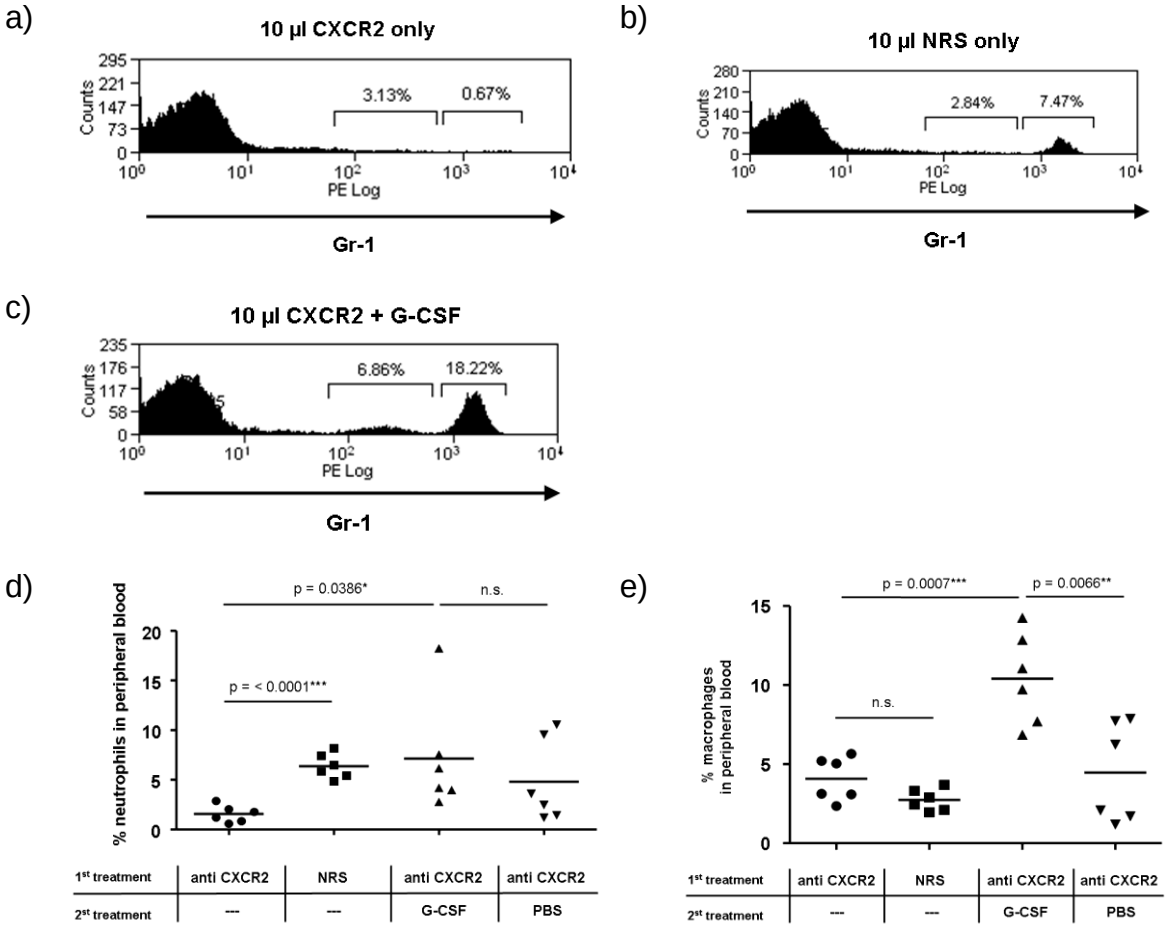

Figure 46 The baseline level of neutrophil counts in the peripheral blood was strongly reduced upon administration of low doses of CXCR2 antiserum. a) A 10th of the usually administered antiserum volume, injected 48h before G-CSF treatment still reduced the basal circulating neutrophil counts to nadir, when analyzed 2 h after G-CSF mobilization b) in contrast to control animals which received the NRS. c) Neutrophils from animals that received the low dose antiserum could be effectively recruited to the blood flow by G-CSF treatment in some cases. d) Statistical analysis of neutrophil behavior under low dose antiserum conditions. e) Statistical analysis of macrophage behavior under low dose antiserum conditions. n = 6 animals were analyzed for each condition.

To further confirm its specific effect on neutrophils the amount of antiserum was titrated down in non G-CSF mobilized animals. A small volume of just 10 µl CXCR2 antiserum led to an almost complete reduction of neutrophil counts (to about 1 %) in the peripheral blood (Figure 46 a) and d)). In control animals which were treated with 10 µl of NRS the normal baseline of around 8 % circulating neutrophils was retained (Figure 46 b) and d)). These results suggested that the CXC receptor 2 might not only play a role in the emergency release of neutrophils but also in regulating the normal baseline of this cell type in peripheral blood. However, a mobilization of neutrophils with G-CSF to at least intermediate but not significant levels was possible at these low doses of anti-CXCR2 serum (Figure 46 c) and d)).

Notably, also in these experiments the number of macrophages was not affected by the CXCR2 antiserum. Macrophages could still be mobilized by G-CSF after administration of 10 µl antiserum and without G-CSF stimulus the number of macrophages stayed on the normal baseline level regardless if antiserum was administered or not (Figure 46 e)).

4.2.8 Inhibition or depletion after CXCR2 treatment?

A very critical point for the analysis was to demonstrate that the anti-CXCR2 serum really bound the receptor thereby blocking the release of neutrophils from BM and not only depleted all neutrophils in the system. To verify the mode of action mice were mobilized with G-CSF after treatment with either 100 µl CXCR2 antiserum (Figure 47 a)), 100 µl NRS (Figure 47 b)) or 100 µl of a monoclonal anti-Gr-1 antibody (RB6-8C5) which is well known to completely eliminate Gr-1 positive cells in living mice (Figure 47 c)) [Stegemann *et al.* 2009]. 2 h after mobilization the number of Gr-1 positive cells in the peripheral blood and bone marrow was assessed. The anti-Gr-1 antibody treatment led to an almost complete depletion of neutrophils in the circulation compared to the anti-CXCR2 serum administration, where a reduction to around 0.5 % cells could be observed. Notably, the difference between both remaining neutrophil populations was highly significant (Figure 47 d)). Moreover not only neutrophils but also the number of macrophages was clearly reduced upon anti-Gr-1 treatment in contrast to the CXCR2 antiserum, which had no influence on macrophage numbers in the peripheral blood (Figure 47 d) and e)).

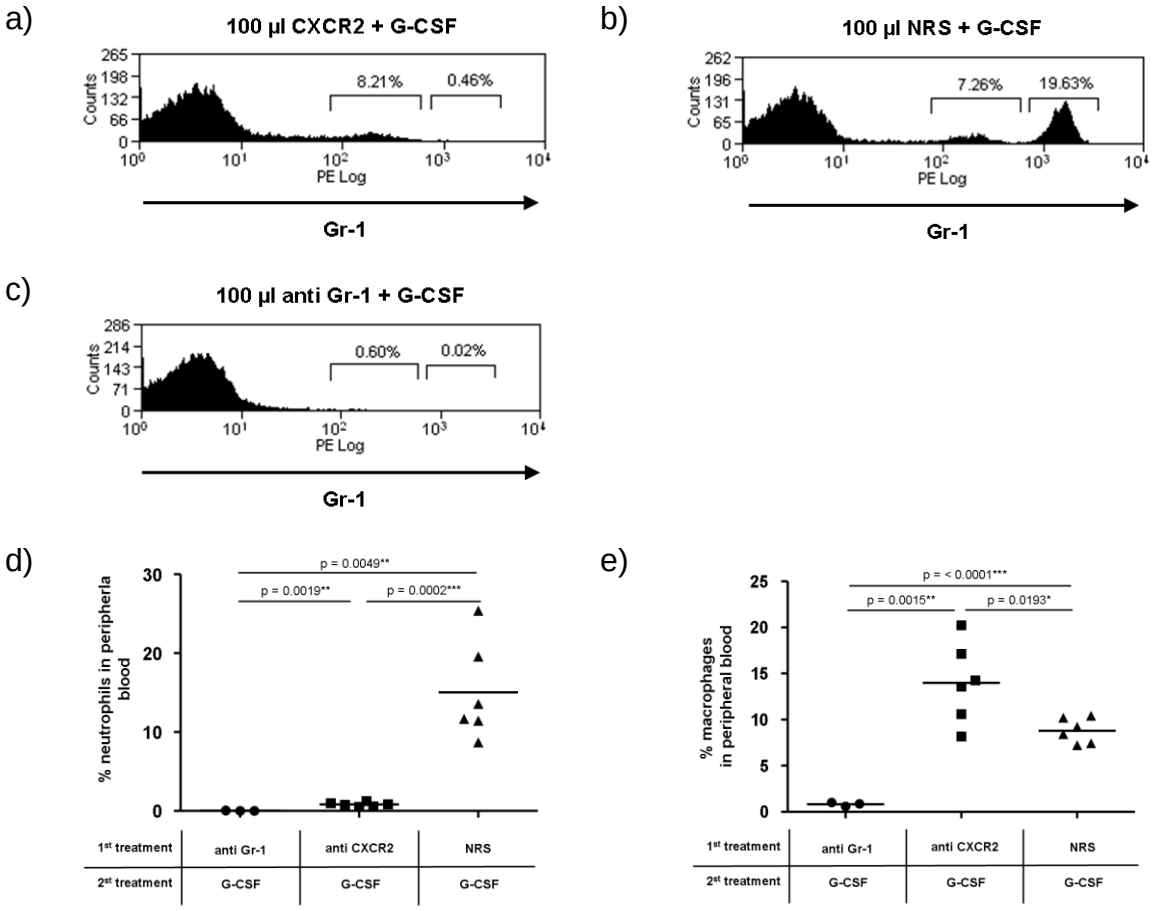

Figure 47 The anti-CXCR2 serum specifically eliminates neutrophils from blood. Animals were treated with either a) 100 µl CXCR2 antiserum, b) 100 µl NRS or c) 100 µl RB6-8C5 and 48 h afterwards stimulated with G-CSF. d) Statistical analysis of blood neutrophil numbers in these groups. e) Statistical analysis of blood macrophage numbers in these groups. n = 3 – 6 animals were analyzed for each condition.

Importantly, within the bone marrow no reduction of Gr-1 positive cells was detectable 48 h upon CXCR2 antiserum treatment. The neutrophil counts in these animals almost remained the same compared to NRS treated mice (Figure 48 a) and b)). In contrast, the administration of an anti-Gr-1 antibody led to a massive 10 fold decimation of neutrophils also in the BM 48 h later (Figure 48 c) and d)).

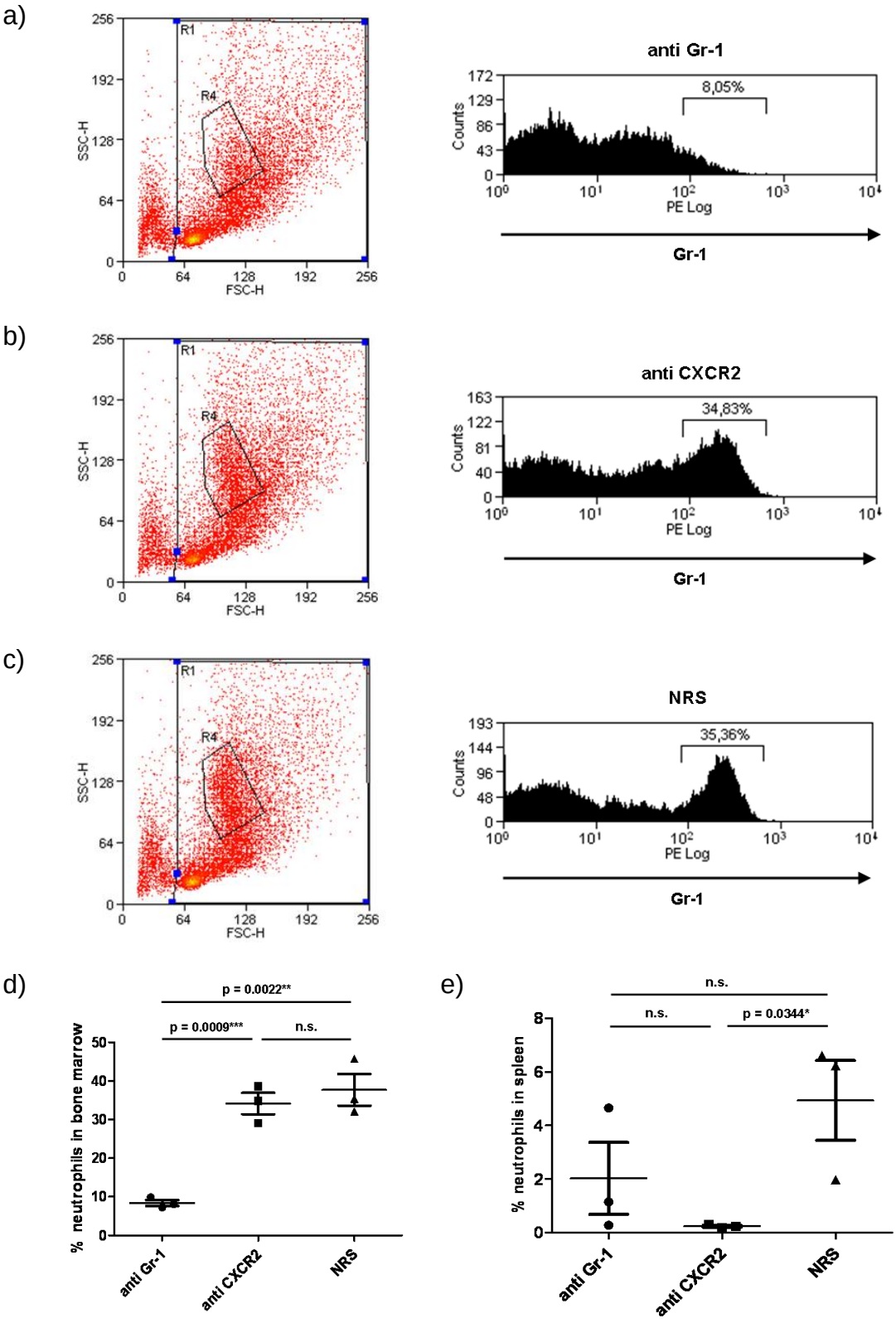

Figure 48 Did anti-CXCR2 serum deplete Gr-1 positive cells? 48 h after treatment wit with either a) NRS, b) CXCR2 antiserum or c) anti Gr-1 bone marrow samples were taken and analyzed for the amount of Gr-1 positive cells. d) Statistical analysis of the neutrophil number in the bone marrow after the different treatments. e) 12 h after treatment with either NRS, CXCR2 antiserum or anti Gr-1 spleen samples were taken and analyzed for the amount of Gr-1 positive cells. n = 3 animals were analyzed for every condition.

These results give an indication that the CXCR2 antiserum did not eliminate Gr-1 positive neutrophils and macrophages from the BM and so maybe also not from the blood like the depleting anti-Gr-1 antibody did. To further proof the depleting ability of the CXCR2 antiserum, the number of neutrophils 12 h after CXCR2 antiserum treatment was determined in the spleen in comparison to the positive depletion with anti Gr-1 and NRS. Notably, in this organ the number of neutrophils was strongly but not significantly reduced after anti Gr-1 whereas after CXCR2 antiserum application the number was stronger decreased (Figure 48 e)). Because of these conflicting data it is still not completely clear how the CXCR2 antiserum influences neutrophils in the peripheral blood.

4.2.9 Influence of CXCR2 antiserum treatment on neutrophil behavior *in vivo*

Next the question arose if the mobilization-inhibitory effect of CXCR2 antiserum was detectable on the migratory activity of individual neutrophils in the BM *in vivo*. Therefore mice were treated as before in the FACS experiments and 2-photon microscopy was started 30 min after G-CSF injection for 3 h. In every experiment three different areas per tibia were investigated consecutively and 20 - 30 cells were analyzed per sequence.

In control mice which just received NRS before G-CSF triggering the cells displayed a very active morphology and also the typical cluster formation of mobilized neutrophils (Figure 49 a)). Unfortunately in this experiment it was not possible to detect the bone structure by technical reasons. In contrast neutrophils of mice which received the CXCR2 antiserum looked more roundish and quiescent (Figure 49 b)). A kinetic overlay clearly underscored that neutrophils were highly motile in the NRS group (Figure 49 c)), whereas cell motility after CXCR2 antiserum treatment was strongly reduced (Figure 49 d)). This was also supported by single cell tracking showing a highly significant decrease of neutrophil velocity after CXCR2 antiserum administration and also a slightly but not significantly diminished cell activity, compared to NRS injection (Figure 49 e) and f)).

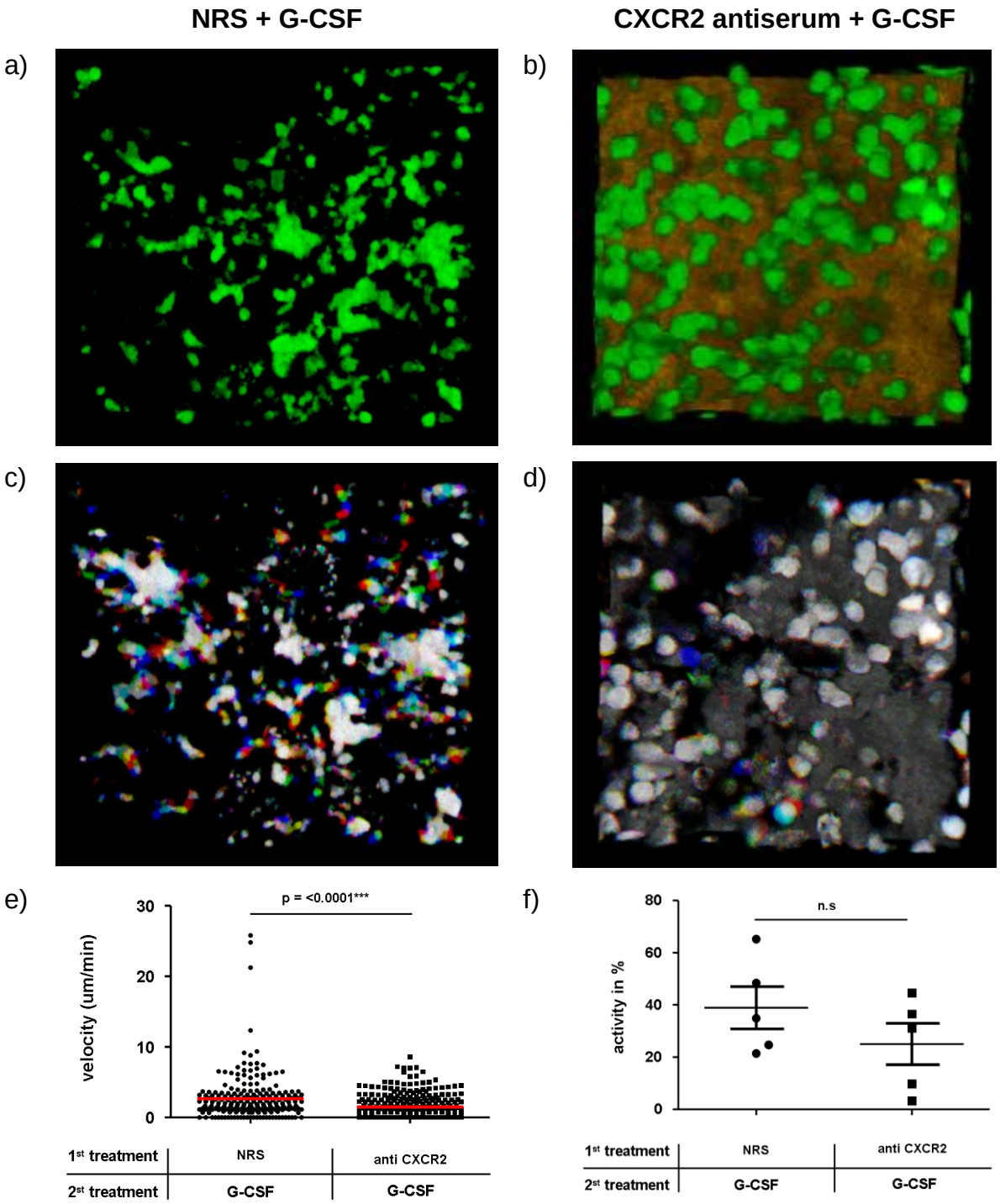

Figure 49 Influence of CXCR2 antiserum treatment on neutrophil single cell behavior. a) 30 min after G-CSF stimulation 2-photon microscopy was carried out in tibial BM of NRS or b) CXCR2 antiserum treated Lys-EGFP mice. c) Kinetic overlay of NRS or d) CXCR2 antiserum sequences. e) Statistical analysis of neutrophil velocity under both conditions. f) Statistical analysis of neutrophil activity under both conditions. n = 5 animals were analyzed independently. View supplemental movie 11.

To further proof the influence of CXCR2 in neutrophil mobilization we looked for CXCR2 knock out mice. Our cooperation partners from the University of California

which also provided us with the CXCR2 antiserum housed these animals in their facility and we asked them to inject G-CSF to the mice. Importantly, CXCR2 ko mice could not mobilize neutrophils into the circulation (data not shown) underlining the important role of CXCR2 during this process.

4.2.10 Triggering of neutrophil motility with the CXCR4 antagonist AMD 3100

In several studies it was shown that the neutrophil surface receptor CXCR4 is responsible for the tethering of neutrophils in the bone marrow by its binding to CXCL12 and that the down regulation of CXCL12 and CXCR4 by G-CSF leads to their mobilization into the blood stream [Levesque *et al.* 2003b; Petit *et al.* 2002; Kim *et al.* 2006; Semerad *et al.* 2005b]. To investigate the impact of CXCR2 inhibition in this system we disrupted the CXCR4-CXCL12 binding by administration of the CXCR4 antagonist AMD3100 [De Clercq *et al.* 1992] in the presence or absence of an additional CXCR2 antiserum treatment.

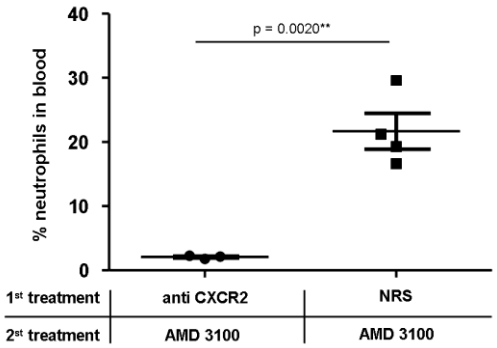

Figure 50 Neutrophil mobilization into the blood stream after AMD3100 treatment. a) Statistical analysis of neutrophil recruitment into peripheral blood 2 h after application of AMD3100. NRS or CXCR2-antiserum was injected 48 h before. n = 3 – 4 animals were analyzed for each condition.

First of all we found that a treatment of mice with AMD3100 48 h after NRS application increased the number of circulating neutrophils to over 20 % when blood was collected 2 h after AMD3100 injection (Figure 50) which is even stronger compared to G-CSF which just led to around 15 % neutrophils in the peripheral blood. This effect could be inhibited by injection of AMD3100 in the presence of the CXCR2 antiserum, thereby suggesting that without CXCR2 triggering neutrophils might be loosened from their CXCL12 anchor but are not able to subsequently enter the blood stream.

This was also confirmed when we evaluated the AMD3100 influence on the single cell behavior *in vivo* by 2-photon microscopy. AMD 3100 treatment led to a mobili-

zation of neutrophils within 1 - 2 h in the majority of mice which was comparable to the situation under G-CSF conditions with respect to activity (Figure 51 d)). A kinetic overlay displays the situation in the same animal 1 - 2 h after AMD3100 injection (Figure 51 a)) and before AMD3100 treatment (Figure 51 b)) as an internal control. Interestingly, the velocity was not increased compared to non mobilized mice, which might further confirm the idea that cells are only detached from the endosteum after AMD3100 (Figure 51 c)) but not induced to migrate faster due to the absence of additional CXCR2 ligands.

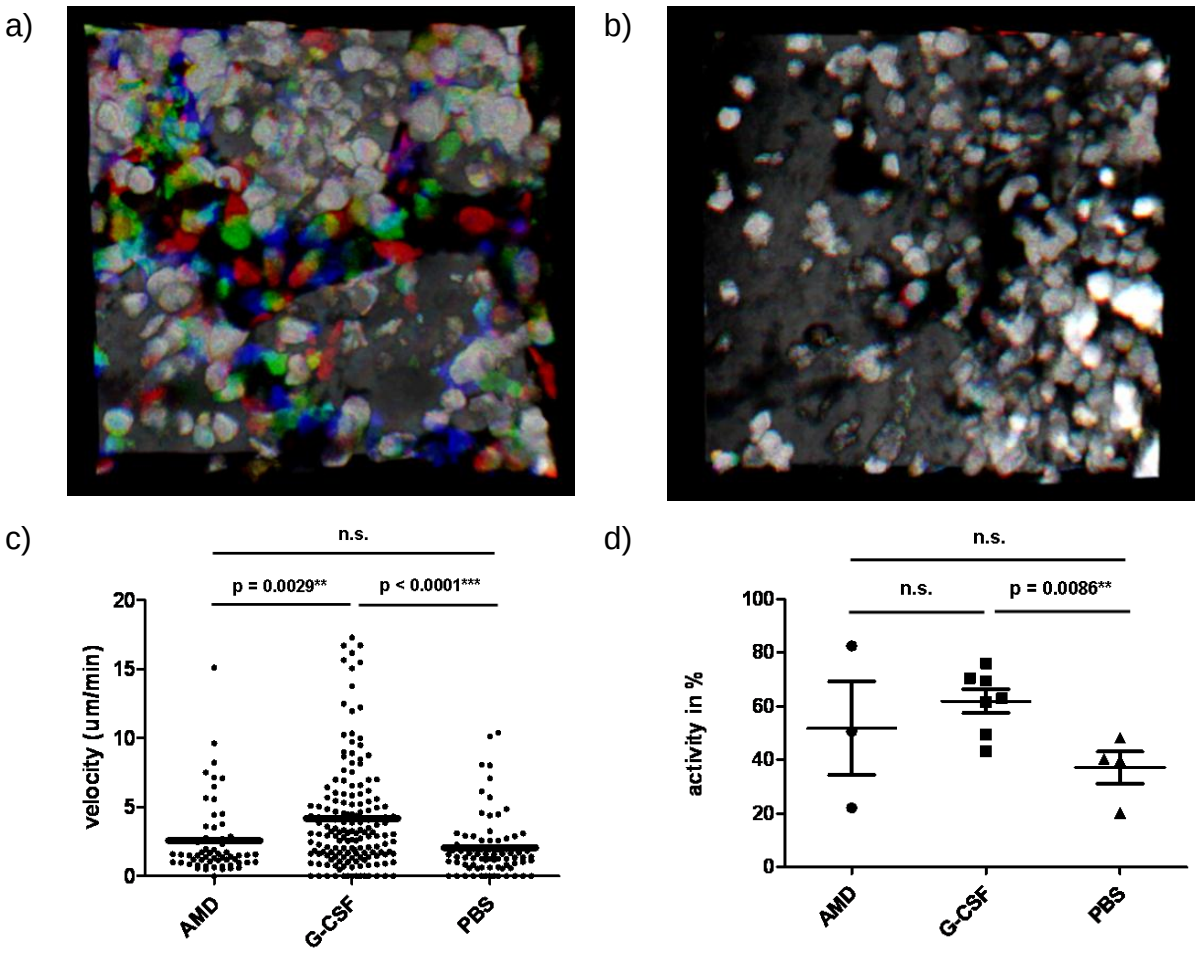

Figure 51 Impact of AMD3100 administration on neutrophil mobilization *in vivo*. a) Kinetic overlay of 2-photon microscopy sequences after AMD3100 mobilization and b) before AMD 3100 injection reveal a strong increase of cell motility after treatment. c) Analysis of cell velocity and d) activity in mice treated with AMD3100 in comparison to the situation 1 – 2 h after G-CSF and PBS. Data were measured in 3 - 7 independently analyzed animals. View supplemental movie 12.

4.2.11 Thrombopoietin (TPO) as mediator of neutrophil mobilization

Taken together our results suggested that G-CSF did not act directly on neutrophils to induce their mobilization. To clarify the underlying mechanisms leading to the observed G-CSF mediated neutrophil mobilization, a cooperative study with the lab of Nancy Hogg (London) was established. With their help it was possible to set up immunohistological analyses of BM sections, showing that both KC and MIP-2 were strongly produced by megakaryocytes located next to sinus vessels that were also positive for both chemokines. 2 h after G-CSF injection, the detectable megakaryocyte and endothelial expression of KC and MIP-2 was strongly reduced (data not shown). The hypothesis of megakaryocytes as the physiological source of neutrophil attracting chemokines was further supported by the demonstration that isolated primary mouse megakaryocytes in cell culture constitutively released KC and MIP-2 into the supernatant under *in vitro* conditions. Notably the addition of G-CSF to the cell culture had no further impact on the cytokine release, suggesting that megakaryocytes themselves are also not the direct targets for G-CSF (data not shown). Further immunohistological studies revealed that neither the majority of neutrophils nor Mac-2-positive macrophages in the BM expressed the receptor for G-CSF, CD114. However, a population of cells exhibiting a stromal cell like morphology was strongly G-CSF receptor positive (data not shown). These cells were predicted to produce factors that would influence the megakaryocytic release of chemokines and should therefore constitute the missing link between G-CSF-treatment, megakaryocytes and PMN mobilization. Megakaryocytes are best known for their function as platelet producers and the hematopoietic cytokine thrombopoietin (TPO) has been described as the major stimulant of this process. Encouraged by this hypothesis we investigated, if the stromal cells might be able to communicate with megakaryocytes via the secretion of TPO and indeed, while the expression level of TPO was found to be very low in unstimulated BM a strong upregulation was detectable upon systemic stimulation with G-CSF within 2 h (data not shown).

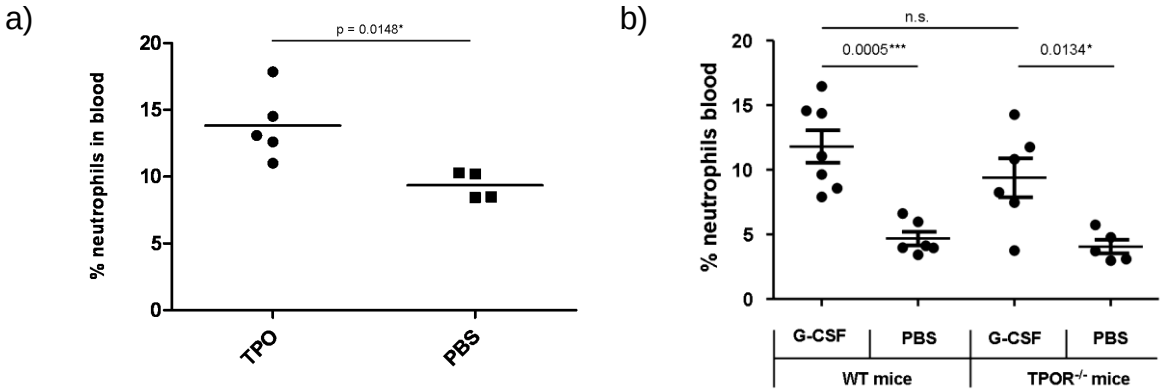

Figure 52 Role of TPO in neutrophil mobilization. a) 2 h after retro orbital injection of TPO a significantly elevated neutrophil number was found in blood circulation. b) After injection of G-CSF or control PBS in TPOR-/- mice, G-CSF still led to neutrophil mobilization, but compared to WT animals the mobilization was diminished. For a) n = 4 – 5 animals were analyzed, for b) between 5 – 7 animals were analyzed.

To finally clarify the potential influence of TPO on neutrophil mobilization *in vivo* TPO was injected i.v. into mice and the mobilization of neutrophils was assessed 2 h later. Confirming the histological and cell-culture observations, a single injection of TPO already led to a significant recruitment of neutrophils into the blood stream (Figure 52 a)). This result further proved that the acute release of TPO constitutes the missing link in the context of G-CSF mediated release of KC and MIP-2 by megakaryocytes. To additionally proof the role of TPO in neutrophil mobilization we injected G-CSF or a PBS control into TPOR-/- mice. Interestingly, neutrophils in TPOR-/- mice were mobilized after G-CSF injection compared to TPOR-/- mice treated with PBS. However, in comparison to WT animals that received G-CSF the mobilization seemed to be slightly but not significantly decreased (Figure 52 b)).

4.2.12 Summary - Part II

In the course of the thesis we further improved our 2-photon microscopy approach and established the staining of blood vessels with rhodamine-dextran. A protocol for mouse injections was developed which allowed the double injection of substances without an interfering pre-stimulation of neutrophils during the mobilization experiments. FACS analysis revealed a strong increase of neutrophils and also of macrophages in the peripheral blood 2 h after G-CSF injection. Additionally we determined the influence of G-CSF on neutrophils via 2-photon microscopy directly in the murine long bones and observed an increase in cell motility with a peak dur-

ing 1 – 2 h after treatment. Interestingly also the entry of neutrophils in the circulation was observable. This increase of motility seems to be a special ability of neutrophils as macrophages and dendritic cells did not show this behavior in response to G-CSF. To figure out the mechanism of G-CSF mobilization we proved the involvement of the chemokines KC and MIP-2 which are known to play a role in neutrophil mobilization during many infection models. Surprisingly the inhibition of neutrophil mobilization with monoclonal antibodies against both chemokines was not successful but blocking the main receptor CXCR2 of the chemokines with a polyclonal antiserum led to a strong reduction of neutrophils in the peripheral blood whereas, interestingly, the number of macrophages was slightly increased. To exclude that the CXCR2 antiserum led to a neutrophil depletion, mice were also treated with a Gr-1 antibody which definitely leads to neutrophil depletion and the bone marrow was analyzed. Our data suggest that the CXCR2 antiserum does not simply deplete neutrophils. Injection of the CXCR2 antiserum 48 h before performing intravital 2-photon microscopy also completely suppressed the neutrophil motility upon G-CSF injection 2 h before starting the imaging. Moreover, we investigated the injection of the CXCR4 antagonist AMD3100 into mice as the important role of CXCR4 in neutrophil mobilization is known for many years. AMD3100 led to a significant increase of neutrophils in the circulation and notably this effect was also blocked by administration of CXCR2 antiserum. Together with our cooperation partners we identified megakaryocytes to be a source of KC and MIP-2 in the bone marrow and the release of both was triggered by TPO. The important role of TPO was also confirmed by the finding that injection of TPO alone led to neutrophil mobilization into the peripheral blood and that G-CSF mobilization of TPOR-/- mice showed a diminished even though not significantly reduced number of neutrophils in the peripheral blood. Taken together, these data reveal a completely new mechanism how G-CSF might induce neutrophil mobilization and suggest for the first time an involvement of megakaryocytes and TPO in this process.

5. Discussion

5.1 Localization and motility of HPCs und eHPCs from young and aged mice in murine long bones

Migratory dynamics and localization relative to the functional structures of the bone matrix are critical for the regulation of stem cell physiology in the bone marrow. This is due to the fact that cell behavior is strongly influenced by the adjacencies, composed of special niche cells either at the calcified bone surface [Adams *et al.* 2006a] or at the blood vessels. It was recently postulated that aged stem cells compared to young cells present with altered, less favorable and stable interactions with their special niche. This might in part explain impaired hematopoiesis in aged individuals [Xing *et al.* 2006; Geiger *et al.* 2007], because the necessary microenvironment for hematopoiesis might no longer be available for the more detached aged cells.

To test this hypothesis directly, we employed intravital 2-photon microscopy to investigate both, the in vivo short-term dynamics of young and aged HPCs, eHPCs and differentiated hematopoietic cells as well as the distance of these cells from the endosteal surface in the marrow of long bones. This study was the first analysis that was performed in long bones. Other *in vivo* studies using intravital microscopy observations of stem cells had so far been done only in the murine calvarium [Lo *et al.* 2009], which is interesting due to the fact that HSCs are normally isolated from the marrow of long bones for different studies. Furthermore marrow of the long bones and jaws is generated from cartilage-based constructions by a process called endochondral ossification [Blumer *et al.* 2008], while flat bones like the calvarium contain marrow that has been formed by intra-membranous ossification, occurring without an intermediate cartilage form [Chan *et al.* 2009]. This has severe functional consequences, e.g. on the functioning of hematopoietic stem cells and the formation of bone with functional niches [Xie *et al.* 2009; Chan *et al.* 2009]. In terms of direct imaging of cells or the blood vessel system in the bone marrow *in vivo* the previously available method for imaging in the calvarium [Mazo *et al.* 1998] will suffer from a possible error made by investigating the not optimal environment.

In our approach, HPCs and eHPCs in long bones resided solitary and were completely immobile after they reached a location in close vicinity to the endosteum.

This is consistent with observations made for HPCs and eHPCs lodging in the bone marrow of the calvarium [Lo *et al.* 2009] and also to HSCs, detected by *ex vivo* real time imaging in bone marrow [Xie *et al.* 2009]. Although the observed cells displayed no locomotion, young primitive hematopoietic cells presented with active cell protrusion movements ("running on the spot") in long bones. Moreover, sustained and very dynamic interactions with the microenvironment were observed that seemed to show some similarities to the movements of T cells during maintenance of the well characterized immunologic synapse (IS) [Reichardt *et al.* 2007]. The IS is the contact plane between T cells and antigen-presenting cells and has been well defined *in vitro* [Gunzer *et al.* 2000; Friedl *et al.* 2005; Gunzer *et al.* 2004] as well as *in vivo* [Henrickson *et al.* 2008; Mempel *et al.* 2004a; Barcia *et al.* 2006]. Because the contact plane of primitive hematopoietic cells with the niche cells in the microenvironment seems to be functionally similar to the IS, it is has been named stem cell synapse [Yin *et al.* 2006; Adams *et al.* 2006b; Scadden 2006b]. Interestingly, eHPCs seem to be located closer to the endosteal surface in the diaphysis of long bones compared with their position to the endosteal region in the calvarium [Lo *et al.* 2009]. This finding might indicate the presence of a special niche architecture in long bones, which is somehow altered in comparison to niches in the calvarium and thus further underscores the functional difference between these two compartments.

By comparing eHPCs and HPCs with respect to their localization and motility it was conspicuous that the HPCs, which resided more distantly from the endosteum showed increased motility compared to eHPCs. The same picture was found by comparing eHPCs from young and old mice for the same parameters. More distantly located cells from old animals displayed a much higher motility than cells from young animals, which had closer contact to the endosteum. This might indicate that the close interaction of cells with their endosteal niche supports the maintenance of quiescence in cells, whereas a larger distance to the endosteal layer leads to a more active cell phenotype. Other studies dealing with the different interactions of stem cells with their several niches support these *in vivo* findings [Arai *et al.* 2007; Scadden 2006a; Adams *et al.* 2006c; Suda *et al.* 2005; Wilson *et al.* 2006b]. Now the question came up, whether the zone close to the endosteum is an area of generally reduced cell migration. First, imaging in CX3CR1-EGFP knock-in mice [Jung *et al.* 2000] could demonstrate that this specific region is not

only engaged by undifferentiated hematopoietic stem cells, a finding that further underline the complexity of the bone marrow microenvironment. In addition, because both EGFP-labeled cell types in these mice, macrophages as well as DCs, were highly motile in comparison to HPCs and eHPCs, it could be concluded that active cell migration near the endosteal surface is possible and thus the lack of locomotion in primitive hematopoietic cells was cell intrinsic rather than hampered by a physical migration barrier in this zone. The data obtained later for neutrophils, which were even more motile in the near-endosteal environment, further strengthens this point. However, interestingly also macrophages and DCs displayed a clear correlation between their motility and localization to the inner bone surface. So this phenomenon seems not to be restricted to primitive hematopoietic cells but applies also for differentiated hematopoietic cell types. The molecular explanation for this observation has remained enigmatic so far.

The complete immobility of eHPCs and HPCs suggest that these cells might have an ability to actively suppress migration once they have reached their destination. Another possibility might be that the activity of several cytokines which should support eHPC migration, like the stromal cell–derived factor 1 (SDF-1), might be restricted to very distinct locations of the endosteal layer *in vivo*. The latter hypothesis is strongly supported by the finding, that stroma cells expressing SDF-1, which can induce migration in primitive hematopoietic cells [Dar *et al.* 2006] are distributed on single distinct spots inside the bone [Sugiyama *et al.* 2006].

Several models try to explain the aging of hematopoietic stem cells. The understanding for this process is of prime importance because it is involved in the impaired tissue homeostasis of different organs that rely on stem cell activity [Rando 2006]. Aging of stem cells is characterized by a reduced proliferative and regenerative capacity, including DNA damage, action of reactive oxygen species and/or telomere attrition [Geiger *et al.* 2002; Geiger *et al.* 2007; Chambers *et al.* 2007; Kamminga *et al.* 2006]. Our results add a model to this list of potential defects in aged stem cells in which localization and in addition altered cell-cell interactions of aged eHPCs with their respective niche in the bone marrow might alter the ability to maintain functionality for a longer period of time. This could lead to the special phenotypes associated with aged eHPCs. Altered interactions of stem cells with the stroma will most likely result in altered differentiation and self-renewal outcomes.

On a molecular level our co-workers found that elevated levels of the α5 integrin chain (CD49e) correlated with reduced adhesion to stroma cells, leading to a more distant localization of young and aged cells from the endosteum [Kohler *et al.* 2009]. This suggested that the level of expression of α5 integrin can modify the localization of primitive hematopoietic cells with respect to the endosteal layer. Moreover it might regulate in which microenvironment a cell will reside in upon transplantation. There are several publications, which are consistent with the finding, that α5 integrins have an influence on stem cell niche interactions. For example the blocking of α5 integrins on HSCs leads to a reduced homing to the BM, but not to the spleen, which does not have endosteal structures [Kiel *et al.* 2005; Kiel *et al.* 2006; Wierenga *et al.* 2006]. Additionally, α5 integrins also regulate engraftment of human hematopoietic stem and progenitor cells [Carstanjen *et al.* 2005] and during the mobilization with G-CSF the cell surface expression level of α5 integrins is increased in bone marrow resident HSCs [Wagers *et al.* 2002]. Unfortunately, our results do not answer the question, which cells in the bone marrow are directly contacted by eHPCs. Using new animal strains in which additional types of hematopoietic [Chiang *et al.* 2007] or stroma cells are fluorescently labeled will result in more profound information about cell-cell interactions of stem cells in long bones. Hopefully, this approach will also allow the monitoring of the endosteal as well as of the perivascular endothelial region within long bones and their influence on aging. This might help to clarify the role and influence of functional stem cell niches in the femur and reveal similarities to recent published *ex vivo* analyses [Xie *et al.* 2009].

To summarize the first part of the thesis, the use of intravital 2-photon microscopy to visualize hematopoietic cells inside the bone marrow cavity of long bones allowed providing the first direct experimental evidence for the existence of eHPC synapses within the niche. In addition, the data implied distinct primitive hematopoietic stem cell stroma interactions for aged eHPCs relative to their analogues from young animals that might impact on both their self-renewal and differentiation potential, probably similar to mechanisms recently described for aged germline stem cells in Drosophila [Cheng *et al.* 2008]. These data thus show, how intravital 2-photon microscopy in the bone marrow of long bones can open new insights for the investigation of mammalian stem cell biology *in vivo* [Sakaue-Sawano *et al.* 2008].

5.2 Investigation of bone structure and blood flow in murine long bones

In the second part of the study a novel explanation how G-CSF mobilizes neutrophils from bone marrow was established, which appears to be much more consistent with all available data on neutrophil mobilization by G-CSF than previous models. Additionally the 3-D bone structure and the blood flow in murine long bones were analyzed in detail for the first time. It was found, that the inner bone surface displays a “crisp bread” structure with lots of emarginations and pores. Many, but not all of these pores were nerved by vessels and blood flow could be observed within. However, the blood flow in long bones is still not fully understood. It is remarkably difficult to investigate the circulation inside the compact bone thoroughly owing to its hard calcified matrix. Methods to study circulation have represented either the bone morphology and the architecture of the canal system [COHEN *et al.* 1958; Smith 1960; VASCIAVEO *et al.* 1961; Albu *et al.* 1973] or the injected vessel network [Brookes *et al.* 1961; HERT *et al.* 1961; Trias *et al.* 1979; Marotti *et al.* 1980]. There is previous evidence that the highly sensitive and complicated bone marrow compartment is not the same in murine long bones and calvarium with respect to hematopoiesis [Xie *et al.* 2009]. Additionally, our 2-photon microscopy data detected remarkable differences between blood vessels in long bones compared to vessels in the calvarium. Murine long bones display big vessels slightly distant from the endosteal layer. Close to the endosteal layer these vessels suddenly branch into a dense network of very small vessels that line the complete inner bone surface. In contrast, in the calvarium the complex structure of small vessels seems to be completely missing and only bigger vessels are visible [Lo *et al.* 2009; Mazo *et al.* 1998]. To which extent this fact might influence cell behavior and if there are other remarkable differences between both distinct bone marrow environments need to be further investigated in the future. Also the overall 3-D architecture of incoming and outgoing vessels in the murine long bone is an important issue worth of in depth investigation in the future.

5.3 Important role for the chemokines KC and MIP-2 and their receptor CXCR2 in neutrophil mobilization from the bone marrow

Neutrophils in murine long bones react on systemic G-CSF administration with a dramatic increase of cell motility. Interestingly the number of migrating cells increase from 35 % to almost 60 % when observed 1 - 3 h after G-CSF injection by intravital 2-photon microscopy. This observation fits to the known fact that G-CSF disrupts the main anchor for neutrophils that provide their retention in the bone marrow, the CXCR4-SDF-1 axis. Notably, neutrophils seem to cluster to distinct places at the blood vessels, where they can immigrate into the circulation (Figure 37). Those special sites are already described for the endothelium [Nourshargh *et al.* 2010; Voisin *et al.* 2010; Wang *et al.* 2006] so it could be speculated that a situation like a traffic jam occurs at these places because too many neutrophils try to leave the bone marrow simultaneously. Usually a few clusters were observed in every microscopy area but exclusively after mobilization. Also the phenomenon that neutrophils aggregate to big clusters was observed in the past and this behavior was named swarming [Peters *et al.* 2008]).

Within this work we discovered that after G-CSF administration the neutrophil-attracting chemokines KC and MIP-2 are produced in the BM. We could also demonstrate that the chemokine receptor CXCR2 which is triggered by these chemokines is required for the induction of profound neutrophil motility in the bone marrow as well as their entry into local blood sinuses after systemic application of G-CSF. During the finalization of this thesis and the submission process of the associated publication the principal finding that CXCR2 is important for G-CSF-mediated neutrophil mobilization was also made by others, thus has now been independently confirmed [Eash *et al.* 2010].

Surprisingly, while a polyclonal anti-CXCR2 antiserum was very effective in blocking increased neutrophil motility *in vivo*, both anti-KC and anti-MIP-2 antibodies did not influence the G-CSF mediated neutrophil motility or their release from bone marrow. This was despite the clear repressing effect of both antibodies on neutrophil mobilization and recruitment, which has been shown in a model of acute peritonitis [Wengner *et al.* 2008]. Also in our hands the anti KC and anti MIP-2 antibodies displayed a significant decrease of neutrophils in the peripheral blood as

well as in the peritoneal lavage 2h after induction of an LPS mediated peritonitis. Why the antibodies did not function within the BM might be explained with the fact, that the LPS-peritonitis model represents a distinct local inflammation, whereas a systemic neutrophil mobilization through G-CSF induces an overall reaction of neutrophils. Possibly this leads to a much stronger neutrophil response, where the dose of antibodies that was chosen in our experiments was not capable to overcome the resulting effect. Another possibility might be that for unknown reasons the antibodies did not reach the BM stroma to interfere with neutrophil motility. Unfortunately from our experiments we also cannot fully exclude that the anti CXCR2 antiserum might deplete neutrophils from blood or peripheral organs. However, in the light of our data on CXCR2 deficient mice which cannot mobilize neutrophils by G-CSF, the recent publication by Eash et al, which confirms a key role of CXCR2 as well as the fact that the CXCR2 antiserum does not bind complement and thus does not kill neutrophils *in vitro* (personal communication, T. Lane, UCI), we might at least assume that the antibody works properly without depletion. An ultimate proof of this concept can only come from additional studies using novel transgenic animal models

5.4 Megakaryocytes produce and release KC and MIP-2 in response to thrombopoietin

There is previous evidence that the receptor for G-CSF does not need to be expressed on neutrophils for efficient mobilization but instead that a trans-acting signal is generated by receptor-expressing bystander cells [Semerad *et al.* 2002]. The nature of this signal has however, remained elusive. Our data fully support these previous findings and identified this trans-acting signal as a combination of thrombopoietin produced by G-CSFR-expressing stromal cells and KC/MIP-2 released at least in parts by megakaryocytes. Other cells important in this respect might be endothelial cells [Eash *et al.* 2010]. This concept also gives new perspectives to the function of megakaryocytes. They are well known as platelet producers [Junt *et al.* 2007] and until now this has remained their sole activity. Our findings suggest a new central role for megakaryocytes as gatekeepers of neutrophil mobilization.

It could be shown that primary mouse BM megakaryocytes secrete KC/MIP-2 without further stimulus in culture and that the baseline levels of circulating neutro-

phils are severely reduced after blockade of the KC/MIP-2-receptor CXCR2. Therefore it could be proposed that megakaryocytes constitutively release small amounts of KC/MIP-2 as a "tonic" signal that maintains steady-state levels of neutrophils in the blood. Consistent with this, our data show the production of the KC/MIP-2 homologue IL-8 by a human megakaryocyte cell line as well as other reports using megakaryocytes derived from human CD34+ progenitor cells [Emadi *et al.* 2005; Higuchi *et al.* 1997]. “Tonic” signalling via chemokine receptors has been demonstrated for neutrophils before in a model of peritoneal inflammation [Zhang *et al.* 2005]. Importantly megakaryocytes can greatly boost the production of CXCR2-binding chemokines following a systemic increase of G-CSF, thereby constituting a hyper-signal capable of mobilizing the large numbers of neutrophils that are needed to fight peripheral infections [Behnsen *et al.* 2007]. Therefore different levels of stimulation via the same chemokine receptor, in this case CXCR2 on neutrophils, might control the circulating levels of a central leukocyte type under both steady state and inflammatory conditions, based on the fact that the CXCR2 antibody does not deplete neutrophils which was already discussed in 4.3. Our demonstration that monocytes were also mobilized via G-CSF but independently of CXCR2 suggests that leukocyte specific receptor-ligand systems might be active for each type of circulating leukocytes to maintain its baseline and trigger-induced levels. The CXCR2-independent mobilization of monocytes by G-CSF also implies that the cytokine will induce the release of factors distinct from neutrophil specific KC/MIP2 which however, are not yet identified. A further complexity is that the rapid release of KC/MIP-2 from megakaryocytes is not a direct effect of G-CSF. Among BM cells, stromal cells and a subtype of F4/80+ macrophages but not neutrophils were identified to express the G-CSFR by our cooperation partners from the group of Nancy Hogg. Based on their localization within the BM it appeared that at least some of the same cells were strong expressors of thrombopoietin following *in vivo* G-CSF treatment. Thrombopoietin has a potent influence on megakaryocyte maturation and function. Its roles extend from acting as main colony-stimulating factor in megakaryopoiesis to controlling the number of mature megakaryocytes able to form pro-platelets [de Sauvage *et al.* 1996].

a)

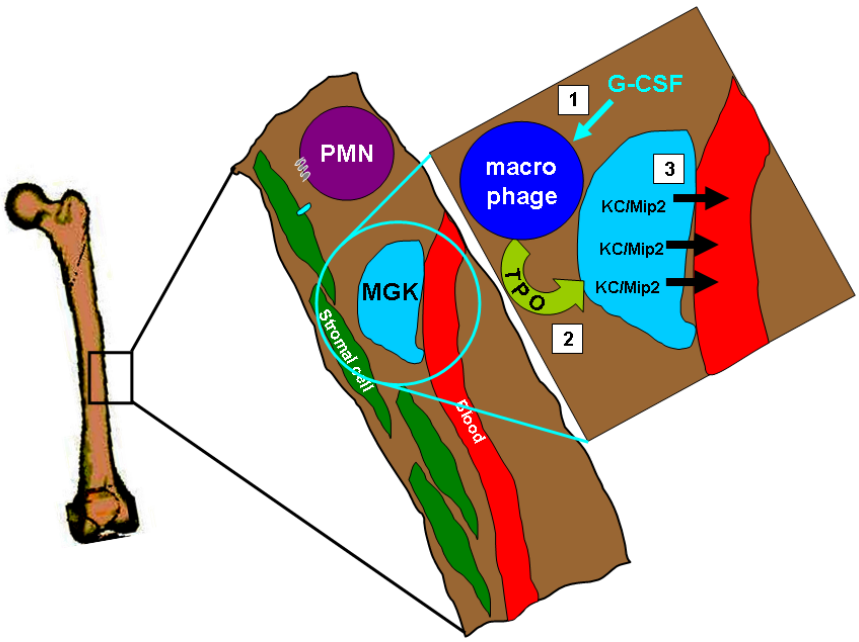

b)

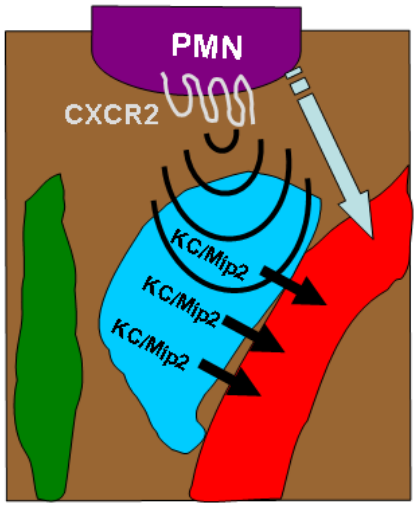

Figure 53 A model summarizing the concept of neutrophil mobilization by G-CSF in keeping with the data of this study. a) (1) A G-CSFR-expressing cell (potentially a F4/80 positive bone marrow macrophage) recognizes G-CSF. (2) As a result this cell produces TPO. (3) TPO enhances the capacity of megakaryocytes to secrete CXCR2 ligands such as KC and MIP-2. b) Neutrophils are mobilized via stimulation of their receptor CXCR2 to find a way out of the bone marrow into blood vessels.

In terms of human stromal cells, high levels of thrombopoietin mRNA are expressed by BM stromal cells from several categories of thrombocytopenic patients but not normal controls [Sungaran *et al.* 1997]. Evidence that thrombopoietin was the link between G-CSF-responsive macrophages and megakaryocyte function came from the finding, that thrombopoietin caused primary mouse megakaryocytes as well as the human MEG-01 cell line, to make enhanced amounts of the neutrophil attracting chemokines. Importantly, thrombopoietin was able to bypass the need for G-CSF and caused neutrophil mobilization directly when injected *in*

vivo. In fact long term exposure to thrombopoietin via a retroviral vector infection gave rise to a fatal myeloproliferative syndrome making the link between thrombopoietin and neutrophils in another way [Villeval *et al.* 1997]. Moreover also osteoblasts that line the endosteal wall within bone marrow are G-CSF receptor positive, are thrombopoietin producers and are intimately involved in retention of quiescent stem cells [Yoshihara *et al.* 2007]. Notably, TPOR-/- mice are still able to mobilize a slightly significant number of neutrophils into the peripheral blood after G-CSF treatment, although the number is decreased compared to wild-type animals. A possible explanation might be that TPO might be just able to induce the release of KC and MIP-2 from megakaryocytes. There are other cell types that also produce both chemokines but which are not known to react to a TPO stimulus, for example endothelial cells in the bone marrow in which we could demonstrate high expression of both chemokines with immunohistochemistry. Other still unknown mechanisms may lead to their release so that we conclude an important but not unique role for TPO in chemokine release which would perfectly explain the given but not fully established neutrophil mobilization in TPOR-/- mice. Furthermore, in terms of stem cell release there is evidence that G-CSF may act outside the bone marrow on the sympathetic nervous system in a network that involves suppression of osteoblast activity and reduction of CXCL12 levels and altering of stem cell release [Katayama *et al.* 2006]. Whether osteoblasts also have a role in the stromal cell/megakaryocyte/neutrophil network what is proposed here is a topic for future investigation. In any case our study demonstrates that CXCR2 is a critical chemokine receptor that mediates stress granulopoiesis induced by G-CSF as meanwhile also confirmed by others [Eash *et al.* 2010].

5.5 Role of the CXCR4 antagonist AMD3100 in neutrophil mobilization

Previous work has highlighted the essential nature of the CXCR4-CXCL12 bond that serves to retain neutrophils in the BM and the disrupting effect of G-CSF on this interaction [Link 2005]. AMD3100 is a major CXCR4 antagonist that can interfere with this chemokine-receptor pair causing neutrophil release from BM [Wengner *et al.* 2008]. In our study we demonstrated that the action of AMD3100 is prevented by CXCR2 blockade thus placing the role of KC/MIP-2 and their CXCR2 receptor downstream of CXCR4-CXCL12. This finding immediately pro-

vides a rational explanation for the well-known synergism of G-CSF and AMD3100, which has been lacking so far [di Persio *et al.* 2009; Flomenberg *et al.* 2005; Pelus 2008]. Our data suggest that AMD3100 breaks the CXCR4-CXCL12 bonds of neutrophils fast and efficiently within the BM but once released, neutrophils need to detect the CXCR2 signal to initiate migration and to be directed towards the BM sinuses. This would be in full accordance with the study of Eash et al [Eash *et al.* 2010] who also observe lack of mobilization by AMD3100 in the absence of CXCR2 on neutrophils. In this concept G-CSF acts synergistically with AMD3100 because it strongly increases the amount of neutrophil mobilising chemokines in the blood thereby enhancing their release into the circulation in much greater numbers than AMD3100 alone. The findings have implications for the clinical treatment of neutropenic patients.

Finally our novel technical approach now allows imaging of BM resident cells in the tibia *in vivo*, a long bone compartment from where both mature neutrophils as well as hematopoietic stem cells are normally isolated for experimental studies in mice. This is a helpful addition to approaches for imaging BM resident cells which have so far concentrated on the bone marrow of the calvarium [Lo *et al.* 2009; Mazo *et al.* 1998]. Using this approach it was possible to provide the first view into the enormous dynamics of neutrophil mobilization in its natural environment *in vivo*.

In summary, the data show that a megakaryocyte/stromal cell axis operates in a finely controlled cooperative fashion to maintain both baseline and emergency levels of neutrophils. Thus, we have identified a network of key signalling molecules, chemokines and cells controlling neutrophil release that is strategically positioned in the BM cavity adjacent to vessels. For future studies it will be important to consider the impact of this cellular axis in response to external perturbations such as peripheral infections requiring immune defense as well as its involvement in the release from the BM of other mature leukocytes or cells from the hematopoietic stem cell compartment.

6. Outlook

The method of intravital 2-photon microscopy opens up a lot of new possibilities for immunologists to directly examine the behavior of immune cells in their natural environment. Due to the enormous complexity of the immune system, this microscopic visualization seems to be an ideal way to really understand cell behavior in different organs and under different conditions. With our new approach of intravital 2-photon microscopy we gained access to a so far unapproachable area of the organism with a tremendous immunological relevance, the long bones.

In the first part of the present work we have analyzed the localization and motility of young and aged eHPCs in this compartment. With our new microscopic tool it will be now possible to further analyze stem cell behavior in their niche with respect to e.g. contact parameters. We are now able to bring light into cell-niche or cell-cell interactions and thereby explaining basic hematopoietic processes. Such experiments could gain further help from a very recent publication in which it has been shown that nestin positive mesenchymal stem cells build up a unique niche [Mendez-Ferrer *et al.* 2010]. Isolated and fluorescently labeled stem cells could subsequently be transferred into *Nes-GFP* transgenic mice which would allow an observation of the interaction between both cell types *in vivo*. Another approach to further investigate this interaction are transgenic mouse models in which different adhesion molecules that are important for stem cells retention could be deeply studied, e.g. by genetic fluorescent labeling and/or deletion. Moreover, the creation of transgenic animals with fluorescently labeled stem cells would be very helpful to visualize the endogenous stem cell population in the long bones. In such a model it would be of great importance to clarify if the endogenous cells behave the same as adoptively transferred entities with respect to localization and motility. For particular experimental questions it could be of interest to analyze stem cells that have been transferred into lethally irradiated recipients. It could well be that in these animals much more stem cells invade the marrow and end up in a closer vicinity to the endosteum, as the niches are not occupied by the recipient's endogenous stem cells. Another important and still unknown question is how adoptively transferred stem cells reach their niche in the bone marrow. Are they leaving the central bone vessel to reach the marrow or are they brought to the marrow in smaller vessels entering the bone all along its shaft? Do these stem cells first enter the vascular niche and then keep moving to the endosteal niche or is it the other way round?

And besides the (re-)population of the bone marrow by stem cells it is also not visualized so far how cells leave this compartment under certain conditions. This stem cell mobilization, for example by G-CSF, can also be studied in detail with our novel intravital 2-photon microscopy approach. Finally, also issues regarding the self-renewing capacity of stem cells will be amenable to intravital imaging. Where and how does asymmetric division occur? At what frequency and which role might play the associated niche cell? Such issues will be open for direct investigation now.

In the second part of the work the mechanisms of neutrophil mobilization after G-CSF treatment have been investigated. The important role of the chemokines KC and MIP-2 and of their receptor CXCR2 was described for the first time in this context. Both chemokines were produced and released by megakaryocytes upon triggering with thrombopoietin. In addition we made the first observations that a subpopulation of macrophages might react to G-CSF stimulation with a release of thrombopoietin. This could be a valid hint that macrophages are the source of TPO that subsequently stimulates megakaryocytes to release the pro-inflammatory chemokines but until now it has not been ultimately shown that macrophages are the only source of TPO and thereby are the key mediators of the proposed model. To prove their involvement in neutrophil mobilization they have to be removed from the system in order to show that this ablation has a direct impact on the mobilization. Furthermore, the chemokines KC and MIP-2 were also detected in an endothelial cell layer of the bone marrow and their release from these cells could be triggered by G-CSF treatment of animals. As this release might not be triggered by TPO a very interesting question for upcoming experiments is to clarify if the endothelial cells, in contrast to megakaryocytes, harbor the G-CSF receptor and thereby possess the ability to directly react to G-CSF stimulation with the release of KC and MIP-2. Further it would be interesting to assess if our proposed model of TPO induced chemokine release also is of relevance under infection conditions. In the literature it is widely accepted that KC and MIP-2 levels are up-regulated as response to different infections and that, as an example, an inactivation of these chemokines by antibody treatment reduces the number of neutrophils in an acute peritonitis model [Wengner *et al.* 2008], but the mediating steps also still remain unknown. Another context in which our proposed model for neutrophil mobilization could be of interest is the regulation of the constantly circulating neutrophil number in the peripheral blood under normal, resting conditions. This steady release of

neutrophils from the BM into the circulation is influenced by G-CSF. To what extent our described mechanism is also involved in this regulation needs to be further investigated.

7. Reference list

1. Abramson S, Miller RG, Phillips RA. The identification in adult bone marrow of pluripotent and restricted stem cells of the myeloid and lymphoid systems. J Exp Med 1977; 145: 1567-1579.

2. Adams GB, Chabner KT, Alley IR *et al*. Stem cell engraftment at the endosteal niche is specified by the calcium-sensing receptor. Nature 2006a; 439: 599-603.

3. Adams GB, Scadden DT. The hematopoietic stem cell in its place. Nat Immunol 2006b; 7: 333-337.

4. Adams GB, Scadden DT. The hematopoietic stem cell in its place. Nat Immunol 2006c; 7: 333-337.

5. Albu I, Georgia R, Stoica E, Giurgiu T, Pop V. [The system of canals of the diaphysial compact layer of human long bones]. Acta Anat (Basel) 1973; 84: 43-51.

6. Ara T, Tokoyoda K, Sugiyama T, Egawa T, Kawabata K, Nagasawa T. Long-term hematopoietic stem cells require stromal cell-derived factor-1 for colonizing bone marrow during ontogeny. Immunity 2003; 19: 257-267.

7. Arai F, Hirao A, Ohmura M *et al*. Tie2/angiopoietin-1 signaling regulates hematopoietic stem cell quiescence in the bone marrow niche. Cell 2004; 118: 149-161.

8. Arai F, Suda T. Maintenance of quiescent hematopoietic stem cells in the osteoblastic niche. Ann N Y Acad Sci 2007; 1106: 41-53.

9. Avalos BR. Molecular analysis of the granulocyte colony-stimulating factor receptor. Blood 1996; 88: 761-777.

10. Avecilla ST, Hattori K, Heissig B *et al*. Chemokine-mediated interaction of hematopoietic progenitors with the bone marrow vascular niche is required for thrombopoiesis. Nat Med 2004; 10: 64-71.

11. Baggiolini M, Dewald B, Moser B. Interleukin-8 and related chemotactic cytokines--CXC and CC chemokines. Adv Immunol 1994; 55: 97-179.

12. Barcia C, Thomas CE, Curtin JF *et al*. In vivo mature immunological synapses forming SMACs mediate clearance of virally infected astrocytes from the brain. J Exp Med 2006; 203: 2095-2107.

13. Behnsen J, Narang P, Hasenberg M *et al*. Environmental Dimensionality Controls the Interaction of Phagocytes with the Pathogenic Fungi Aspergillus fumigatus and Candida albicans. PLoS Pathog 2007; 3: e13.

14. Blumer MJ, Longato S, Fritsch H. Structure, formation and role of cartilage canals in the developing bone. Ann Anat 2008; 190: 305-315.

15. Bozic CR, Gerard NP, von Uexkull-Guldenband C *et al*. The murine inter-

leukin 8 type B receptor homologue and its ligands. Expression and biological characterization. J Biol Chem 1994; 269: 29355-29358.

16. Bozic CR, Kolakowski LF, Jr., Gerard NP *et al*. Expression and biologic characterization of the murine chemokine KC. J Immunol 1995; 154: 6048-6057.

17. Bradfute SB, Graubert TA, Goodell MA. Roles of Sca-1 in hematopoietic stem/progenitor cell function. Exp Hematol 2005; 33: 836-843.

18. Branehog I, Ridell B, Swolin B, Weinfeld A. Megakaryocyte quantifications in relation to thrombokinetics in primary thrombocythaemia and allied diseases. Scand J Haematol 1975; 15: 321-332.

19. Brinkmann V, Reichard U, Goosmann C *et al*. Neutrophil extracellular traps kill bacteria. Science 2004; 303: 1532-1535.

20. Brinkmann V, Zychlinsky A. Beneficial suicide: why neutrophils die to make NETs. Nat Rev Microbiol 2007; 5: 577-582.

21. Brookes M, Lloyd EG. Marrow vascularization and oestrogen-induced endosteal bone formation in mice. J Anat 1961; 95: 220-228.

22. Broxmeyer HE, Orschell CM, Clapp DW *et al*. Rapid mobilization of murine and human hematopoietic stem and progenitor cells with AMD3100, a CXCR4 antagonist. J Exp Med 2005; 201: 1307-1318.

23. Bruns S, Kniemeyer O, Hasenberg M *et al*. Production of extracellular traps against Aspergillus fumigatus in vitro and in infected lung tissue is dependent on invading neutrophils and influenced by hydrophobin RodA. PLoS Pathog 2010; 6: e1000873.

24. Bunting S, Widmer R, Lipari T *et al*. Normal platelets and megakaryocytes are produced in vivo in the absence of thrombopoietin. Blood 1997; 90: 3423-3429.

25. Burdon PC, Martin C, Rankin SM. Migration across the sinusoidal endothelium regulates neutrophil mobilization in response to ELR + CXC chemokines. Br J Haematol 2008; 142: 100-108.

26. Burdon PC, Martin C, Rankin SM. The CXC chemokine MIP-2 stimulates neutrophil mobilization from the rat bone marrow in a CD49d-dependent manner. Blood 2005; 105: 2543-2548.

27. Burgess AW, Metcalf D. Characterization of a serum factor stimulating the differentiation of myelomonocytic leukemic cells. Int J Cancer 1980; 26: 647-654.

28. Cahalan MD, Parker I, Wei SH, Miller MJ. Two-photon tissue imaging: seeing the immune system in a fresh light. Nat Rev Immunol 2002; 2: 872-880.

29. Carlson T, Kroenke M, Rao P, Lane TE, Segal B. The Th17-ELR+ CXC chemokine pathway is essential for the development of central nervous sys-

tem autoimmune disease. J Exp Med 2008b; 205: 811-823.

30. Carlson T, Kroenke M, Rao P, Lane TE, Segal B. The Th17-ELR+ CXC chemokine pathway is essential for the development of central nervous system autoimmune disease. J Exp Med 2008a; 205: 811-823.

31. Carstanjen D, Gross A, Kosova N, Fichtner I, Salama A. The alpha4beta1 and alpha5beta1 integrins mediate engraftment of granulocyte-colony-stimulating factor-mobilized human hematopoietic progenitor cells. Transfusion 2005; 45: 1192-1200.

32. Cataisson C, Pearson AJ, Tsien MZ *et al*. CXCR2 ligands and G-CSF mediate PKCalpha-induced intraepidermal inflammation. J Clin Invest 2006; 116: 2757-2766.

33. Chambers SM, Shaw CA, Gatza C, Fisk CJ, Donehower LA, Goodell MA. Aging hematopoietic stem cells decline in function and exhibit epigenetic dysregulation. PLoS Biol 2007; 5: e201.

34. Chan CK, Chen CC, Luppen CA *et al*. Endochondral ossification is required for haematopoietic stem-cell niche formation. Nature 2009; 457: 490-494.

35. Chen J, Astle CM, Harrison DE. Genetic regulation of primitive hematopoietic stem cell senescence. Exp Hematol 2000; 28: 442-450.

36. Cheng J, Turkel N, Hemati N, Fuller MT, Hunt AJ, Yamashita YM. Centrosome misorientation reduces stem cell division during ageing. Nature 2008; 456: 599-604.

37. Cheng T, Rodrigues N, Shen H *et al*. Hematopoietic stem cell quiescence maintained by p21cip1/waf1. Science 2000; 287: 1804-1808.

38. Cheshier SH, Morrison SJ, Liao X, Weissman IL. In vivo proliferation and cell cycle kinetics of long-term self-renewing hematopoietic stem cells. Proc Natl Acad Sci U S A 1999; 96: 3120-3125.

39. Chiang EY, Hidalgo A, Chang J, Frenette PS. Imaging receptor microdomains on leukocyte subsets in live mice. Nat Methods 2007; 4: 219-222.

40. Civin CI, Gore SD. Antigenic analysis of hematopoiesis: a review. J Hematother 1993; 2: 137-144.

41. COHEN J, HARRIS WH. The three-dimensional anatomy of haversian systems. J Bone Joint Surg Am 1958; 40-A: 419-434.

42. Cox G, Kable E, Jones A, Fraser I, Manconi F, Gorrell MD. 3-dimensional imaging of collagen using second harmonic generation. J Struct Biol 2003; 141: 53-62.

43. Crawford J, Ozer H, Stoller R *et al*. Reduction by granulocyte colony-stimulating factor of fever and neutropenia induced by chemotherapy in patients with small-cell lung cancer. N Engl J Med 1991; 325: 164-170.

44. CUDKOWICZ G, UPTON AC, SHEARER GM, HUGHES WL. LYMPHOCYTE CONTENT AND PROLIFERATIVE CAPACITY OF SERIALLY TRANSPLANTED MOUSE BONE MARROW. Nature 1964; 201: 165-167.

45. Curry JL, Trentin JJ, Wolf N. Hemopoietic spleen colony studies. II. Erythropoiesis. J Exp Med 1967; 125: 703-720.

46. Cutler C, Antin JH. Peripheral blood stem cells for allogeneic transplantation: a review. Stem Cells 2001; 19: 108-117.

47. Dar A, Kollet O, Lapidot T. Mutual, reciprocal SDF-1/CXCR4 interactions between hematopoietic and bone marrow stromal cells regulate human stem cell migration and development in NOD/SCID chimeric mice. Exp Hematol 2006; 34: 967-975.

48. De Clercq E, Yamamoto N, Pauwels R *et al*. Potent and selective inhibition of human immunodeficiency virus (HIV)-1 and HIV-2 replication by a class of bicyclams interacting with a viral uncoating event. Proc Natl Acad Sci U S A 1992; 89: 5286-5290.

49. de Haan G, Van ZG. Dynamic changes in mouse hematopoietic stem cell numbers during aging. Blood 1999; 93: 3294-3301.

50. de Sauvage FJ, Carver-Moore K, Luoh SM *et al*. Physiological regulation of early and late stages of megakaryocytopoiesis by thrombopoietin. J Exp Med 1996; 183: 651-656.

51. Demetri GD, Griffin JD. Granulocyte colony-stimulating factor and its receptor. Blood 1991; 78: 2791-2808.

52. Demetri GD, Zenzie BW, Rheinwald JG, Griffin JD. Expression of colony-stimulating factor genes by normal human mesothelial cells and human malignant mesothelioma cells lines in vitro. Blood 1989; 74: 940-946.

53. Denk W, Strickler JH, Webb WW. Two-photon laser scanning fluorescence microscopy. Science 1990; 248: 73-76.

54. Deutsch VR, Tomer A. Megakaryocyte development and platelet production. Br J Haematol 2006; 134: 453-466.

55. di Persio JF, Uy GL, Yasothan U, Kirkpatrick P. Plerixafor. Nat Rev Drug Discov 2009; 8: 105-106.

56. Dick JE, Magli MC, Huszar D, Phillips RA, Bernstein A. Introduction of a selectable gene into primitive stem cells capable of long-term reconstitution of the hemopoietic system of W/Wv mice. Cell 1985; 42: 71-79.

57. Dilulio NA, Engeman T, Armstrong D, Tannenbaum C, Hamilton TA, Fairchild RL. Groalpha-mediated recruitment of neutrophils is required for elicitation of contact hypersensitivity. Eur J Immunol 1999; 29: 3485-3495.

58. Eash KJ, Greenbaum AM, Gopalan PK, Link DC. CXCR2 and CXCR4 antagonistically regulate neutrophil trafficking from murine bone marrow. J

Clin Invest 2010.

59. Emadi S, Clay D, Desterke C *et al*. IL-8 and its CXCR1 and CXCR2 receptors participate in the control of megakaryocytic proliferation, differentiation, and ploidy in myeloid metaplasia with myelofibrosis. Blood 2005; 105: 464-473.

60. Ernst TJ, Ritchie AR, Demetri GD, Griffin JD. Regulation of granulocyte- and monocyte-colony stimulating factor mRNA levels in human blood monocytes is mediated primarily at a post-transcriptional level. J Biol Chem 1989; 264: 5700-5703.

61. Fahey TJ, III, Sherry B, Tracey KJ *et al*. Cytokine production in a model of wound healing: the appearance of MIP-1, MIP-2, cachectin/TNF and IL-1. Cytokine 1990; 2: 92-99.

62. Faust N, Varas F, Kelly LM, Heck S, Graf T. Insertion of enhanced green fluorescent protein into the lysozyme gene creates mice with green fluorescent granulocytes and macrophages. Blood 2000; 96: 719-726.

63. Fibbe WE, van DJ, Billiau A *et al*. Interleukin 1 induces human marrow stromal cells in long-term culture to produce granulocyte colony-stimulating factor and macrophage colony-stimulating factor. Blood 1988; 71: 430-435.

64. Fleming WH, Alpern EJ, Uchida N, Ikuta K, Spangrude GJ, Weissman IL. Functional heterogeneity is associated with the cell cycle status of murine hematopoietic stem cells. J Cell Biol 1993; 122: 897-902.

65. Flomenberg N, Devine SM, DiPersio JF *et al*. The use of AMD3100 plus G-CSF for autologous hematopoietic progenitor cell mobilization is superior to G-CSF alone. Blood 2005; 106: 1867-1874.

66. Friedl P, den Boer AT, Gunzer M. Tuning immune responses: diversity and adaptation of the immunological synapse. Nat Rev Immunol 2005; 5: 532-545.

67. Friedl P, Wolf K, von Andrian UH, Harms G. Biological second and third harmonic generation microscopy. Curr Protoc Cell Biol 2007; Chapter 4: Unit.

68. Furze RC, Rankin SM. Neutrophil mobilization and clearance in the bone marrow. Immunology 2008; 125: 281-288.

69. Gabrilove JL, Jakubowski A, Fain K *et al*. Phase I study of granulocyte colony-stimulating factor in patients with transitional cell carcinoma of the urothelium. J Clin Invest 1988a; 82: 1454-1461.

70. Gabrilove JL, Jakubowski A, Scher H *et al*. Effect of granulocyte colony-stimulating factor on neutropenia and associated morbidity due to chemotherapy for transitional-cell carcinoma of the urothelium. N Engl J Med 1988b; 318: 1414-1422.

71. Geiger H, Koehler A, Gunzer M. Stem cells, aging, niche, adhesion and

Cdc42: a model for changes in cell-cell interactions and hematopoietic stem cell aging. Cell Cycle 2007; 6: 884-887.

72. Geiger H, Rennebeck G, Van ZG. Regulation of hematopoietic stem cell aging in vivo by a distinct genetic element. Proc Natl Acad Sci U S A 2005; 102: 5102-5107.

73. Geiger H, Van ZG. The aging of lympho-hematopoietic stem cells. Nat Immunol 2002; 3: 329-333.

74. Göppert-Mayer M. Über Elementarakte mit zwei Quantensprüngen. Ann Phys 1931; 273-295.

75. Gordon JR, Li F, Zhang X, Wang W, Zhao X, Nayyar A. The combined CXCR1/CXCR2 antagonist CXCL8(3-74)K11R/G31P blocks neutrophil infiltration, pyrexia, and pulmonary vascular pathology in endotoxemic animals. J Leukoc Biol 2005; 78: 1265-1272.

76. Gregory AD, Hogue LA, Ferkol TW, Link DC. Regulation of systemic and local neutrophil responses by G-CSF during pulmonary Pseudomonas aeruginosa infection. Blood 2007; 109: 3235-3243.

77. Gunzer M, Schafer A, Borgmann S *et al*. Antigen presentation in extracellular matrix: interactions of T cells with dendritic cells are dynamic, short lived, and sequential. Immunity 2000; 13: 323-332.

78. Gunzer M, Weishaupt C, Hillmer A *et al*. A spectrum of biophysical interaction modes between T cells and different antigen-presenting cells during priming in 3-D collagen and in vivo. Blood 2004; 104: 2801-2809.

79. Gurney AL, Carver-Moore K, de Sauvage FJ, Moore MW. Thrombocytopenia in c-mpl-deficient mice. Science 1994; 265: 1445-1447.

80. Hanson P, Mathews V, Marrus SH, Graubert TA. Enhanced green fluorescent protein targeted to the Sca-1 (Ly-6A) locus in transgenic mice results in efficient marking of hematopoietic stem cells in vivo. Exp Hematol 2003; 31: 159-167.

81. Harrington LE, Hatton RD, Mangan PR *et al*. Interleukin 17-producing CD4+ effector T cells develop via a lineage distinct from the T helper type 1 and 2 lineages. Nat Immunol 2005; 6: 1123-1132.

82. Hauser AE, Junt T, Mempel TR *et al*. Definition of germinal-center B cell migration in vivo reveals predominant intrazonal circulation patterns. Immunity 2007; 26: 655-667.

83. Hendrix CW, Flexner C, MacFarland RT *et al*. Pharmacokinetics and safety of AMD-3100, a novel antagonist of the CXCR-4 chemokine receptor, in human volunteers. Antimicrob Agents Chemother 2000; 44: 1667-1673.

84. Henrickson SE, Mempel TR, Mazo IB *et al*. T cell sensing of antigen dose governs interactive behavior with dendritic cells and sets a threshold for T cell activation. Nat Immunol 2008; 9: 282-291.

85. Herrmann F, Cannistra SA, Griffin JD. T cell-monocyte interactions in the production of humoral factors regulating human granulopoiesis in vitro. J Immunol 1986; 136: 2856-2861.

86. HERT J, HLADIKOVA J. [The vascular supply of the Haversian bones.]. Acta Anat (Basel) 1961; 45: 344-361.

87. Higuchi T, Koike K, Sawai N *et al*. Megakaryocytes derived from CD34-positive cord blood cells produce interleukin-8. Br J Haematol 1997; 99: 509-516.

88. Hill CP, Johnston NL, Cohen RE. Crystal structure of a ubiquitin-dependent degradation substrate: a three-disulfide form of lysozyme. Proc Natl Acad Sci U S A 1993a; 90: 4136-4140.

89. Hill CP, Osslund TD, Eisenberg D. The structure of granulocyte-colony-stimulating factor and its relationship to other growth factors. Proc Natl Acad Sci U S A 1993b; 90: 5167-5171.

90. Hoebe K, Janssen E, Beutler B. The interface between innate and adaptive immunity. Nat Immunol 2004; 5: 971-974.

91. Holmes WE, Lee J, Kuang WJ, Rice GC, Wood WI. Structure and functional expression of a human interleukin-8 receptor. Science 1991; 253: 1278-1280.

92. Horuk R. Chemokine receptors. Cytokine Growth Factor Rev 2001; 12: 313-335.

93. Hosking MP, Liu L, Ransohoff RM, Lane TE. A Protective Role for ELR+ Chemokines during Acute Viral Encephalomyelitis. PLoS Pathog 2009; 5: e1000648.

94. Huang S, Paulauskis JD, Godleski JJ, Kobzik L. Expression of macrophage inflammatory protein-2 and KC mRNA in pulmonary inflammation. Am J Pathol 1992; 141: 981-988.

95. Ito CY, Li CY, Bernstein A, Dick JE, Stanford WL. Hematopoietic stem cell and progenitor defects in Sca-1/Ly-6A-null mice. Blood 2003; 101: 517-523.

96. Jagels MA, Chambers JD, Arfors KE, Hugli TE. C5a- and tumor necrosis factor-alpha-induced leukocytosis occurs independently of beta 2 integrins and L-selectin: differential effects on neutrophil adhesion molecule expression in vivo. Blood 1995; 85: 2900-2909.

97. Jagels MA, Hugli TE. Neutrophil chemotactic factors promote leukocytosis. A common mechanism for cellular recruitment from bone marrow. J Immunol 1992; 148: 1119-1128.

98. Janzen V, Forkert R, Fleming HE *et al*. Stem-cell ageing modified by the cyclin-dependent kinase inhibitor p16INK4a. Nature 2006; 443: 421-426.

99. Jordan CT, Lemischka IR. Clonal and systemic analysis of long-term hema-

topoiesis in the mouse. Genes Dev 1990; 4: 220-232.

100. Ju ST, Panka DJ, Cui H *et al*. Fas(CD95)/FasL interactions required for programmed cell death after T-cell activation. Nature 1995; 373: 444-448.

101. Jung S, Aliberti J, Graemmel P *et al*. Analysis of fractalkine receptor CX(3)CR1 function by targeted deletion and green fluorescent protein reporter gene insertion. Mol Cell Biol 2000; 20: 4106-4114.

102. Jung Y, Wang J, Havens A *et al*. Cell-to-cell contact is critical for the survival of hematopoietic progenitor cells on osteoblasts. Cytokine 2005; 32: 155-162.

103. Junquiera LC, Carneiro J. Histologie. Heidelberg: Springer Medizin Verlag; 2005.

104. Junt T, Schulze H, Chen Z *et al*. Dynamic visualization of thrombopoiesis within bone marrow. Science 2007; 317: 1767-1770.

105. Kagi D, Vignaux F, Ledermann B *et al*. Fas and perforin pathways as major mechanisms of T cell-mediated cytotoxicity. Science 1994; 265: 528-530.

106. Kalajzic I, Kalajzic Z, Kaliterna M *et al*. Use of type I collagen green fluorescent protein transgenes to identify subpopulations of cells at different stages of the osteoblast lineage. J Bone Miner Res 2002; 17: 15-25.

107. Kamminga LM, de HG. Cellular memory and hematopoietic stem cell aging. Stem Cells 2006; 24: 1143-1149.

108. Katayama Y, Battista M, Kao WM *et al*. Signals from the sympathetic nervous system regulate hematopoietic stem cell egress from bone marrow. Cell 2006; 124: 407-421.

109. Kaushansky K. Lineage-specific hematopoietic growth factors. N Engl J Med 2006; 354: 2034-2045.

110. Keller G, Paige C, Gilboa E, Wagner EF. Expression of a foreign gene in myeloid and lymphoid cells derived from multipotent haematopoietic precursors. Nature 1985; 318: 149-154.

111. Kiel MJ, Morrison SJ. Maintaining hematopoietic stem cells in the vascular niche. Immunity 2006; 25: 862-864.

112. Kiel MJ, Yilmaz OH, Iwashita T, Yilmaz OH, Terhorst C, Morrison SJ. SLAM family receptors distinguish hematopoietic stem and progenitor cells and reveal endothelial niches for stem cells. Cell 2005; 121: 1109-1121.

113. Kielian T, Barry B, Hickey WF. CXC chemokine receptor-2 ligands are required for neutrophil-mediated host defense in experimental brain abscesses. J Immunol 2001; 166: 4634-4643.

114. Kim HK, De La Luz SM, Williams CK, Gulino AV, Tosato G. G-CSF down-regulation of CXCR4 expression identified as a mechanism for mobilization

of myeloid cells. Blood 2006; 108: 812-820.

115. King AG, Horowitz D, Dillon SB *et al*. Rapid mobilization of murine hematopoietic stem cells with enhanced engraftment properties and evaluation of hematopoietic progenitor cell mobilization in rhesus monkeys by a single injection of SB-251353, a specific truncated form of the human CXC chemokine GRObeta. Blood 2001; 97: 1534-1542.

116. Knapp S, Hareng L, Rijneveld AW *et al*. Activation of neutrophils and inhibition of the proinflammatory cytokine response by endogenous granulocyte colony-stimulating factor in murine pneumococcal pneumonia. J Infect Dis 2004; 189: 1506-1515.

117. Kobayashi Y. Neutrophil infiltration and chemokines. Crit Rev Immunol 2006; 26: 307-316.

118. Koch AE, Polverini PJ, Kunkel SL *et al*. Interleukin-8 as a macrophage-derived mediator of angiogenesis. Science 1992; 258: 1798-1801.

119. Koeffler HP, Gasson J, Ranyard J, Souza L, Shepard M, Munker R. Recombinant human TNF alpha stimulates production of granulocyte colony-stimulating factor. Blood 1987; 70: 55-59.

120. Koeffler HP, Gasson J, Tobler A. Transcriptional and posttranscriptional modulation of myeloid colony-stimulating factor expression by tumor necrosis factor and other agents. Mol Cell Biol 1988; 8: 3432-3438.

121. Kohler A, Schmithorst V, Filippi MD *et al*. Altered cellular dynamics and endosteal location of aged early hematopoietic progenitor cells revealed by time-lapse intravital imaging in long bones. Blood 2009; 114: 290-298.

122. Kondo M, Wagers AJ, Manz MG *et al*. Biology of hematopoietic stem cells and progenitors: implications for clinical application. Annu Rev Immunol 2003; 21: 759-806.

123. Krause DS, Theise ND, Collector MI *et al*. Multi-organ, multi-lineage engraftment by a single bone marrow-derived stem cell. Cell 2001; 105: 369-377.

124. Lally F, Smith E, Filer A *et al*. A novel mechanism of neutrophil recruitment in a coculture model of the rheumatoid synovium. Arthritis Rheum 2005; 52: 3460-3469.

125. Lapidot T, Dar A, Kollet O. How do stem cells find their way home? Blood 2005; 106: 1901-1910.

126. Lapidot T, Petit I. Current understanding of stem cell mobilization: the roles of chemokines, proteolytic enzymes, adhesion molecules, cytokines, and stromal cells. Exp Hematol 2002; 30: 973-981.

127. Laterveer L, Lindley IJ, Hamilton MS, Willemze R, Fibbe WE. Interleukin-8 induces rapid mobilization of hematopoietic stem cells with radioprotective capacity and long-term myelolymphoid repopulating ability. Blood 1995; 85:

2269-2275.

128. Le Beau MM, Lemons RS, Carrino JJ *et al*. Chromosomal localization of the human G-CSF gene to 17q11 proximal to the breakpoint of the t(15;17) in acute promyelocytic leukemia. Leukemia 1987; 1: 795-799.

129. Le Y, Zhou Y, Iribarren P, Wang J. Chemokines and chemokine receptors: their manifold roles in homeostasis and disease. Cell Mol Immunol 2004; 1: 95-104.

130. Leeuwenberg JF, Smeets EF, Neefjes JJ *et al*. E-selectin and intercellular adhesion molecule-1 are released by activated human endothelial cells in vitro. Immunology 1992; 77: 543-549.

131. Levesque JP, Hendy J, Takamatsu Y, Simmons PJ, Bendall LJ. Disruption of the CXCR4/CXCL12 chemotactic interaction during hematopoietic stem cell mobilization induced by GCSF or cyclophosphamide. J Clin Invest 2003a; 111: 187-196.

132. Levesque JP, Hendy J, Takamatsu Y, Simmons PJ, Bendall LJ. Disruption of the CXCR4/CXCL12 chemotactic interaction during hematopoietic stem cell mobilization induced by GCSF or cyclophosphamide. J Clin Invest 2003b; 111: 187-196.

133. Liang Y, Van ZG, Szilvassy SJ. Effects of aging on the homing and engraftment of murine hematopoietic stem and progenitor cells. Blood 2005; 106: 1479-1487.

134. Liles WC, Broxmeyer HE, Rodger E *et al*. Mobilization of hematopoietic progenitor cells in healthy volunteers by AMD3100, a CXCR4 antagonist. Blood 2003; 102: 2728-2730.

135. Link DC. Neutrophil homeostasis: a new role for stromal cell-derived factor-1. Immunol Res 2005; 32: 169-178.

136. Lo CC, Fleming HE, Wu JW *et al*. Live-animal tracking of individual haematopoietic stem/progenitor cells in their niche. Nature 2009; 457: 92-96.

137. Ma Q, Jones D, Borghesani PR *et al*. Impaired B-lymphopoiesis, myelopoiesis, and derailed cerebellar neuron migration in C. Proc Natl Acad Sci U S A 1998; 95: 9448-9453.

138. Marotti G, Zallone AZ. Changes in the vascular network during the formation of Haversian systems. Acta Anat (Basel) 1980; 106: 84-100.

139. Mazo IB, Gutierrez-Ramos JC, Frenette PS, Hynes RO, Wagner DD, von Andrian UH. Hematopoietic progenitor cell rolling in bone marrow microvessels: parallel contributions by endothelial selectins and vascular cell adhesion molecule 1. J Exp Med 1998; 188: 465-474.

140. McColl SR, Clark-Lewis I. Inhibition of murine neutrophil recruitment in vivo by CXC chemokine receptor antagonists. J Immunol 1999; 163: 2829-2835.

141. McDonald B, Pittman K, Menezes GB *et al*. Intravascular danger signals guide neutrophils to sites of sterile inflammation. Science 2010; 330: 362-366.

142. Mempel TR, Henrickson SE, von Andrian UH. T-cell priming by dendritic cells in lymph nodes occurs in three distinct phases. Nature 2004a; 427: 154-159.

143. Mempel TR, Scimone ML, Mora JR, von Andrian UH. In vivo imaging of leukocyte trafficking in blood vessels and tissues. Curr Opin Immunol 2004b; 16: 406-417.

144. Mempel TR, Scimone ML, Mora JR, von Andrian UH. In vivo imaging of leukocyte trafficking in blood vessels and tissues. Curr Opin Immunol 2004c; 16: 406-417.

145. Mendez-Ferrer S, Michurina TV, Ferraro F *et al*. Mesenchymal and haematopoietic stem cells form a unique bone marrow niche. Nature 2010; 466: 829-834.

146. Metcalf D. Hematopoietic cytokines. Blood 2008; 111: 485-491.

147. Metcalf D, Robb L, Dunn AR, Mifsud S, Di RL. Role of granulocyte-macrophage colony-stimulating factor and granulocyte colony-stimulating factor in the development of an acute neutrophil inflammatory response in mice. Blood 1996; 88: 3755-3764.

148. Miura M, Fu X, Zhang QW, Remick DG, Fairchild RL. Neutralization of Gro alpha and macrophage inflammatory protein-2 attenuates renal ischemia/reperfusion injury. Am J Pathol 2001; 159: 2137-2145.

149. Morrison SJ, Hemmati HD, Wandycz AM, Weissman IL. The purification and characterization of fetal liver hematopoietic stem cells. Proc Natl Acad Sci U S A 1995; 92: 10302-10306.

150. Morrison SJ, Wandycz AM, Akashi K, Globerson A, Weissman IL. The aging of hematopoietic stem cells. Nat Med 1996; 2: 1011-1016.

151. Morstyn G, Campbell L, Souza LM *et al*. Effect of granulocyte colony stimulating factor on neutropenia induced by cytotoxic chemotherapy. Lancet 1988; 1: 667-672.

152. Murdoch C, Finn A. Chemokine receptors and their role in inflammation and infectious diseases. Blood 2000; 95: 3032-3043.

153. Murone M, Carpenter DA, de Sauvage FJ. Hematopoietic deficiencies in c-mpl and TPO knockout mice. Stem Cells 1998; 16: 1-6.

154. Murphy K, Travers P, Walport M. Janeway`s Immunobiology. 2008.

155. Murphy PM. Neutrophil receptors for interleukin-8 and related CXC chemokines. Semin Hematol 1997; 34: 311-318.

156. Murphy PM. Chemokines and the molecular basis of cancer metastasis. N Engl J Med 2001; 345: 833-835.

157. Murphy PM. The molecular biology of leukocyte chemoattractant receptors. Annu Rev Immunol 1994; 12: 593-633.

158. Murphy PM, Baggiolini M, Charo IF *et al*. International union of pharmacology. XXII. Nomenclature for chemokine receptors. Pharmacol Rev 2000; 52: 145-176.

159. Nagata S, Tsuchiya M, Asano S *et al*. Molecular cloning and expression of cDNA for human granulocyte colony-stimulating factor. Nature 1986a; 319: 415-418.

160. Nagata S, Tsuchiya M, Asano S *et al*. The chromosomal gene structure and two mRNAs for human granulocyte colony-stimulating factor. EMBO J 1986b; 5: 575-581.

161. Nagata S, Tsuchiya M, Asano S *et al*. The chromosomal gene structure and two mRNAs for human granulocyte colony-stimulating factor. EMBO J 1986c; 5: 575-581.

162. Nakae S, Nambu A, Sudo K, Iwakura Y. Suppression of immune induction of collagen-induced arthritis in IL-17-deficient mice. J Immunol 2003; 171: 6173-6177.

163. Neiva K, Sun YX, Taichman RS. The role of osteoblasts in regulating hematopoietic stem cell activity and tumor metastasis. Braz J Med Biol Res 2005; 38: 1449-1454.

164. Nilsson SK, Haylock DN, Johnston HM, Occhiodoro T, Brown TJ, Simmons PJ. Hyaluronan is synthesized by primitive hemopoietic cells, participates in their lodgment at the endosteum following transplantation, and is involved in the regulation of their proliferation and differentiation in vitro. Blood 2003; 101: 856-862.

165. Nilsson SK, Johnston HM, Coverdale JA. Spatial localization of transplanted hemopoietic stem cells: inferences for the localization of stem cell niches. Blood 2001; 97: 2293-2299.

166. Nilsson SK, Johnston HM, Whitty GA *et al*. Osteopontin, a key component of the hematopoietic stem cell niche and regulator of primitive hematopoietic progenitor cells. Blood 2005; 106: 1232-1239.

167. Nilsson SK, Simmons PJ. Transplantable stem cells: home to specific niches. Curr Opin Hematol 2004; 11: 102-106.

168. Nourshargh S, Hordijk PL, Sixt M. Breaching multiple barriers: leukocyte motility through venular walls and the interstitium. Nat Rev Mol Cell Biol 2010; 11: 366-378.

169. Ohmori Y, Hamilton TA. Cell type and stimulus specific regulation of chemokine gene expression. Biochem Biophys Res Commun 1994a; 198: 590-

596.

170. Ohmori Y, Hamilton TA. IFN-gamma selectively inhibits lipopolysaccharide-inducible JE/monocyte chemoattractant protein-1 and KC/GRO/melanoma growth-stimulating activity gene expression in mouse peritoneal macrophages. J Immunol 1994b; 153: 2204-2212.

171. Opdenakker G, Fibbe WE, van DJ. The molecular basis of leukocytosis. Immunol Today 1998; 19: 182-189.

172. Osawa M, Hanada K, Hamada H, Nakauchi H. Long-term lymphohematopoietic reconstitution by a single CD34-low/negative hematopoietic stem cell. Science 1996; 273: 242-245.

173. Oster W, Lindemann A, Mertelsmann R, Herrmann F. Granulocyte-macrophage colony-stimulating factor (CSF) and multilineage CSF recruit human monocytes to express granulocyte CSF. Blood 1989; 73: 64-67.

174. P.A.Franken AEHCWPaGW. Generation of Optical Harmonics. Phys Rev Lett 1961; 7: 118.

175. Pannarale L, Morini S, D'Ubaldo E, Gaudio E, Marinozzi G. SEM corrosion-casts study of the microcirculation of the flat bones in the rat. Anat Rec 1997; 247: 462-471.

176. Papayannopoulou T. Current mechanistic scenarios in hematopoietic stem/progenitor cell mobilization. Blood 2004; 103: 1580-1585.

177. Papayannopoulou T. Bone marrow homing: the players, the playfield, and their evolving roles. Curr Opin Hematol 2003; 10: 214-219.

178. Park H, Li Z, Yang XO *et al*. A distinct lineage of CD4 T cells regulates tissue inflammation by producing interleukin 17. Nat Immunol 2005; 6: 1133-1141.

179. Pelus LM. Peripheral blood stem cell mobilization: new regimens, new cells, where do we stand. Curr Opin Hematol 2008; 15: 285-292.

180. Peters NC, Egen JG, Secundino N *et al*. In vivo imaging reveals an essential role for neutrophils in leishmaniasis transmitted by sand flies. Science 2008; 321: 970-974.

181. Petit I, Szyper-Kravitz M, Nagler A *et al*. G-CSF induces stem cell mobilization by decreasing bone marrow SDF-1 and up-regulating CXCR4. Nat Immunol 2002; 3: 687-694.

182. Ponomaryov T, Peled A, Petit I *et al*. Induction of the chemokine stromal-derived factor-1 following DNA damage improves human stem cell function. J Clin Invest 2000; 106: 1331-1339.

183. Rando TA. Stem cells, ageing and the quest for immortality. Nature 2006; 441: 1080-1086.

184. Reichardt P, Gunzer F, Gunzer M. Analyzing the physicodynamics of immune cells in a three-dimensional collagen matrix. Methods Mol Biol 2007; 380: 253-269.

185. Rossi DJ, Bryder D, Zahn JM *et al*. Cell intrinsic alterations underlie hematopoietic stem cell aging. Proc Natl Acad Sci U S A 2005; 102: 9194-9199.

186. Rovai LE, Herschman HR, Smith JB. The murine neutrophil-chemoattractant chemokines LIX, KC, and MIP-2 have distinct induction kinetics, tissue distributions, and tissue-specific sensitivities to glucocorticoid regulation in endotoxemia. J Leukoc Biol 1998; 64: 494-502.

187. Russell JH, Ley TJ. Lymphocyte-mediated cytotoxicity. Annu Rev Immunol 2002; 20: 323-370.

188. Safirstein R, Megyesi J, Saggi SJ *et al*. Expression of cytokine-like genes JE and KC is increased during renal ischemia. Am J Physiol 1991; 261: F1095-F1101.

189. Sakaue-Sawano A, Kurokawa H, Morimura T *et al*. Visualizing spatiotemporal dynamics of multicellular cell-cycle progression. Cell 2008; 132: 487-498.

190. Scadden DT. The stem-cell niche as an entity of action. Nature 2006b; 441: 1075-1079.

191. Scadden DT. The stem-cell niche as an entity of action. Nature 2006a; 441: 1075-1079.

192. Schiebler TH. Anatomie. 2005.

193. Schofield R. The relationship between the spleen colony-forming cell and the haemopoietic stem cell. Blood Cells 1978; 4: 7-25.

194. Semerad CL, Christopher MJ, Liu F *et al*. G-CSF potently inhibits osteoblast activity and CXCL12 mRNA expression in the bone marrow. Blood 2005a; 106: 3020-3027.

195. Semerad CL, Christopher MJ, Liu F *et al*. G-CSF potently inhibits osteoblast activity and CXCL12 mRNA expression in the bone marrow. Blood 2005b; 106: 3020-3027.

196. Semerad CL, Liu F, Gregory AD, Stumpf K, Link DC. G-CSF is an essential regulator of neutrophil trafficking from the bone marrow to the blood. Immunity 2002; 17: 413-423.

197. Shahbazian LM, Quinton LJ, Bagby GJ, Nelson S, Wang G, Zhang P. Escherichia coli pneumonia enhances granulopoiesis and the mobilization of myeloid progenitor cells into the systemic circulation. Crit Care Med 2004; 32: 1740-1746.

198. Sharpless NE, DePinho RA. Telomeres, stem cells, senescence, and cancer. J Clin Invest 2004; 113: 160-168.

199. Sherry B, Horii Y, Manogue KR, Widmer U, Cerami A. Macrophage inflammatory proteins 1 and 2: an overview. Cytokines 1992; 4: 117-130.

200. SIMINOVITCH L, TILL JE, MCCULLOCH EA. DECLINE IN COLONY-FORMING ABILITY OF MARROW CELLS SUBJECTED TO SERIAL TRANSPLANTATION INTO IRRADIATED MICE. J Cell Physiol 1964; 64: 23-31.

201. Simmers RN, Webber LM, Shannon MF *et al*. Localization of the G-CSF gene on chromosome 17 proximal to the breakpoint in the t(15;17) in acute promyelocytic leukemia. Blood 1987; 70: 330-332.

202. Smith JW. Collagen fibre patterns in mammalian bone. J Anat 1960; 94: 329-344.

203. Souza LM, Boone TC, Gabrilove J *et al*. Recombinant human granulocyte colony-stimulating factor: effects on normal and leukemic myeloid cells. Science 1986; 232: 61-65.

204. Spangrude GJ, Johnson GR. Resting and activated subsets of mouse multipotent hematopoietic stem cells. Proc Natl Acad Sci U S A 1990; 87: 7433-7437.

205. Stegemann S, Dahlberg S, Kröger A *et al*. Increased susceptibility for superinfection with *Streptococcus pneumoniae* during influenza virus infection is not caused by TLR7-mediated lymphopenia. PLoS one 2009; 4: e4840.

206. Strieter RM, Kunkel SL, Elner VM *et al*. Interleukin-8. A corneal factor that induces neovascularization. Am J Pathol 1992; 141: 1279-1284.

207. Suda T, Arai F, Hirao A. Hematopoietic stem cells and their niche. Trends Immunol 2005; 26: 426-433.

208. Sudo K, Ema H, Morita Y, Nakauchi H. Age-associated characteristics of murine hematopoietic stem cells. J Exp Med 2000; 192: 1273-1280.

209. Sugiyama T, Kohara H, Noda M, Nagasawa T. Maintenance of the hematopoietic stem cell pool by CXCL12-CXCR4 chemokine signaling in bone marrow stromal cell niches. Immunity 2006; 25: 977-988.

210. Sumen C, Mempel TR, Mazo IB, von Andrian UH. Intravital microscopy: visualizing immunity in context. Immunity 2004; 21: 315-329.

211. Sungaran R, Markovic B, Chong BH. Localization and regulation of thrombopoietin mRNa expression in human kidney, liver, bone marrow, and spleen using in situ hybridization. Blood 1997; 89: 101-107.

212. Suratt BT, Petty JM, Young SK *et al*. Role of the CXCR4/SDF-1 chemokine axis in circulating neutrophil homeostasis. Blood 2004; 104: 565-571.

213. Szilvassy SJ. The biology of hematopoietic stem cells. Arch Med Res 2003; 34: 446-460.

214. Szilvassy SJ, Cory S. Efficient retroviral gene transfer to purified long-term repopulating hematopoietic stem cells. Blood 1994; 84: 74-83.

215. Tachibana K, Hirota S, Iizasa H *et al*. The chemokine receptor CXCR4 is essential for vascularization of the gastrointestinal tract. Nature 1998; 393: 591-594.

216. Terashima T, English D, Hogg JC, van Eeden SF. Release of polymorphonuclear leukocytes from the bone marrow by interleukin-8. Blood 1998; 92: 1062-1069.

217. Thomas J, Liu F, Link DC. Mechanisms of mobilization of hematopoietic progenitors with granulocyte colony-stimulating factor. Curr Opin Hematol 2002; 9: 183-189.

218. Torella D, Rota M, Nurzynska D *et al*. Cardiac stem cell and myocyte aging, heart failure, and insulin-like growth factor-1 overexpression. Circ Res 2004; 94: 514-524.

219. Trias A, Fery A. Cortical circulation of long bones. J Bone Joint Surg Am 1979; 61: 1052-1059.

220. Tromberg BJ, Shah N, Lanning R *et al*. Non-invasive in vivo characterization of breast tumors using photon migration spectroscopy. Neoplasia 2000; 2: 26-40.

221. Tsuchiya M, Asano S, Kaziro Y, Nagata S. Isolation and characterization of the cDNA for murine granulocyte colony-stimulating factor. Proc Natl Acad Sci U S A 1986; 83: 7633-7637.

222. Uchida N, Fleming WH, Alpern EJ, Weissman IL. Heterogeneity of hematopoietic stem cells. Curr Opin Immunol 1993; 5: 177-184.

223. van Zant G, Liang Y. The role of stem cells in aging. Exp Hematol 2003; 31: 659-672.

224. VASCIAVEO F, BARTOLI E. Vascular channels and resorption cavities in the long bone cortex. The bovine bone. Acta Anat (Basel) 1961; 47: 1-33.

225. Vellenga E, Rambaldi A, Ernst TJ, Ostapovicz D, Griffin JD. Independent regulation of M-CSF and G-CSF gene expression in human monocytes. Blood 1988; 71: 1529-1532.

226. Villeval JL, Cohen-Solal K, Tulliez M *et al*. High thrombopoietin production by hematopoietic cells induces a fatal myeloproliferative syndrome in mice. Blood 1997; 90: 4369-4383.

227. Visnjic D, Kalajzic I, Gronowicz G *et al*. Conditional ablation of the osteoblast lineage in Col2.3deltatk transgenic mice. J Bone Miner Res 2001; 16: 2222-2231.

228. Visnjic D, Kalajzic Z, Rowe DW, Katavic V, Lorenzo J, Aguila HL. Hematopoiesis is severely altered in mice with an induced osteoblast deficiency.

Blood 2004; 103: 3258-3264.

229. Visser JW, Van Bekkum DW. Purification of pluripotent hemopoietic stem cells: past and present. Exp Hematol 1990; 18: 248-256.

230. Voisin MB, Probstl D, Nourshargh S. Venular basement membranes ubiquitously express matrix protein low-expression regions: characterization in multiple tissues and remodeling during inflammation. Am J Pathol 2010; 176: 482-495.

231. von Andrian UH, Mempel TR. Homing and cellular traffic in lymph nodes. Nat Rev Immunol 2003; 3: 867-878.

232. von Vietinghoff S, Ley K. Homeostatic regulation of blood neutrophil counts. J Immunol 2008; 181: 5183-5188.

233. Wagers AJ, Allsopp RC, Weissman IL. Changes in integrin expression are associated with altered homing properties of Lin(-/lo)Thy1.1(lo)Sca-1(+)c-kit(+) hematopoietic stem cells following mobilization by cyclophosphamide/granulocyte colony-stimulating factor. Exp Hematol 2002; 30: 176-185.

234. Wang JM, Deng X, Gong W, Su S. Chemokines and their role in tumor growth and metastasis. J Immunol Methods 1998; 220: 1-17.

235. Wang S, Voisin MB, Larbi KY *et al*. Venular basement membranes contain specific matrix protein low expression regions that act as exit points for emigrating neutrophils. J Exp Med 2006; 203: 1519-1532.

236. Weissman IL. Stem cells: units of development, units of regeneration, and units in evolution. Cell 2000; 100: 157-168.

237. Wengner AM, Pitchford SC, Furze RC, Rankin SM. The coordinated action of G-CSF and ELR + CXC chemokines in neutrophil mobilization during acute inflammation. Blood 2008; 111: 42-49.

238. Wierenga PK, Weersing E, Dontje B, de HG, van OR. Differential role for very late antigen-5 in mobilization and homing of hematopoietic stem cells. Bone Marrow Transplant 2006; 38: 789-797.

239. Wieser M, Bonifer R, Oster W, Lindemann A, Mertelsmann R, Herrmann F. Interleukin-4 induces secretion of CSF for granulocytes and CSF for macrophages by peripheral blood monocytes. Blood 1989; 73: 1105-1108.

240. Williams B.Swaim. Overview over Confocal microscopy. 2010.

241. Wilson A, Murphy MJ, Oskarsson T *et al*. c-Myc controls the balance between hematopoietic stem cell self-renewal and differentiation. Genes Dev 2004; 18: 2747-2763.

242. Wilson A, Trumpp A. Bone-marrow haematopoietic-stem-cell niches. Nat Rev Immunol 2006b; 6: 93-106.

243. Wilson A, Trumpp A. Bone-marrow haematopoietic-stem-cell niches. Nat Rev Immunol 2006a; 6: 93-106.

244. Witowski J, Ksiazek K, Warnecke C *et al*. Role of mesothelial cell-derived granulocyte colony-stimulating factor in interleukin-17-induced neutrophil accumulation in the peritoneum. Kidney Int 2007; 71: 514-525.

245. Wright DE, Bowman EP, Wagers AJ, Butcher EC, Weissman IL. Hematopoietic stem cells are uniquely selective in their migratory response to chemokines. J Exp Med 2002; 195: 1145-1154.

246. Xie Y, Yin T, Wiegraebe W *et al*. Detection of functional haematopoietic stem cell niche using real-time imaging. Nature 2009; 457: 97-101.

247. Xing Z, Ryan MA, Daria D *et al*. Increased hematopoietic stem cell mobilization in aged mice. Blood 2006; 108: 2190-2197.

248. Yin T, Li L. The stem cell niches in bone. J Clin Invest 2006; 116: 1195-1201.

249. Yoshihara H, Arai F, Hosokawa K *et al*. Thrombopoietin/MPL signaling regulates hematopoietic stem cell quiescence and interaction with the osteoblastic niche. Cell Stem Cell 2007; 1: 685-697.

250. Zhang H, Meng F, Chu CL, Takai T, Lowell CA. The Src family kinases Hck and Fgr negatively regulate neutrophil and dendritic cell chemokine signaling via PIR-B. Immunity 2005; 22: 235-246.

251. Zhang J, Niu C, Ye L *et al*. Identification of the haematopoietic stem cell niche and control of the niche size. Nature 2003; 425: 836-841.

252. Zou YR, Kottmann AH, Kuroda M, Taniuchi I, Littman DR. Function of the chemokine receptor CXCR4 in haematopoiesis and in cerebellar development. Nature 1998; 393: 595-599.

253. Zsebo KM, Yuschenkoff VN, Schiffer S *et al*. Vascular endothelial cells and granulopoiesis: interleukin-1 stimulates release of G-CSF and GM-CSF. Blood 1988; 71: 99-103.

8. Appendix – DVD-Content

Supplemental movie 1 Behavior of eHPCs from young mice in long bones. eHPCS were isolated from 8 weeks old C57Bl/6 mice, stained with CFSE and adoptively transferred into a naÏve 8 weeks old recipient. 2-photon microscopy was carried out in the tibia at a total magnification of 200x, 18 h after cell transfer. The recording time was 10 min, one z-stack consisted of 31 steps with an interval of 3 µm and the repetition time for each z-stack acquisition was 80 s. The bone structure, displayed in brown was detected by its SHG signal.

Supplemental movie 2 Behavior of eHPCs from old mice in long bones. eHPCS were isolated from 18-20 months old C57Bl/6 mice, stained with CFSE and adoptively transferred into a naÏve 8 weeks old recipient. 2-photon microscopy was carried out in the tibia at a total magnification of 200x, 18 h after cell transfer. The recording time was 9 min, one z-stack consisted of 31 steps with an interval of 4 µm and the repetition time for each z-stack acquisition was 60 s. The bone structure, displayed in brown was detected by its SHG signal.

Supplemental movie 3 Behavior of HPCs from young mice in long bones. HPCS were isolated from 8 weeks old C57Bl/6 mice, stained with CFSE and adoptively transferred into a naÏve 8 weeks old recipient. 2-photon microscopy was carried out in the tibia at a total magnification of 200x, 40 h after cell transfer. The recording time was 14 min, one z-stack consisted of 31 steps with an interval of 4 µm and the repetition time for each z-stack acquisition was 80 s. The bone structure, displayed in brown was detected by its SHG signal.

Supplemental movie 4 Behavior of HPCs from old mice in long bones. HPCS were isolated from old 18-20 months old C57Bl/6 mice, stained with CFSE and adoptively transferred into a naÏve 8 weeks old recipient. 2-photon microscopy was carried out in the tibia at a total magnification of 200x, 40 h after cell transfer. The recording time was 10 min, one z-stack consisted of 31 steps with an interval of 4 µm and the repetition time for each z-stack acquisition was 60 s. The bone structure, displayed in brown was detected by its SHG signal.

Supplemental movie 5 High resolution z-stack of murine tibia. The z-stack was recorded in a Lys-EGFP mouse. Blood vessels were stained with rhodamine-dextran and displayed in red, cells were detected via their green fluorescence and the bone structure by its SHG signal which was displayed in brown. The z-stack consisted of 99 steps with an interval of 2 µm and was recorded at a magnification of 200x.

Supplemental movie 6 Neutrophil observation in a Lys-EGFP mouse under steady-state conditions. Blood vessels were stained with rhodamine-dextran and displayed in red, cells were detected via their green fluorescence and the bone structure by its SHG signal which was displayed in brown. The recording time was 59 min, one z-stack consisted of 31 steps with an interval of 4 µm and the repetition time for each z-stack acquisition was 60 s. Pictures were taken at a magnification of 200x.

Supplemental movie 7 Neutrophil observation in a Lys-EGFP mouse 2 h after G-CSF mobilization. Blood vessels were stained with rhodamine-dextran and displayed in red, cells were detected via their green fluorescence and the bone structure by its SHG signal which was displayed in brown. The recording time was 39 min, one z-stack consisted of 31 steps with an interval of 4 µm and the repetition time for each z-stack acquisition was 60 s. Pictures were taken at a magnification of 200x.

Supplemental movie 8 Neutrophils of a Lys-EGFP mouse entering blood vessels after G-CSF treatment. Blood vessels were stained with rhodamine-dextran and displayed in red, cells were detected via their green fluorescence and the bone structure by its SHG signal which was displayed in brown. The recording time was 44 min, one z-stack consisted of 31 steps with an interval of 4 µm and the repetition time for each z-stack acquisition was 60 s. Pictures were taken at a magnification of 200x.

Supplemental movie 9 Macrophage and DC observation in a CX3CR1-EGFP mouse 2 h after mobilization with G-CSF. Blood vessels were stained with rhodamine-dextran and displayed in red, cells were detected via their green fluores-

cence and the bone structure by its SHG signal which was displayed in brown. The recording time was 29 min, one z-stack consisted of 31 steps with an interval of 4 µm and the repetition time for each z-stack acquisition was 60 s. Pictures were taken at a magnification of 200x.

Supplemental movie 10 Neutrophil behavior in a Lys-EGFP mouse treated with anti-KC/anti-MIP-2 antibodies and subsequently with G-CSF. G-CSF was applied 46 h after simultaneous i.p. antibody administration. Blood vessels were stained with rhodamine-dextran and displayed in red, cells were detected via their green fluorescence and the bone structure by its SHG signal which was displayed in brown. The recording time was 29 min, one z-stack consisted of 31 steps with an interval of 4 µm and the repetition time for each z-stack acquisition was 60 s. Pictures were taken at a magnification of 200x.

Supplemental movie 11 Neutrophil behavior in a Lys-EGFP mouse treated with an anti-CXCR2 antiserum and subsequently with G-CSF. G-CSF was applied 46 h after i.p. injection of the antiserum. Blood vessels were stained with rhodamine-dextran and displayed in red, cells were detected via their green fluorescence and the bone structure by its SHG signal which was displayed in brown. The recording time was 38 min, one z-stack consisted of 31 steps with an interval of 4 µm and the repetition time for each z-stack acquisition was 60 s. Pictures were taken at a magnification of 200x.

Supplemental movie 12 Neutrophil behavior in a Lys-EGFP mouse before treatment with AMD3100. Blood vessels were stained with rhodamine-dextran and displayed in red, cells were detected via their green fluorescence and the bone structure by its SHG signal which was displayed in brown. The recording time was 14 min, one z-stack consisted of 31 steps with an interval of 4 µm and the repetition time for each z-stack acquisition was 60 s. Pictures were taken at a magnification of 200x.

Supplemental movie 13 Neutrophil behavior in a Lys-EGFP mouse 2 h after i.v. treatment with AMD3100. Blood vessels were stained with rhodamine-dextran and displayed in red, cells were detected via their green fluorescence and

the bone structure by its SHG signal which was displayed in brown. The recording time was 14 min, one z-stack consisted of 31 steps with an interval of 4 µm and the repetition time for each z-stack acquisition was 60 s. Pictures were taken at a magnification of 200x.

9. Acknowledgement

First of all I want to thank my supervisor Prof. Matthias Gunzer for the extremely interesting subject of my PhD thesis. He introduced me to the world of immune cells and 2-photon microscopy and gave me time and support to establish and enhance the microscopy in murine long bones. The always very inspiring discussions and ideas concerning my project were irreplaceable and his positive manner motivated me also in periods of time when experiments seemed to be in a stalemate.

I would like to thank Prof. Burkhart Schraven and the whole Institute of Molecular and Clinical Immunology in Magdeburg for the support during the last three years.

A big thanks goes to all former and present members of the “Immunodynamics” for the good time in the lab and beyond. I thank our technicians Julia and especially Susi for the help every time when I needed much more than two hands. I thank Linda for her support in many mouse businesses and the shoe discussions and I thank Marco for many laughs and the delicious cakes. Kathleen R. showed me how to perfectly write a lab book and I thank Monika for nice times at the 2-photon microscope. Further I thank Lars for the sweets and Eloho and Kathleen B. for their good mood and support whenever I needed it.

I would like to thank the group of Nancy Hogg and especially Katia de Fillipo for performing all the immunohistochemistry and ELISA measurements and for the nice cooperation during the whole neutrophil story.

I would like to thank Tom Lane and Martin Hosking for providing me with CXCR2 antiserum and for performing the experiments with the CXCR2 ko mice.

I would like to thank Dr. Roland Hartig for all the stem cell sorts.

I would like to thank Dr. Anja Hauser and Katrin Roth from the DRFZ in Berlin for the helpful discussions all around the manifold and often unexpected problems during 2-photon microscopy and for the good brainstorming about fixing a mouse for intravital microscopy.

I would like to thank the group of Uschi Bommhard next door not only for allowing me to always use their lab equipment when ours was overcrowded but also for their support with coffee, milk and cookies during long days.

I would like to thank all members of the Tuesday's Badminton group for all the great fun on the court and afterwards.

Besides the members of my group a special thank goes to Swen, Clemens, Elisa and Anna for the fun at work and for the nice evenings and weekends which made my life in Magdeburg much more acceptable than I had expected before.

I would like to thank my family and especially my parents who always supported me in all my decisions and made everything possible to push me forward in life. It was their help and their exemplary and heartily way of education that guided me to this key point in my life where I stand now.

Last but not least I want to thank Mike for his comprehensive help in all circumstances. He always gave me the energy to overcome all problems in the lab and in our private life. Our discussions about science helped me a lot during my thesis but the most important thing is that I can always count on you. Thank you so much!

10. Curriculum vitae

Dipl. Biol. Anja Köhler

Olvenstedter Str. 65
39108 Magdeburg

tel.: +49(0)391-4021296
mobil: +49(0)170-2931618
e-mail: *anja.koehler@med.ovgu.de*

Personal Information

- Nationality: German
- Date of birth: 05.07.1980
- Place of birth: Peine
- Parents: Heinrich Köhler; electrician; 04.01.1950
  Ingrid Köhler; maiden name Wagner;
  office clerk; 03.07.1955
- Siblings: Markus Köhler, birthday: 16.12.1982

Education

- 1987 – 1991: Basic primary school in Edemissen, Germany
- 1991 – 1993: Orientation school in Edemissen, Germany
- 1993 – 2000: Secondary school (Gymnasium am Silberkamp) in Peine, Germany
- October 2000: Begin of Biology studies at the Technical University Braunschweig, Germany
- December 2003: Intermediate diploma at the Technical University Braunschweig, Germany

▪ March 2006 – May 2006:	Diploma exams at the Technical University Braunschweig, Germany
July 2006 – April 2007:	Diploma thesis at the Helmholtz Centre for Infection Research (Braunschweig, Germany) in the group of Prof. Matthias Gunzer. Title: „Analysis of the migartion behavior of mematopoietic stem cells in the bone marrow of mice"
▪ June 2007:	Begin of Ph.D. project at the Helmholtz Centre for Infection Research (Braunschweig, Germany) in the group of Prof. Matthias Gunzer
▪ Since December 2007:	Continuance of Ph.D. project at the Otto-von-Guericke University Magdeburg, Germany; Institute of Molecular and Clinical Immunology in the group of Prof. Matthias Gunzer

Graduations/Degrees

- 07.07.2000: high school graduation (German Abitur)
- 08.12.2003: pre-degree in Biology
- 02.05.2007: Diploma in Biology
  - main subject: Microbiology
  - minor subject 1: Genetics
  - minor subject 2: Phytology

Magdeburg, _____ Signature: _____